Probing HIV-1 Vaccination Through Deep B Cell Repertoire Sequencing and Functional Characterization

Shawn Michael Couture Herring

A dissertation

submitted in partial fulfillment of the

requirements for the degree of

Doctor of Philosophy

University of Washington

2026

Reading Committee:

D. Noah Sather, Chair

Donald L. Sodora, Chair

Andrew T. McGuire

Program Authorized to Offer Degree:

Pathobiology

Abstract

Probing HIV-1 Vaccination Through Deep B Cell Repertoire Sequencing and Functional Characterization

Shawn Michael Couture Herring

Chair of the Supervisory Committee:

D. Noah Sather

Department of Global Health

Understanding why vaccine-engaged B cells fail to mature into functional lineages remains a challenge in Human Immunodeficiency Virus 1 (HIV-1) vaccine development. This dissertation examined antibody function and repertoire maturation in rhesus macaques (*Macaca mulatta*) immunized with HIV-1 10014.F8 (F8) Envelope glycoprotein (Env), derived from an individual with broad neutralizing activity. F8 Env was presented as a SOSIP trimer, ferritin-displayed Env, or liposome-displayed Env to test whether antigen format altered humoral function and B cell evolution. Serum activity was linked to lineage-level maturation using serology, bulk memory B cell immunoglobulin heavy chain sequencing, single-cell V(D)J sequencing, monoclonal antibody expression, and Hinge-Seq. F8 trimer immunization induced Env-binding antibodies and detectable Fc activity, but neutralization breadth remained limited. Functionally anchored repertoire analysis showed Env-specific lineages were recruited yet less mutated than non-Env-binding background lineages. Ferritin display increased binding titers and avidity but did not improve neutralization, Fc activity, or lineage maturation. This series of findings indicates that F8 Env vaccination achieved antigen engagement without coordinated functional maturation, and antigen valency alone was insufficient to overcome this bottleneck.

TABLE OF CONTENTS

Acknowledgements

Undertaking a PhD was unlike anything I could have expected or prepared for. The number of people who have supported me along the way is too great to list. That being said, there are several to whom I owe never-ending thanks for their support.

First, to my P.I., Dr. Noah Sather, who provided a steadying voice and unbridled scientific encouragement, and without whom I would never have made it to my second year as a PhD student. I will always be grateful for his guidance, which will shape how I approach science, mentorship, and collaboration for the rest of my life. I could not have hoped for a better mentor or friend.

Second, I offer my sincere thanks to my dissertation committee. Their advice, time, and thoughtful feedback allowed me to pursue my science with rigor and drive. I recognize that their roles do not leave them with extra time in their workdays, and I deeply appreciate their willingness to supervise my PhD and contribute to the training of future generations of scientists. Thank you again to Drs. Andrew McGuire, Rhea Coler, William DeWitt, and Don Sodora.

Third, to the members of the Sather Lab who were with me throughout this journey. From the moment I arrived at SCRI to the writing of this dissertation, I have been surrounded by encouragement, humor, understanding, and solidarity. I cannot imagine what this experience would have been like without Andrew, Nicholas, Vlad, Madeline, Ganesh, Alex, and Will.

Fourth, to my cohort, who were with me through every step of this PhD journey. I will always appreciate our get-togethers, Slack chats, and friendship. I hope each of you forever receive the same support, encouragement, and solidarity that you have given me throughout my time here.

Fifth, to my many friends who kept me sane all these years. I never could have imagined a life so rich and full of connection. As you read this, please know that you are my chosen family, and I can't wait to make unlimited "Trust me, I'm a doctor" jokes.

Sixth, to my big sister Vanessa, you have always been my inspiration. Thank you for showing me what a life devoted to helping others looks like, and what it means to pursue that work with conviction, compassion, and purpose.

Finally, to Grace, without whom none of this would have been possible. You are my light, and I dedicate all of this to you.

Materials and Methods

Animal Care and Ethics Statement

All rhesus macaque studies were conducted at Oregon Health and Science University under an approved Institutional Animal Care and Use Committee (IACUC) protocol (IP00001105; Principal Investigator: Ann Hessell; approved February 6, 2019). All procedures involving animals were performed in accordance with institutional animal care policies and applicable federal guidelines governing the ethical use and welfare of laboratory animals. Animals were managed in compliance with regulations and guidance established by the United States Department of Agriculture, the Public Health Service Policy on Humane Care and Use of Laboratory Animals, the National Research Council Guide for the Care and Use of Laboratory Animals, the Institute for Laboratory Animal Research, the Centers for Disease Control, and the Weatherall Report on the Use of Nonhuman Primates in Research. Animal care and housing were provided in facilities accredited by the Association for Assessment and Accreditation of Laboratory Animal Care (AAALAC) International.

Rhesus macaques (*Macaca mulatta)* were housed in socially compatible pairs and maintained on a standard primate diet supplemented with fruits and vegetables, with environmental enrichment provided according to institutional standards. Immunizations and blood collections were performed under appropriate anesthesia in accordance with veterinary protocols to minimize discomfort.

Envelope Immunogen

The HIV-1 envelope sequence used in this study, hereafter referred to as 10014.F8, was derived from an early infection Env clone isolated from subject VC10014 in the Vanderbilt cohort and engineered for production of a soluble trimeric gp140 immunogen as previously

described[1–3]. In brief, the primary furin cleavage site, REKR, was changed to RRRRRR to enhance cleavage[4,5]. The 10014.F8 gp120 subunit sequence was grafted onto the BG505 gp41 subunit using a SOSIP motif as previously described[6,7]. Briefly, a disulfide bond is introduced between gp120 and gp41 (A501C/T605C) via site-directed mutagenesis (Agilent Technologies, Santa Clara, CA) along with gp41 (I559P) for stabilization. Additionally, gp120-gp41 interface stabilizing mutations 543N, 553S, 588R, 662A and a V3 stabilizing engineered disulfide bond (L201C/A433C) were added[8]. To improve trimer homogeneity and solubility a stop codon was introduced at residue 683 (HXB2 numbering)[9]. The native leader sequence was replaced with the tissue plasminogen activator. The entire construct was cloned into the pcDNA3.4 (Thermo Fisher, Waltham, MA) mammalian expression vector, then produced in HEK293F cells and purified using a combination of lectin affinity chromatography, anion exchange and size exclusion chromatography.

Study Design and Immunization Cohort

Eighteen female rhesus macaques were immunized with HIV-1 10014.F8.SOSIP Env immunogens derived from the 10014.F8 envelope sequence[10] in a prime-boost regimen consisting of a DNA prime at week 0 followed by protein boosts at weeks 4, 10, and 20 (Fig. 1a). Animals were divided into three vaccine groups of six animals each to compare the effects of antigen presentation format while holding the Env sequence constant. Vaccine groups included soluble 10014.F8.SOSIP trimer, ferritin-displayed 10014.F8.SOSIP Env nanoparticles, and liposome-displayed 10014.F8.SOSIP Env trimers. The soluble trimer group represented the lowest-valency antigen format (1-copy), the ferritin group represented an intermediate-valency nanoparticle display format (8-copy), and the liposome group represented a higher-density membrane-associated Env display format (100+-copy).

For protein immunizations, animals received a total of 50 μg of Env immunogen per immunization, administered as bilateral intramuscular injections of 25 μg in each deltoid. For the ferritin-displayed Env group, animals received 100 μg of conjugated ferritin nanoparticle material per immunization, corresponding to approximately 88 μg of Env and 12 μg of ferritin scaffold. Soluble 10014.F8.SOSIP trimer and ferritin-displayed 10014.F8.SOSIP Env immunogens were formulated in 20% Adjuplex adjuvant. Liposome-displayed 10014.F8.SOSIP Env trimers were formulated with MPLA and QS-21. Peripheral blood samples were collected longitudinally throughout the immunization schedule for serological, cellular, and repertoire-based analyses.

Sample Collection

Peripheral blood samples were collected from immunized animals at multiple timepoints throughout the vaccination schedule for downstream immunological and repertoire analyses. Whole blood was processed to isolate plasma for serological assays and peripheral blood mononuclear cells (PBMCs) for cellular and sequencing-based assays.

PBMCs used for bulk B cell receptor (BCR) repertoire sequencing were collected two weeks following the final immunization (week 22). In a subset of animals, PBMCs collected at weeks 21/22 were additionally used for single-cell B cell sorting and 10x Genomics 5’ V(D)J sequencing to recover paired heavy and light chain antibody sequences for mAb expression and functional characterization.

Plasma samples were collected longitudinally during the immunization schedule and were used for serological analyses including Env-specific binding enzyme-linked immunosorbent assay (ELISA), avidity measurements, neutralization assays, and fragment crystallizable region (Fc)-mediated effector function assays.

Bio-Layer Interferometry

Monoclonal antibody binding to 10014.F8 Env antigens was assessed by Bio-Layer Interferometry (BLI) using a GatorBio GatorPlus instrument. 10014.F8.SOSIP trimer and 10014.F8 gp120 proteins were biotinylated and immobilized onto streptavidin biosensors (Gator Probes PN: 16002). After antigen loading, sensors were equilibrated in KB running buffer, consisting of 1× PBS, 0.1 mg/mL bovine serum albumin (BSA), 0.05% sodium azide, and 0.02% Tween-20, and then dipped into wells containing monoclonal antibody to measure antigen-antibody association. Binding responses were recorded as BLI wavelength shifts and compared against background signals from the KB running buffer alone. Monoclonal antibodies were considered Env-binding hits if binding to 10014.F8.SOSIP, 10014.F8 gp120, or both antigens exceeded the background signal observed with buffer alone. Response shifts were used to compare relative binding across antibodies and antigens.

Serological Assays

Env-Binding ELISA

Longitudinal plasma samples were collected and analyzed for IgG binding titers to the respective SOSIP via ELISA at weeks 1, 2, and 3 (post-first immunization), weeks 5, 6, and 8 (post-second immunization), weeks 11, 12, and 14 (post-third immunization), and weeks 21, 22, and 24 (post-fourth immunization). Autologous 10014.F8.SOSIP Env-specific IgG endpoint titers were determined using a direct ELISA. Plasma was heat-inactivated for 1 hour at 56°C prior to the assay. Immulon 2HB 96-well plates (Thermo Scientific) were coated with fifty nanograms (50 ng) per well of 10014.F8.SOSIP trimer in 0.1 M $NaHCO_3$, pH 9.5. Plates were washed between each ELISA step with PBS containing 0.2% Tween-20. Coated plates were blocked with PBS, 10% non-fat milk, and 0.3% Tween-20 for 1 hour at 37°C. Following blocking, plasma samples

were serially diluted five-fold over a range of 1:50 to 1:3,906,250 in 100 µL of PBS, 10% non-fat milk, 0.03% Tween-20 and incubated for 1 hour at 37°C. Bound antibodies were detected using goat anti-human IgG (H+L)-HRP (Invitrogen, A18805) diluted 1:1000 in PBS, 10% non-fat milk, 0.03% Tween-20 and incubated for 1 hr at 37°C. Plates were developed using 50 µL of TMB Peroxidase Substrate (SeraCare Life Sciences Inc), then stopped after 3 minutes with an equal volume of 1 N H2SO4. Absorbance at 450 nm was determined with the BioTek ELx800 microplate reader. Endpoint titers were defined as the reciprocal of plasma dilution at OD450 = 0.1 after the subtraction of any non-specific signal from pre-immunization plasma.

Avidity ELISA

To evaluate the quality of the antibody response elicited by immunization with 10014.F8.SOSIP, ammonium thiocyanate (NH4SCN) avidity ELISAs were performed using a modified version of the previously described ELISA protocol. In this assay, plasma titrations were performed in quadruplicate. After incubation with primary antibodies, half of the samples were treated with either 1× PBS or 4 M NH4SCN for 20 minutes at room temperature. Following treatment, the ELISA proceeded with secondary staining and was developed as described above.

Avidity index was determined as the ratio of the area under the binding curve (AUC) after transforming the x-axis by 1/x for NH_4SCN-treated samples to the AUC of the corresponding PBS-treated controls, calculated across the full dilution series. Values approaching 1 indicate high-avidity antibody binding resistant to chaotropic disruption, whereas lower values reflect reduced binding strength and increased sensitivity to dissociation.

Neutralization Assays

Tier 1 and Tier 2 panels of pseudoviruses from clades, A, B, C, and G, as well as the recombinant forms CRF01_AE, CRF07_BC, and AC, were used to assess the neutralization activity in samples collected one week post-third immunization. TZM-bl cells were plated at a density of 4 x 10^3 per well of a 96-well plate (Falcon, 353075) 24 hours prior to the assay, and polybrene reagent was added to the cells at 2 µg/ml 30 minutes prior to inoculation with test samples. Heat-inactivated plasma at 1:50 final dilution was pre-incubated with pseudovirus for 90 minutes at 37°C. Following the incubation, the medium was aspirated, and the virus/plasma mixture was added to the TZM-bl cells. After 72 hours at 37°C, cell supernatant was replaced with 100 µL of Promega Steady Glo reagent, cells were allowed to lyse for 5 minutes at room temperature, and luciferase activity was measured as relative light units (RLU) using a Fluoroskan Ascent FL luminometer. RLU values used to determine percent neutralization are the average of triplicate wells of pre- and post-immune plasma samples tested on the same plate. Percent neutralization for the tier 1 and 2 panels was calculated using the following equation:

$$([\text{RLUpre} - \text{RLUcell background}] - [\text{RLUpost} - \text{RLUcell background}]) \div (\text{RLUpre} - \text{RLUcell background}) \times 100$$

Titrated autologous neutralization was determined by titrating plasma samples over the range of a dilution factor of 20 to 1,562,500 and the following equation:

$$1-((\text{RLUsample}-\text{RLUcell\_control})/(\text{RLUvirus\_control} - \text{RLUcell background})) \times 100$$

Values below 50% neutralization were classified as non-neutralizing.

Antibody Dependent Cellular Phagocytosis

To measure Antibody Dependent Cellular Phagocytosis (ADCP), we conducted the assay as previously described[11]. Briefly, 1 µm fluorescent NeutrAvidin beads (Invitrogen, F8776) were coated with biotinylated 10014.F8 gp120 overnight at 4°C, then subsequently washed in 0.1% BSA in 1× PBS. Plasma collected two weeks post-third immunization was heat-inactivated for 1 hour at 56°C and incubated at a 1:50 dilution with 2 x 10^6 beads for 2 hours at 37°C in a 96-well U-bottom plate (Corning, 353227). THP-1 monocytes (ATCC® TIB-202TM) were cultured as recommended by ATCC and 20,000 cells were added to each well in 100 µl volume. The plates were incubated overnight at 37°C to allow for phagocytosis. The following morning cells were fixed with 100 µl of 4% PFA (Electron Microscopy Sciences, 15710) and analyzed on the BD LSRII flow cytometer. The phagocytic activity is represented by the integrated Mean Fluorescence Intensity (iMFI), which is the product of the median fluorescence intensity and the frequency of bead-positive (FITC+) cells.

Antibody Dependent Cellular Cytotoxicity

Antibody Dependent Cellular Cytotoxicity (ADCC) was determined with the assay previously described[12]. Briefly, MT4-CCR5-Luc cells were infected with 300 ng p24/million cells viral inoculum or mock-infected by spinnoculating at 1200 g for 2 hours at room temperature. Cells were cultured for three days and confirmed to have a minimum of 10x RLU compared to mock-infected cells. MT4 cells were diluted to 0.2 x 10^6 cells/mL in RPMI + (1x PSG + IL-2) then incubated with plasma at a 1:50 dilution. 100 µL of KHYG-1 cells at 1 x 10^6 cells/mL (in RPMI + 1x PSG + IL-2) was then added to the MT4/antibody mixture and incubated for 24 hours to generate ADCC. Percent ADCC was calculated using the following equation:

$$(\text{RLUpre} - \text{RLUpost}) \div (\text{RLUpre} - \text{RLUcell background}) \times 100$$

B Cell Isolation

PBMCs from 2-week post-final boost were thawed in RPMI containing 10% FBS, 2 mM L-glutamine, 0.1 mg/mL DNase I, and 5 mM MgCl2. PBMCs were then enriched using the EasySep Human Memory B Cell Isolation Kit (STEMCELL Technologies) according to the manufacturer's instructions with the following exception. Following magnetic separation in step 6, the supernatant containing the negatively selected cell fraction, typically reserved for optional naïve B cell isolation, was instead collected, quantified, and stained for FACS sorting to isolate plasmablasts (defined as CD3-, CD11c-, CD14-, CD16-, CD123-, CD20-/int, CD80+, and HLA-DR+ as previously described)[13]. Plasmablasts were sorted directly into FBS, centrifuged, quantified, and prepared for single-cell RNA sequencing using the 10x Genomics 5' Single Cell v2 protocol according to the manufacturer's instructions.

The remaining positive fraction containing the magnet-bound memory B cells was processed through the remainder of the EasySep Human Memory B Cell Isolation Kit protocol. Isolated memory B cells were then cultured in ImmunoCult Human B Cell Expansion Medium (STEMCELL Technologies) at a concentration of 0.2×10^6 cells/mL. These stimulated cells were maintained for a total of seven days, with a media split performed on day 5 to return the culture density back to 0.2×10^6 cells/mL. On day 7, the cultured cells were harvested and sorted via FACS to isolate CD3- and double antigen-positive populations directly into FBS. Following the sort, these stimulated cells were centrifuged, quantified, and prepared for single-cell RNA sequencing using the 10x Genomics 5' Single Cell v2 protocol according to the manufacturer's instructions.

Single-cell V(D)J Sequencing and Monoclonal Antibody Recovery

Single-cell V(D)J libraries were generated from sorted B cell populations using the Chromium Next GEM Single Cell 5' V(D)J Reagent Kit v1.1 according to the manufacturer's protocol through cDNA amplification and QC. Briefly, sorted cells were loaded onto the 10x Genomics Chromium Controller for GEM generation, reverse transcription, and single-cell barcoding. The resulting cDNA was amplified, purified, and assessed for quality prior to downstream immune-repertoire amplification. The 10x workflow captures the full-length, 10X-barcoded cDNA from polyadenylated transcripts, with each transcript retaining a cell barcode and unique molecular identifier for assignment to individual cells.

For antibody recovery, the standard 10X V(D)J enrichment workflow was modified after cDNA amplification by using custom immunoglobulin-specific primers. Initial amplification was performed from amplified 10X cDNA using a 5' primer compatible with the 10X read 1/cell barcode/UMI structure and chain-specific 3' primers targeting rhesus immunoglobulin constant regions. Nested amplification was then performed using a common forward primer and reverse primers targeting IgG, IgM, IgA, IgK, and IgL constant regions. PCR products were purified using SPRIselect beads, quantified by Qubit, indexed, and prepared for Illumina sequencing. Sample-specific index primers were used to distinguish libraries during sequencing.

Indexed libraries were pooled and sequenced on an Illumina NextSeq 2000 using a 600-cycle kit (Illumina, 20100981) on a P1 flow cell. Libraries were sequenced using paired-end reads, with sequencing performed from both ends of each library molecule to generate forward and reverse reads spanning the V(D)J amplicons. Sequencing was performed using standard sequencing-by-synthesis workflows with onboard cluster generation, base calling, and demultiplexing to generate FASTQ files.

Single-cell V(D)J Sequencing Data Processing

Raw base call files generated from the Illumina NextSeq 2000 were demultiplexed to FASTQ files and processed using Cell Ranger version 9.0.0. FASTQ files were analyzed using the Cell Ranger V(D)J workflow to associate sequencing reads with 10x cell barcodes and unique molecular identifiers, assemble immunoglobulin contigs, and generate per-cell V(D)J annotations. Cell Ranger output files containing assembled contigs and cell-level V(D)J annotations were used to identify productive immunoglobulin heavy and light chain contigs and recover paired antibody sequences from individual cells. Cell barcodes were used to associate heavy and light chain sequences originating from the same sorted cell. Candidate paired antibody sequences were selected for downstream mAb expression based on recovery of productive paired heavy and light chain rearrangements.

Monoclonal Antibody Expression and Purification

Recovered paired immunoglobulin heavy and light chain sequences were synthesized and expressed by a commercial provider (Biointron). Antibodies were expressed as *Macaca mulatta* IgG1-kappa in HEK293F cells using transient PEI Max co-transfection of heavy and light chains encoded in pcDNA3.4 expression vectors. Antibodies were purified by affinity chromatography by passing supernatants over an MAb-select SURE column (GE) and eluting with 0.1 M Glycine-HCl, pH 3.0, and then neutralized in 1 M Tris-HCl, pH 9.0. Purified antibodies were provided following standard quality control procedures, including endotoxin testing (<1 EU/mg), SDS-PAGE purity assessment (>95%), and size-exclusion chromatography by HPLC (SEC-HPLC) for evaluation of aggregation and monodispersity.

Monoclonal Antibody Functional Characterization

Monoclonal antibodies were evaluated for binding and functional activity using the same assay platforms described for plasma samples. Binding to HIV-1 Env antigens was assessed by ELISA and Bio-Layer Interferometry, and neutralization activity was measured using TZM-bl-based pseudovirus assays. Fc-mediated effector functions were evaluated using ADCP and ADCC assays as described above.

Bulk BCR Repertoire Sequencing (HINGE-Seq)

The bulk BCR repertoire was characterized using a targeted high-throughput sequencing method adapted for rhesus macaque IgG chains. This methodology involves the development of sequencing libraries targeting the variable, CDR3, and constant regions of the immunoglobulin heavy chain (IgH). The process begins with cDNA synthesis utilizing a 5’ cap technique and incorporating a template switch adapter containing a Unique Molecular Identifier (UMI) tag. Synthesis is initiated using a specific reverse primer targeting the gamma chain. Following cDNA generation, libraries are constructed using two rounds of sequential PCR amplification and a final indexing PCR step. The final products are designed as paired, barcoded, overlapping reads suitable for multiplexed sequencing.

PBMC Processing and B Cell Enrichment

Starting material consisted of frozen peripheral blood mononuclear cells (PBMCs). Upon thawing, PBMCs were enriched for B cells using the EasySep™ Human B Cell Isolation Kit (STEMCELL Technologies). This negative selection method depletes cells expressing CD2, CD3, CD14, CD16, CD36, CD43, CD56, CD66b, and GlyA via antibody-magnetic labeling. B cells were then cultured for one week in ImmunoCult™ B Cell Expansion Medium to increase B

cell numbers and improve RNA integrity before extraction. B cells were then pelleted and frozen in 50,000-cell aliquots in RLT buffer.

RNA Extraction and cDNA Synthesis

B cell aliquots were processed using the Monarch® Total RNA Miniprep Kit (New England Biolabs), with homogenization performed using a Qiagen QIAshredder before column purification. RNA cleanup and concentration were carried out using RNAClean XP beads (Beckman Coulter), involving RNA binding, ethanol washes, and elution in nuclease-free water. Purified RNA was immediately reverse transcribed using a SMARTScribe Reverse Transcriptase kit (Takara Bio). A template-switch adapter containing the UMI was included in the reaction. Following cDNA synthesis, Uracil-DNA Glycosylase was added to hydrolyze uracil residues within residual template-switch adapters, preventing carryover into PCR and reducing background amplification.

Library Preparation

Multiplex nested PCR was performed using Q5 High-Fidelity 2X master mix (New England Biolabs). Library construction was designed to generate two overlapping amplicons originating from the same template molecule: a variable-region amplicon spanning the V(D)J and complementarity determining region 3 (CDR3) of the IgH transcript, and a constant-region amplicon targeting the hinge and constant region of the heavy chain to enable subclass assignment. Both amplicons were linked through the shared UMI introduced during template-switch cDNA synthesis, allowing sequences originating from the same transcript to be computationally paired during downstream analysis.

This dual-amplicon strategy was implemented to overcome limitations of short-read sequencing technologies. While Illumina sequencing provides high base-calling accuracy and

high Phred quality scores that are advantageous for analyzing highly diverse immunoglobulin variable regions, read lengths are insufficient to reliably span both the variable and constant regions of the IgH transcript in a single contiguous read. By separately amplifying the variable and constant regions and linking them through a shared UMI, this approach enables accurate characterization of antigen-binding regions while still allowing assignment of IgG subclass identity.

PCR1 and PCR2 products were purified after each amplification step using SPRIselect beads (Beckman Coulter), followed by ethanol washes and elution in nuclease-free water. Purified PCR2 products underwent end-repair and adaptor ligation using the NEBNext Ultra II DNA Library Prep Kit for Illumina (New England Biolabs). Libraries were then indexed with NEBNext Multiplex Oligos (New England Biolabs) to incorporate unique indices for sample barcoding. Library concentrations were determined using the KAPA Library Quantification Kit (Roche). Each library was quantified in duplicate, and molar concentrations were calculated from the standard curve. Libraries were pooled to a target concentration of 4 nM using KAPA derived molarities. The pooled library was assessed by KAPA quantification to verify final concentration before sequencing.

Because subclass identity was determined from the constant-region amplicon, assignment of IgG subclass required successful recovery of both the variable-region and constant-region amplicons sharing the same UMI. In cases where the variable-region amplicon was successfully recovered but the corresponding constant-region amplicon was not retained through sequencing or library processing, subclass identity could not be assigned. As a result, a subset of otherwise productive IgH sequences lacked subclass annotation in downstream analyses.

Bulk Sequencing Data Processing

Raw paired-end MiSeq reads were merged to reconstruct full-length amplicons using FLASH. Merged reads were filtered to retain sequences containing expected amplification primers, which were subsequently trimmed using cutadapt. Reads containing low-confidence base calls (N's) were removed using the FASTX-Toolkit.

UMIs introduced during cDNA synthesis were used to collapse sequencing reads originating from the same template molecule. Consensus sequences were defined as Molecular Identifier Groups (MIGs), retaining only MIGs supported by at least three sequencing reads to ensure high-confidence sequence reconstruction.

Processed sequences were annotated using IgBLAST against a customized rhesus macaque immunoglobulin gene reference database. V and J gene segment assignments were determined based on highest-scoring alignments. Due to ambiguity in short D segment alignments, D gene calls were excluded from downstream analyses. Sequences failing productive rearrangement criteria (including stop codons, frameshifts, or incomplete V(D)J assignments) were removed. Constant-region amplicons were linked to corresponding variable-region sequences through shared UMI identifiers, enabling assignment of IgG subclass identity.

Bulk Repertoire Bioinformatics

Clonal families were inferred from productive IgH sequences using the SCOPer package within the Immcantation toolkit [14,15]. Sequences were first grouped by shared V/J family assignment and CDRH3 length, after which pairwise distances between CDRH3 nucleotide sequences were calculated. Clonal clustering was performed using a hierarchical clustering approach with an adaptive threshold determined using the *findThreshold* method to separate

intra-clone from inter-clone sequence distances. Clone size was defined as the number of unique MIG-supported sequences assigned to each clonal lineage.

For analyses of bulk repertoire structure, clonal clustering was performed independently for each animal to prevent assignment of sequences from different animals to the same lineage. However, for integration of mAb sequences recovered from single-cell experiments, some antibody sequences could not be unambiguously attributed to a single animal due to limitations in sample demultiplexing during single-cell processing. In these cases, clonal clustering was performed using bulk repertoire sequences only from the subset of animals from which the antibody could have originated. These pooled clustering analyses included no more than three animals at a time and allowed recovered mAbs to be assigned to the animal with the most closely related bulk clonal lineage while minimizing the possibility of spurious cross-animal lineage assignment. Because the animals were unrelated and immunized independently, the probability of highly similar IgH sequences arising independently across animals is low, further reducing the likelihood of erroneous cross-animal lineage assignment.

Functional Anchoring of Bulk Repertoires

To link bulk repertoire data with experimentally validated antibody functionality, IGH sequences derived from single-cell V(D)J sequencing were incorporated into the bulk IGH dataset prior to clonal inference. Clonal clustering was then performed jointly, allowing mAb sequences to be assigned alongside bulk IGH sequences to clusters based on shared V and J gene family usage and highly similar CDRH3 nucleotide sequences.

Productive IGH sequences were subjected to clonal inference using SCOPer on a per-animal basis[14,15]. To mitigate uncertainty in germline gene assignment in rhesus macaques, sequences were grouped by shared V and J gene family rather than exact gene assignment prior to distance calculation. This approach increases sensitivity for detecting clonal

relationships by reducing artificial lineage fragmentation arising from ambiguous or incomplete germline annotation.

Pairwise distances between sequences were calculated using length-normalized nucleotide Hamming distance, and nearest-neighbor distance distributions were used to estimate clonal clustering thresholds via the SHazaM *findThreshold* function. Thresholds were inferred using a Gaussian mixture model with a gamma–gamma formulation and the optimal cutoff criterion, without subsampling. Clustering was performed using single-linkage hierarchical clustering on length-normalized nucleotide distances. Only sequences meeting a retained-count threshold of at least three were included in downstream analyses.

Clonal families containing sequences matched to mAbs demonstrating Env binding were classified as vaccine-specific lineages, whereas clonal families matched to non-binding mAbs were classified as non-binding lineages. Clonal families without a corresponding single-cell mAb match were annotated as functionally uncharacterized.

Clonal expansion and lineage analysis

Cluster-specific phylogenies were inferred from MAFFT-aligned nucleotide sequences using IQ-TREE2 under a GTR+G substitution model with 1,000 bootstrap replicates[16,17]. Trees were inferred independently for each clone, and alignments containing fewer than three sequences were excluded from phylogenetic analysis. Branch lengths represent substitutions per site and were used as a proxy for SHM accumulation within clonal lineages.

Somatic Hypermutation Analysis

SHM levels were calculated by comparing each sequence to its inferred germline V gene using the SHazaM package[14]. Mutation frequency was quantified as the number of nucleotide substitutions per aligned V gene region relative to the germline sequence. SHM levels were calculated for the full V region and separately for framework regions (FWR) and CDRs. Clone

level mutation statistics were computed by averaging mutation frequencies across sequences within each clonal family.

IgG Subclass Analysis

IgG subclass identity was determined by alignment of constant region sequences to rhesus macaque germline constant region references. Subclass usage was quantified at both the sequence and clonal lineage levels.

Statistical Analysis

Statistical analyses were performed using R version 4.5.1. Statistical tests were selected based on the structure of each comparison, including whether data were paired within animals, repeated across time, or compared between independent groups. Unless otherwise indicated, tests were two-sided, and statistical significance was defined as $p < 0.05$.

Longitudinal avidity measurements were analyzed using repeated-measures one-way analysis of variance with Geisser-Greenhouse correction, followed by Tukey's multiple-comparisons test. Paired pre- and post-immunization functional assays, including antibody-dependent cellular phagocytosis and antibody-dependent cellular cytotoxicity, were analyzed using paired two-sided t tests.

Repertoire-derived comparisons between vaccine-specific and non-Env-binding lineages were analyzed using non-parametric tests. Two-group comparisons were performed using Mann-Whitney U tests. For comparisons involving more than two groups, Kruskal-Wallis tests were used, followed by pairwise comparisons where appropriate. Multiple testing correction was performed using the Benjamini-Hochberg false discovery rate procedure. Adjusted p-values < 0.05 were considered significant.

For clone-level analyses, each antibody-anchored clone was treated as the unit of analysis unless otherwise stated. Clone-level summary values were calculated from the median sequence-level value within each clone before statistical testing.

Chapter 1. Introduction to Human Immunodeficiency Virus 1 (HIV-1)

1.1 The Need for an HIV-1 Vaccine and Barriers to Its Development

1.1.1 The Global Burden of HIV-1 and the Need for Preventive Vaccination

HIV-1 remains a major global health challenge, demanding effective preventive measures despite progress in treatment. Since the beginning of the HIV epidemic, 91.4 million people have been infected with HIV-1, and 44.1 million have died from Acquired Immunodeficiency Syndrome (AIDS)-related illnesses. The mortality burden of HIV-1 has been compared to the total number of battle deaths across the twentieth century, underscoring the extraordinary scale of the epidemic[18]. An estimated 40.8 million people worldwide were living with HIV-1 in 2024 according to the 2025 Joint United Nations Programme on HIV and AIDS (UNAIDS) Global HIV Factsheet[19]. This included 39.4 million adults aged 15 years or older and 1.4 million children aged 0-14. In 2024 alone, 1.3 million new HIV-1 infections occurred. Although this represents a 61% decrease from the peak in 1996, which had just over 3.4 million new infections, and a 40% decline since 2010, which had 2.2 million new infections, it still falls short of the UNAIDS target of fewer than 370,000 new infections by 2025. This gap becomes especially consequential in light of the recent disruptions in United States (US) foreign aid, including stop-work orders affecting the US President's Emergency Plan for AIDS Relief (PEPFAR) and dissolution of the US Agency for International Development (USAID).

The scale and persistence of the problem highlights the urgent need for a safe, effective, affordable, and widely available vaccine to control and end the HIV-1 epidemic. While

combination antiretroviral therapy (cART) has turned HIV-1 into a manageable chronic disease, with an estimated 31.6 million of the 40.8 million people living with HIV (PLWH) globally accessing treatment in 2024, it does not eliminate the virus, which rapidly rebounds upon treatment interruption[19,20]. However, despite effective viral suppression, PLWH on cART still experience persistently heightened inflammation, an elevated risk of serious non-AIDS comorbidities (such as cardiovascular diseases, cancers, and metabolic disorders) and a shortened life expectancy compared to the general population[21]. These biological limitations when coupled with the logistical burden of maintaining lifelong adherence and care highlight the critical need for a preventive HIV-1 vaccine that can provide durable and broad protection with only a few doses. However, creating such a vaccine remains highly challenging due to major scientific obstacles.

1.1.2 Genetic and Structural Barriers to HIV-1 Vaccine Design

The development of an HIV-1 vaccine faces significant challenges due to the nature of the virus and how it interacts with the host immune system. The extensive genetic variability of HIV-1, particularly its viral envelope (Env) glycoprotein, is one such challenge[10,21]. The virus's high mutation rate enables it to rapidly evade neutralizing antibodies and other immune responses. The HIV-1 genome encodes an error-prone viral reverse transcriptase, leading to an elevated mutation rate within replication cycles. HIV-1 is categorized into four groups (M, O, N, P), with Group M consisting of nine subtypes/clades (A, B, C, D, F, G, H, J, K). Amino acid variations can be as high as 30% within subtypes and up to 42% between them, making the development of a universal vaccine difficult[21].

The difficulty in addressing the mutation rate is compounded by the Env trimer exhibiting high levels of conformational flexibility and a dense shield of host-derived glycans. This "glycan shield" acts as a form of molecular camouflage, occluding conserved epitopes from antibody recognition[22]. While a subset of antibodies can penetrate or even exploit the glycan shield, such

responses are rare and typically require high levels of sequence divergence from germline-encoded immunoglobulin genes. The combination of HIV-1's extreme sequence diversity, conformational masking, and glycan shielding presents a virus that has thus far stymied the production of an effective HIV-1 vaccine.

1.1.3 The Challenge of Eliciting Broadly Neutralizing Antibodies

Eliciting broadly neutralizing antibodies (bNAbs) is a major goal for vaccine research due to their ability to neutralize a broad diversity of viral isolates despite their overall genetic diversity. This breadth depends on two related features. First, many bNAbs target Env sites that are evolutionarily constrained, meaning that the virus cannot extensively mutate these regions without reducing viral fitness. Second, bNAbs often bind these sites with sufficient affinity and structural compatibility that limited sequence variation within the antibody-binding footprint can be tolerated without fully disrupting neutralization. In this sense, breadth reflects both the conservation of the targeted epitope and the ability of the antibody-antigen interaction to withstand the modest amino acid variation that remains across viral isolates. These bNAbs naturally develop in approximately 20-30% of HIV-1-infected individuals, usually within the first three years of infection and often in the context of moderate, sustained viral loads[1,23]. Eliciting them through traditional vaccination protocols has proven challenging[3,10,24]. Many bNAbs display high levels of somatic hypermutation (SHM), diverging from germline sequences by as much as 46%[10,24]. In addition to unusually high SHM, many possess unusual repertoire features that are rare in normal B cell populations, including long CDRH3 regions, restricted germline-gene usage, and frequent polyreactivity or autoreactivity. The inferred germline precursors of some bNAbs may lack detectable binding to recombinant HIV-1 Env proteins, making it difficult to drive their maturation[24,25]. In addition, some potent bNAb families, like the VRC01 class, are genetically restricted, primarily using the IGHV1-2*02 human VH allele[26–28]. Other barriers to vaccine development include gaps in understanding of the immune correlates of protection, the

lack of perfect animal models, and historical safety concerns that prevent the use of traditional live attenuated or whole-inactivated virus methods for HIV-1 because of the risk of proviral HIV DNA integration into the host genome[21]. These barriers help explain why, despite more than 250 human HIV-1 vaccine trials since the epidemic began, no licensed HIV-1 vaccine has been developed[29].

1.2 Historical Context of HIV-1 Vaccine Trials and Emerging Correlates of Protection

1.2.1 Early Vaccine Approaches and Limited Efficacy

The history of HIV-1 vaccine development is marked by decades of intense research and clinical trials, yet no licensed HIV-1 vaccine is currently available. After HIV-1 was first isolated in 1983-84, there was optimism that a vaccine could be developed within a few years[30,31]. However, researchers quickly realized they had underestimated the challenge, as HIV-1 is fundamentally different from other viral diseases for which successful vaccines were empirically developed. As a retrovirus, HIV-1 integrates into the host genome as an obligate step in its life cycle, allowing infection to become lifelong once a viral reservoir is established[32]. An effective prophylactic vaccine likely needs to prevent infection (and subsequent integration) entirely, or at least be capable of responses able to destroy founder proviral cells before systemic dissemination and reservoir establishment.

HIV-1 also presents an extreme antigenic-diversity problem. Its error-prone, low-fidelity reverse transcriptase leads to extensive viral diversity both within and between infected individuals. As a result, humoral and cellular responses against one Env variant may have limited activity against contemporaneous or subsequently emerging variants. The scale of this variation is unusual among human viruses. The genetic diversity of HIV-1 within a single infected individual can be comparable to the global genetic diversity of influenza viruses

circulating in a given year[33]. This extraordinary diversity has made it difficult for conventional vaccine approaches to elicit responses with sufficient breadth. This requirement has driven vaccine-development strategies based on rationally designed platforms.

Early work was inspired by the success of the hepatitis B vaccine and often focused on recombinant DNA technologies using genetically engineered antigens of HIV's outer envelope glycoproteins, gp120 or gp160[21]. The first experimental immunization of humans against HIV-1/AIDS, conducted in Zaire (modern-day Democratic Republic of Congo) in 1986, involved vaccinating a small group with a vaccinia vector expressing gp160 (recombinant HIV-1-vaccinia virus)[34,35]. Initial responses were weak, but in one individual, subsequent boosts with autologous vaccinia-infected cells and purified gp160 protein elicited stronger and longer-lasting immune responses, including neutralizing antibodies and cell-mediated reactivity. This study demonstrated for the first time that humans could be immunized against HIV-1 and mount detectable antiviral immunity, but its impractical design and inconsistent results highlighted the difficulty of developing a scalable, protective vaccine.

Subsequent trials revisited recombinant gp160 (e.g., VaxSyn) and vaccinia virus vectors (e.g., HIVAC-1e). VaxSyn demonstrated safety and tolerability, but immune responses were modest, required multiple doses, diminished within 18 months, and had little neutralizing activity[36]. HIVAC-1e produced short-lived T cell responses but often failed to produce HIV-specific antibodies[37]. A "prime-boost" approach, combining HIVAC-1e with VaxSyn, showed enhanced humoral and cellular responses while inducing neutralizing antibodies. However, safety concerns about vaccinia vectors in previously vaccinated individuals and potential severe disease in immunosuppressed recipients led to replication-competent vaccinia vectors being abandoned. Researchers then shifted focus to non-replicating or attenuated poxviruses[21].

Later efficacy trials, such as VAX003 and VAX004 (1998-2003), tested bivalent gp120 protein formulations (AIDSVAX B/B or B/E) with alum as an adjuvant[38,39]. Despite protecting chimpanzees and showing safety and immunogenicity in early-phase human trials, these

vaccines failed to prevent HIV-1 acquisition or reduce disease in large cohorts of men who have sex with men and intravenous drug users. These trials, along with later T cell-focused trials like STEP/HVTN502, and Phambili/HVTN503, ultimately failed to prove effective, leading to significant setbacks and a reevaluation of HIV-1 vaccine design strategies. These early attempts at vaccination exposed a limitation in neutralizing antibody strategies. The vaccinations were immunogenic and could elicit humoral responses, including neutralization of autologous or laboratory-adapted HIV-1 strains, but these responses did not have the breadth needed to neutralize circulating isolates. At the time, only a limited number of viral isolates had been deeply characterized, and the full scale of HIV-1 genetic diversity was not yet understood. As more sequence and neutralization data became available, it became clear that a protective neutralizing antibody response would need to target conserved Env vulnerabilities across many viral variants.

1.2.2 The RV144 "Thai Trial" and Non-Neutralizing Antibody Function

A shift in HIV-1 vaccine research came with the RV144 “Thai Trial”, a randomized, double-blind phase 3 efficacy trial, which provided the first, though modest, success by demonstrating 59.9% efficacy within the first 12 months, dropping to 31.2% efficacy against HIV-1 infection at the conclusion of the trial[21,40–43]. The RV144 regimen used a prime-boost strategy, with four priming injections of a recombinant canarypox vector vaccine, ALVAC-HIV (vCP1521), expressing Env (clade E), Gag (clade B), and Pro (clade B), followed by two booster injections of an alum-adjuvanted bivalent HIV-1 gp120 subunit vaccine (AIDSVAX B/E). This approach combined two vaccines that had previously failed to achieve protection alone.

Protection observed in RV144 was not associated with viral neutralization or cytotoxic T cell responses; instead, immune correlates analyses revealed that protection correlated with non-neutralizing immunoglobulin G (IgG) antibodies binding to the HIV Env variable loops 1 and 2 (V1V2). Antibody-dependent cellular cytotoxicity (ADCC), an IgG-mediated fragment

crystallizable region (Fc)-effector function in which antibodies recruit effector cells to kill infected target cells, was also associated with a reduced risk of infection alongside polyfunctional Env-specific CD4+ T cell responses.

In contrast to RV144, the VAX003 trial, which tested only the AIDSVAX B/E bivalent recombinant gp120 protein with alum in seven doses, provided no protection from infection. Comparative analysis highlighted that while VAX003 induced total HIV-specific IgG levels, these antibodies were of a “less functional nature”[44]. The difference between VAX003 and RV144 highlighted that the quality and functional properties of vaccine-induced antibodies, rather than their sheer quantity, were critical for protection. Building on RV144, trials such as RV305, RV306, and RV328 explored strategies to enhance vaccine responses, particularly through booster shot components and timing[45–48]. The follow-on trials HVTN 097 and HVTN 100 adapted the RV144 regimen for various HIV-1 subtypes and demographics, but the subsequent HVTN 702 Uhambo efficacy trial could not replicate RV144's success, underscoring the challenge of achieving broad efficacy across diverse populations and viral strains[49–51].

1.2.3 Neutralizing and Fc-mediated Antibody Functions as Vaccine Goals

The findings from the RV144 trial, and subsequent analyses from other trials such as HVTN505 and HVTN705, emphasized the role of Fc-effector functions in protective immunity against HIV-1[52,53]. While HVTN505 and HVTN705 did not replicate RV144’s efficacy profile, follow-up analyses did show that Fc-effector functions correlated with protection in HVTN705 (Imbokodo study). These functions involve the Fc domain of antibodies engaging with Fc gamma receptors (FcγRs) on effector cells to recruit direct antiviral activity[42,54]. In addition to previously described mechanisms like ADCC, this also includes antibody-dependent cellular phagocytosis (ADCP). During ADCP, phagocytic cells such as macrophages and neutrophils internalize and degrade antibody-opsonized virions or immune complexes. The nature of these

interactions is modulated by IgG subclass, which exhibits differential affinities for Fc receptors and tightly modulates the type and strength of Fc-mediated effector functions.

Fc-mediated antibody functions and bNAb activity should not be viewed as mutually exclusive vaccine goals. Neutralization reflects fragment variable region (Fv)-mediated recognition of vulnerable Env epitopes and can directly block infection, whereas Fc-effector functions depend on the antibody Fc domain and can promote clearance of virions or infected cells after antibody binding. An ideal HIV-1 vaccine would likely coordinate both arms of antibody function: inducing antibodies with sufficient breadth and potency to neutralize diverse viruses while also promoting subclass, glycosylation, and Fc receptor engagement profiles capable of recruiting immune effector mechanisms. This distinction is important because a vaccine response may appear strong by one functional measure while remaining incomplete by another. It is important to evaluate HIV-1 vaccine responses not only by binding magnitude or neutralization breadth, but also the Fc-dependent activities that may contribute to protection.

While Fc-mediated functions offer one promising avenue for protection, bNAbs remain a major focus of HIV-1 vaccine research due to their potential to protect against diverse HIV-1 strains and have been identified as an experimental correlate of protection. The AMP trials, HVTN 703/HPTN 081 and HVTN 704/HPTN 085, tested passive immunization with the bNAb VRC01 in high-risk populations across sub-Saharan Africa and the Americas[55]. Despite not achieving overall efficacy, these trials provided insights: VRC01 was 75% effective against sensitive HIV-1 strains, validating the concept of bNAb-based prevention in humans for the first time. However, because only about 30% of circulating viruses were sensitive to VRC01, the results underscored the need for bNAbs with greater breadth and potency, or possibly a combination of antibodies targeting multiple HIV-1 epitopes. This emphasizes the high threshold required to achieve protection through neutralizing antibodies alone. Current vaccines have been unable to induce these antibodies in humans at levels comparable to those seen in natural infection. However, the natural development of bNAbs in some individuals provides a model for

vaccine strategies. Research efforts are focused on methods like creating SOSIP mimics of the HIV-1 Env protein to accurately represent its native structure[4,6,56], targeting germline B cell precursors[56–61], and applying lineage-based approaches to steer B cell evolution[62,63]. More recent human studies have provided important proof-of-concept for these strategies. The eOD-GT8 60-mer immunogen is a germline-targeting nanoparticle designed to activate rare VRC01-class precursor B cells[59,60]. Unlike earlier versions of recombinant gp120 or gp140 immunogens, which presented larger portions of Env and often elicited binding antibodies without broad neutralization, eOD-GT8 uses an engineered gp120 outer domain to focus recognition on the CD4 binding site and engage the inferred naive precursors of a specific bNAb class. This was successfully trialed in humans, activating VRC01-class precursor B cells, demonstrating that rare bNAb precursor populations can be targeted by vaccination[64]. Separately, lineage-based MPER immunization uses sequential immunogens focused on the membrane-proximal external region of gp41, rather than full gp120/gp140 Env, to guide B cell lineages through defined maturation steps. This approach has shown that vaccine-induced human B cell lineages can acquire heterologous HIV-1 neutralizing activity[65]. These techniques aim to replicate the natural immune response to HIV-1 through vaccination.

1.3 B Cell Maturation and Germinal Center Selection in Vaccine Responses

1.3.1 Germinal Center Maturation and Antibody Diversification

B cells are the primary mediators of protective immunity for most licensed human vaccines because they generate antibodies that provide both immediate defense and long-term immunological memory[66]. Understanding how B cells mature and interact with antigens is

central to rational vaccine design, particularly in the context of HIV-1, where generating broadly protective antibodies is a challenge.

As reviewed by Victora & Nussenzweig, B cells develop in the bone marrow and acquire diverse antigen receptors through V(D)J recombination[67]. After entering the peripheral lymphoid compartment, mature naive B cells can encounter cognate antigen in lymph nodes or the spleen. Productive activation requires both B cell receptor (BCR) engagement and additional signals from CD4+ T cells. After antigen binding, B cells internalize antigen through the BCR, process it, and present antigen-derived peptides on major histocompatibility complex class II (MHC-II)[68]. B cells that successfully engage cognate CD4+ T cells receive costimulatory and cytokine signals that support proliferation, survival, class-switch recombination, and entry into the germinal center (GC) reaction.

GCs are specialized structures that form within B cell follicles after infection or immunization. They provide the anatomical and cellular context for affinity maturation, a process in which antigen-specific B cell clones diversify and are selected based on improved antigen recognition. Within GCs, B cells undergo iterative rounds of proliferation, mutation, selection, and fate decisions. This process is spatially organized into dark and light zone phases. In the dark zone, GC B cells proliferate rapidly and undergo SHM of their immunoglobulin variable-region genes, generating related daughter cells with altered BCR sequences and potentially altered antigen affinity or specificity. These mutated cells then migrate to the light zone, where they compete for antigen and T cell help.

Selection in the light zone depends on both antigen capture and T follicular helper (Tfh) cell interactions. Antigen is retained on follicular dendritic cells (FDCs), allowing GC B cells to test their newly mutated BCRs through antigen binding. B cells with higher-affinity receptors generally acquire more antigen, present more peptide MHC-II, and receive stronger Tfh-derived survival and proliferation signals[69]. Tfh help is delivered through direct Tfh-B cell interactions, including T cell receptor engagement of peptide-MHC-II and costimulatory signaling, as well as

cytokines that influence GC maintenance, selection stringency, proliferation, class switching, and differentiation. Cells that receive sufficient help can reenter the dark zone for additional rounds of proliferation and SHM, while cells receiving differentiation cues can exit the GC as memory B cells, plasmablasts, or plasma cells. Cells that fail to compete effectively for antigen or Tfh help are progressively lost from the response (e.g., death-by-neglect).

In addition to affinity maturation, activated B cells undergo class-switch recombination (CSR), which changes the antibody constant region while preserving antigen specificity. CSR allows antigen-specific B cells to produce different antibody isotypes and subclasses with distinct effector properties, including differences in Fc receptor engagement. Although SHM and CSR are both initiated by activation-induced cytidine deaminase-dependent mechanisms, they are biologically separable. SHM continues during GC cycling as B cells diversify and undergo affinity-based selection, whereas recent work indicates that CSR is often initiated during early T cell-B cell interactions before full GC differentiation and then declines after B cells enter the GC[70]. These processes are shaped by Tfh-derived signals and cytokine environments that influence whether responding B cells continue cycling, switch isotype, or differentiate into memory or antibody-secreting compartments.

The GC response should be understood as a linked developmental process rather than a single maturation event. Antigen-engaged B cells must be recruited into the response, receive sufficient T cell help, expand clonally, diversify through SHM, compete for antigen and Tfh-derived selection signals, reenter additional rounds of mutation and selection, undergo appropriate class switching, and ultimately differentiate into memory or antibody-secreting cells. This framework is central to interpreting vaccine responses because a regimen may succeed at one stage, such as antigen-specific recruitment or clonal expansion, while failing at another, such as SHM accumulation, subclass programming, or functional antibody maturation. For HIV-1 vaccination, where protective humoral immunity may require both neutralizing and

Fc-mediated antibody functions, understanding how a vaccine regimen shapes each step of this process is essential for identifying where antibody development becomes limited.

1.3.2 Memory B Cells, Plasmablasts, and Vaccine Response Quality

The GC reaction also serves as a decision point for B cell fate. B cells that survive selection can remain in the GC for additional rounds of diversification, or they can differentiate along two major pathways: memory B cells (MBCs), which form a long-lived, antigen-specific reservoir capable of rapid reactivation upon re-exposure, and plasmablasts (PBs), short-lived antibody secreting cells that can further mature into long-lived plasma cells (PCs)[71]. These outcomes are not interchangeable: MBCs preserve the capacity for future adaptation, whereas PBs and PCs provide the circulating antibody that mediates immediate serum and mucosal protection.

These two pathways provide complementary layers of protection. PBs and PCs drive the immediate production of serum and mucosal antibodies, while MBCs preserve the capacity for recall and further evolution after re-exposure. Upon boosting or (re)infection, antigen-specific MBCs can rapidly proliferate, differentiate into antibody-secreting cells, or in some settings reenter GC reactions for additional rounds of SHM and selection. This recall capacity is relevant for sequential vaccination, where repeated antigen exposure may expand previously recruited lineages and further shape their affinity, specificity, subclass usage, and functional output.

Studies also suggest that memory and GC B cells differ in their affinity profiles. GC-resident cells tend to be enriched for high-affinity clones, whereas some memory B cells persist with lower-affinity receptors but remain important for diverse recall responses[71]. The balance between MBC and PB outputs is therefore another key determinant of vaccine efficacy, influenced by antigen presentation, adjuvant choice, immunization schedule, and antigen multimerization.

1.3.3 B Cell Maturation as a Barrier to HIV-1 Antibody Development

Effective GC maturation is especially important in HIV-1 vaccine development. Because of the virus's profound genetic diversity and sophisticated immune evasion mechanisms, protective antibodies must achieve exceptionally high levels of affinity and breadth. For bNAbs, affinity maturation is not only important for strengthening binding to one Env variant, but also for stabilizing interactions across related Env variants. Mutations acquired during B cell maturation can increase the number, strength, or structural complementarity of antibody contacts across a conserved epitope, allowing the antibody to retain binding and neutralizing activity even when some residues within the footprint vary among viral isolates. Broadly neutralizing antibodies typically require extensive SHM to acquire this breadth. For example, V3-glycan-directed bNAbs isolated from adult PLWH often accumulate between 6% and 29% SHM (averaging ~18%), a mutational burden far higher than what conventional vaccination protocols typically produce[24,72]. Furthermore, the inferred germline precursors of many bNAbs show little or no detectable binding to recombinant Env proteins, further underscoring the extraordinary degree of mutation required to develop these specificities and recognize the target antigen[10]. These factors collectively highlight a fundamental bottleneck in GC biology. The duration, stringency, and overall quality of the GC response, including the sustained availability of antigen over time, largely determine whether vaccine-elicited B cells can undergo the iterative rounds of selection needed to acquire the mutations required for efficacy[73].

1.4 Antigen Multimerization as a Vaccine Design Strategy

1.4.1 Antigen Valency and Repetitive Antigen Display

Antigen multimerization, which presents multiple copies of an antigenic epitope in a repetitive array, has emerged as a promising strategy to strengthen adaptive immunity[74,75]. This differs significantly from monomeric or soluble antigen presentation, where a single copy of the

antigen is displayed, often leading to weaker avidity and less potent immune responses[66,76,77]. Early vaccine successes, such as virus-like particles (VLPs) for hepatitis B virus and human papillomavirus, showed the advantages of multimerized antigen display, where multivalency was a key factor in their effectiveness[66,77].

1.4.2 Multimerized HIV-1 Env Immunogen Platforms

For HIV-1, initial attempts at protective immunity began with soluble gp120, which produced binding antibodies but weak neutralizing responses[21,78–80]. A significant advancement came with the development of stabilized Env trimers, such as SOSIP, which allowed more authentic display of key quaternary epitopes and better replication of the native viral spike[6,74,77,81]. However, accurate structural mimicry alone may be insufficient if vaccination does not also drive the B cell maturation needed for neutralizing activity. Because many bNAbs require extensive SHM and affinity maturation to recognize conserved Env epitopes across diverse viral isolates, one explanation for the limited success of Env immunogens is that they can recruit Env-binding B cells without sustaining the iterative selection required for those lineages to acquire broad neutralizing function. Stabilized trimers therefore remain central to HIV-1 vaccine design, but their success depends not only on antigen structure, but also on whether the vaccine regimen can guide recruited B cell lineages through productive maturation.

To further enhance immunogenicity, researchers developed nanoparticle and scaffolded Env platforms designed to array these trimers at high density[74,77]. Numerous approaches have been utilized to multimerize antigens including C4b-binding protein (5/7-meric)[82–84], ferritin nanoparticles (24-meric)[74,77], E2p and lumazine synthase (60-meric)[77], and liposomes (100+-meric)[74,85] to name several. Current research is actively moving these high-valency platforms into non-human primate (NHP) models and early human clinical trials to evaluate their capacity to overcome B cell maturation bottlenecks[3,86–88].

1.4.3 Effects of Multimerization on B Cell Recruitment and Maturation

Antigen multimerization strongly shapes B cell responses[66,74,76,77]. The repetitive structure of multimerized antigens promotes BCR cross-linking, which provides a stronger activating stimulus to cognate B cells. This multivalent binding can increase the avidity of antigen-BCR interactions, stabilize antigen capture at the B cell surface, and strengthen antigen-dependent signalling. This stronger activation is important because it promotes the early expression of transcription factors such as IRF4 and Bcl6, which drive both extrafollicular plasma cell responses and germinal center formation. Multimerization likely affects B cell responses through additional mechanisms as well, including how B cells internalize and present captured antigen to Tfh cells via the MHC-II complex, and how they receive T cell help. Multimerized antigens may also have altered drainage to lymph nodes, retention time on FDCs, and may modulate antigen interactions between B cells and FDCs. The combination of these effects may influence the survival of lower-affinity B cell clones, alter the founder population entering GCs, and further modulate downstream GC dynamics. Antigen multimerization may allow lower-affinity B cells to compete successfully alongside higher-affinity clones within GCs by overcoming strict affinity thresholds. This process increases GC recruitment and clonal diversity, with preclinical studies showing tens to hundreds of unique B cell clones per GC[67,89,90].

1.5 Rhesus Macaques as a Preclinical Model for HIV-1 Vaccine Research

1.5.1 Strengths of the Rhesus Macaque Model

Rhesus macaques (RMs) are widely used in HIV-1 vaccine research because of their close genetic similarity and conservation of immune cell populations with humans[91,92]. They share more than 93% overall sequence identity with humans, including high homology across

their immunoglobulin heavy (IGH), kappa (IGK), and lambda (IGL) V alleles. Importantly, RMs produce rearranged B cells by the exact same mechanisms as humans through V(D)J recombination, as opposed to smaller animal models that either use different methods of rearrangement (e.g., gene conversion) or have highly divergent subclasses and IgH/K/L variable genes. Importantly, RMs as a model can also be infected with a close relative of HIV-1, Simian Immunodeficiency Virus (SIV), and have similar infection kinetics and disease sequelae as HIV-1 infection in humans. SIV can also be made chimeric to express an HIV-1 Env in an SIV structural backbone, making it possible to directly test vaccination and protection challenge studies in vivo. This close evolutionary relationship enables RMs to serve as a surrogate for the human immune system in HIV-1 vaccine research.

1.5.2 Limitations for Interpreting Humoral Immunity and Fc Function

However, the RM model is not without its challenges, particularly when interpreting humoral immunity and Fc-mediated antibody function. A significant translational gap exists between preclinical animal research and human clinical outcomes due to fundamental differences in IgG subclass biology and FcγR expression profiles[44,92]. For example, the extended hinge region found in human IgG3, which may play a role in antigen recognition and effector function, is absent in RMs and other NHPs[93]. These differences may create a “blind spot” when interpreting Fc-mediated antibody function in NHP vaccine studies.

Furthermore, Vigdorovich et al. noted that while some convergence in B cell repertoires is observed after antigen exposure, certain genetic features, such as the human IGHV1-2*02 allele and 5-amino acid (AA) CDRL3s required for certain VRC01-class bNAbs, are less abundant or undetectable in RMs. These differences suggest that RMs may be limited in their ability to develop antibody lineages that depend on genetic features not encoded, or only rarely encoded, in their germline repertoires. These caveats underscore the need for cautious interpretation of data from RMs and a mindful appreciation of the species’ differences when

extending conclusions to human immunity, and that understanding the exact ways in which they differ from humans in a research context is a key effort to make the model more predictive.

1.6 Dissertation Aims and Contributions

1.6.1 Rationale for Studying 10014.F8.SOSIP Env-Induced B Cell Maturation

Despite intensive research efforts across disciplines since the early 1980s, HIV-1 remains a global health challenge. The development of a safe, effective, cost-efficient, and accessible preventative vaccine is a critical step to control and eventually end the epidemic. As reviewed by Ng'uni et al, prevention efforts have been repeatedly stymied due to factors including formidable viral diversity, immune evasion, gaps in understanding of protective immune correlates, and the persistent inability of past vaccine candidates to translate promising preclinical results into durable human efficacy[21]. The limited successes along the way, including RV144, underscore the need to define how vaccine parameters influence B cell maturation, SHM, and the selection of appropriate antibody subclasses to optimize both neutralizing (Fv-related) and non-neutralizing (Fc-mediated) humoral immunity. Defining how a specific vaccine regimen shapes each of these steps is essential for iterative vaccine design, because different immunogen formats, adjuvants, and dosing schedules may need to be optimized for different stages of the B cell response. Despite evidence that antigen multimerization can enhance B cell activation and GC recruitment, its impact on B cell fate decisions and clonal dynamics in NHPs and humans remains poorly understood[66].

One approach the HIV-1 research field is pursuing is studying Env variants circulating in human subjects who naturally developed bNAbs. The rationale is that these are the envelopes that helped drive bNAb development, and they may have features that intrinsically make them predisposed to elicit antibodies with bNAb properties. Identifying and utilizing Env variants that

emerged during critical periods of natural antibody maturation might shortcut the pathway to vaccine-derived protective immunity[94].

The 10014.F8.SOSIP Envelope immunogen evaluated in this dissertation originates from HIV-1 *env* gene sequences cloned from subject VC10014, a clade B-infected individual who developed bNAb activity approximately one to three years post-infection[1,10]. A key observation in VC10014 was that the appearance of bNAbs coincided with a marked stepwise increase in plasma IgG anti-Env binding affinity, suggesting that active, affinity-driven antibody maturation was a critical element driving the development of neutralization breadth[10]. While 10014.F8-derived immunogens have shown promise in eliciting tier 2-like autologous neutralization and Env-specific T follicular helper cell activation in rhesus macaques[94], their precise impact on global B cell fate decisions, repertoire-level SHM, and lineage maturation remains unknown.

To evaluate these developmental mechanisms, the initial focus of this dissertation (Chapter 2) is two-fold. First, we explore the baseline *in vivo* immunogenicity of the 10014.F8 vaccine when presented as a stabilized, native-like SOSIP trimer. Because earlier iterations of 10014.F8-derived immunogens demonstrated significant promise in prior studies, we sought to determine whether this specific trimer format successfully drives the extensive clonal expansion and deep SHM required for functional maturation[1,10,94–100]. Second, to evaluate this biological response at an unprecedented depth and scale in NHPs, Chapter 2 focuses on increasing the throughput of B cell receptor sequence analysis. We apply a repertoire mining approach ("Hinge-Seq") that pairs deep bulk IgG MBC BCR IgH next-generation sequencing (NGS) with single-cell-derived, characterized, expressed monoclonal antibodies (mAbs). This methodology allows us to directly assign massive volumes of bulk IgG MBC BCR IgH sequences to functionally validated mAbs, fleshing out the evolutionary lineages of antigen-specific B cells and linking sequence features encoded in the B cell receptor with functional outcomes.

Building upon this baseline, Chapter 3 addresses whether the functional and maturation limits observed after soluble native-like trimer immunization could be improved by increasing antigen valency. Despite evidence that antigen multimerization can enhance early B cell activation, GC recruitment, and the survival of lower-affinity clones, its comparative impact on long-term B cell fate decisions and clonal dynamics *in vivo* during vaccination remains poorly understood[66,71,89,101]. Therefore, we extend our functional repertoire analysis across a multimerization cohort, immunizing RMs with the HIV-1 10014.F8.SOSIP Env presented with increasing multivalency: soluble SOSIP trimer (monomeric trimer), ferritin nanoparticles (8-copy trimer), and liposomal display (100+-copy trimer).

The primary goal of this research is to define how these specific vaccine parameters, the 10014.F8.SOSIP immunogen and its multivalent presentation formats, shape the clonal diversity, subclass selection, and maturation characteristics of the B cell repertoire and define the functional fate of the antibodies that make up the circulating antibody response.

Chapter 2. Deep repertoire profiling reveals a somatic hypermutation ceiling in HIV-1 vaccine-elicited B cell lineages

This chapter is adapted from a manuscript submitted to *npj Vaccines*.

Herring, S[a]; Raappana, A[b,#]; Vigdorovich, V[b]; Dambrauskas, N[b,#]; Glad, M[b]; Pandey, S[c]; Hessell, A[c,d]; Sather, DN[b,e,#].

[a]Department of Global Health, University of Washington, Seattle WA USA
[b]Seattle Children's Research Institute, Seattle WA USA
[c]Oregon National Primate Research Center, Beaverton OR USA
[d]Oregon Health and Science University, Portland OR USA
[e]Department of Pediatrics, University of Washington, Seattle WA USA
[#]Current address: Center for Global Health and Interdisciplinary Research, University of South Florida, Tampa FL USA

Corresponding Author: dnsather@usf.edu

2.1 Abstract

Eliciting antibodies with broad antiviral activity remains a central challenge for HIV-1 vaccine development, in part because protective broadly neutralizing antibodies require extensive and sustained B cell maturation. Here, we evaluated the humoral and B cell repertoire response elicited by soluble HIV-1 10014.F8.SOSIP Env trimer immunization in rhesus macaques. Vaccination induced strong Env-specific plasma IgG binding titers, increasing avidity, and Fc-mediated effector activity, including ADCP and ADCC. However, neutralizing activity remained limited, with weak autologous neutralization and narrow heterologous activity across Tier 1 and Tier 2 pseudovirus panels. To define the B cell features underlying this functional limitation, we paired single-cell V(D)J sequencing and monoclonal antibody validation with deep

bulk IgG memory B cell repertoire profiling using Hinge-Seq, enabling functional anchoring of Env-specific lineages within the broader repertoire. Fifteen Env-binding monoclonal antibodies were recovered, spanning diverse genetic rearrangements and epitope specificities, but most displayed weak or absent antiviral function. Repertoire analysis showed that vaccine-specific lineages underwent clonal expansion and class-switch recombination, indicating successful recruitment into antigen-experienced IgG memory pathways. However, these lineages accumulated lower somatic hypermutation than non-Env-binding comparator lineages and remained concentrated in intermediate mutation states. These findings indicate that soluble 10014.F8.SOSIP trimer vaccination can recruit and expand Env-specific B cells but fails to sustain the degree of maturation required for potent antiviral antibody function. Functional anchoring of B cell repertoires may therefore help identify specific maturation bottlenecks limiting HIV-1 Env vaccine efficacy.

2.2 Introduction and Rationale

Eliciting protective broadly neutralizing antibodies (bNAbs) against HIV-1 remains a central objective of HIV-1 vaccine development[102–105]. However, generating these protective responses requires recruiting specific, rare B cell precursors and guiding them through extensive, iterative, and sustained germinal center (GC) reactions[60,67,106]. A major biological hurdle in this developmental pathway is the need to acquire the specific antibody sequence features required for breadth, which often includes extensive SHM but can also involve rare structural features such as long CDRH3 loops or particular germline-encoded contacts. Within the GC, B cells must undergo rigorous cycles of proliferation, mutation, and selection. Unlike typical vaccine-induced antibodies that achieve efficacy with modest affinity maturation[107,108], prototypical anti-HIV-1 bNAbs isolated from natural chronic infections are highly evolved[106]. They frequently exhibit unusually high levels of SHM, often reaching 15–30% sequence

divergence from their unmutated common ancestors[26,109,110]. This extensive maturation is necessary to accommodate immense viral diversity and navigate the dense, shifting Env glycan shield to access highly conserved, occluded epitopes[111–113]. Achieving this level of breadth and potency often necessitates complex, improbable genetic adaptations, including exceptionally long heavy-chain third complementarity-determining regions (CDRH3) or rare framework insertions and deletions[106,109,114–116].

While current-generation SOSIP native-like Env trimer immunogens represent a major breakthrough, they face distinct immunological barriers *in vivo*[6,104]. These immunogens effectively engage B cells and induce robust, class-switched IgG titers, confirming successful initial antigen recognition and GC entry[117–119]. Yet, they consistently fail to drive the deep, prolonged affinity maturation required to reproduce the evolutionary trajectories of natural bNAbs. Instead of focusing selective pressure on subdominant, broadly neutralizing epitopes, the immune response is often distracted by the immunodominance of highly accessible, strain-specific sites, such as variable loops, glycan holes, or the artificial trimer base[120–123]. As a result, current prime-boost regimens typically stall in intermediate maturation states[65,124]. Even when they succeed in eliciting robust autologous tier 2 NAb titers, they ultimately yield antibodies with narrow autologous neutralization or some degree of weak breadth. Although germline-targeting immunogens are able to more selectively stimulate bNAb progenitors, they currently face similar maturation ceilings[64,124,125].

Developing novel vaccine approaches that overcome these barriers requires the accurate diagnosis of specific bottlenecks in B cell maturation. While traditional serological readouts can confirm antigen engagement, neutralization, and Fc-mediated effector functions, such as antibody dependent cellular phagocytosis and antibody dependent cytotoxicity, they only reflect the aggregate, polyclonal end-products of the immune response. They lack the cellular resolution required to identify the precise immunological mechanisms or failure points occurring within the B cell compartment itself. It is critical to define features encoded within the B

cell repertoire that implicate specific maturation checkpoints, such as an initial failure to activate the correct precursors, a defect in class-switch recombination, or an inability to sustain the GC selective pressures required for deep SHM. Doing so requires capturing a broad sampling of diverse Env-specific lineages and obtaining sufficient, high-resolution B cell receptor (BCR) repertoire data to reconstruct their evolutionary histories, clonal diversity, and mutational trajectories.

To define potential maturation bottlenecks during Env SOSIP vaccination, we developed a novel approach that couples deep IgG memory B cell receptor IgH repertoires combined with single cell sequencing and functional anchoring, allowing the direct linkage of sequence features with functional outcomes. We analyzed a cohort of rhesus macaques immunized with the HIV-1 10014.F8.SOSIP trimer in a prime and three-boost immunization regimen (Fig. 1a). This immunogen was derived from a clade B-infected subject that developed bNAbs within the first three years of infection and has been evaluated in previous generation antigen formats[10,94,95]. To overcome the limitations of standard short-read sequencing, we developed Hinge-Seq, a dual-amplicon sequencing pipeline that directly links theFv and Fc regions of the immunoglobulin heavy chain with exceptional depth (detailed in Fig. 2a). In concert, we isolated 15 unique, experimentally validated monoclonal antibodies (mAbs) against Env that target diverse epitopes and possess unique genetic rearrangements, alongside a comparator group of non-Env-specific mAbs. By mapping these mAbs back to the repertoires obtained through deep IgG MBC BCR IgH profiling using HingeSeq, we were able to retrieve related sequences, construct large clonal families with diverse attributes, and ultimately reconstruct the maturation history of extensive Env-specific lineages.

Our functionally-anchored profiling revealed that the 10014.F8.SOSIP vaccine successfully recruited B cells into GC pathways. Vaccine-specific lineages readily proliferated and underwent class-switch recombination, distributing across multiple IgG subclasses (predominantly IgG1 and IgG2) at frequencies similar to non-binding lineages, demonstrating

that class-switching is not a restrictive bottleneck. Instead, we identified a distinct commonality within Env-specific lineages that implicated truncated B cell maturation processes. Despite robust clonal expansion, the anti-Env mAbs and their associated vaccine-specific clonal variants hit a distinct maturation barrier, remaining clustered within intermediate SHM niches and exhibiting significantly lower absolute SHM compared to the heavily diversified, non-specific compartments of the IgG MBC BCR IgH repertoire. This truncated maturation provides a mechanistic explanation for why vaccination generated high binding titers and measurable Fc-effector functions but failed to achieve potent antiviral neutralization. Ultimately, these findings underscore that robust clonal diversification is not a sufficient indicator of burgeoning vaccine efficacy, and highlights the need for vaccine strategies that overcome this specific SHM bottleneck to sustain prolonged germinal center evolution.

2.3 Results

2.3.1 Serum Responses Reflect Strong Antigen Engagement but Limited Functional Maturation and Breadth

Six female rhesus macaques aged 7-11.9 years (Table 1) were immunized with recombinant SOSIP trimer Envelope, 10014.F8.SOSIP according to the schedule shown in Fig. 1a. This Env protein was derived from the circulating *env* sequences in subject 10014 at the time that they developed broadly neutralizing activity, around three years post infection[10], and has been tested previously as fused gp140 trimers in rabbits and NHPs[94,95]. The SOSIP version of 10014.F8 was constructed by grafting the BG505 gp41 region to the 10014.F8 gp120, and by introducing stabilizing mutations known to increase stability and protein production yields[4,6,126]. After production, the presence of native-like trimer was confirmed by assessing binding of the trimer-specific antibody PGT151 by Bio-Layer Interferometry (Supplemental Fig. 1). Vaccines were formulated with 50 μg recombinant 10014.F8.SOSIP and 20% Adjuplex adjuvant, and

animals were immunized a total of four times at weeks 0, 4, 10, and 20 (Fig. 1a). Animals were also simultaneously administered DNA plasmid encoding 10014.08.SOSIP via gene gun to the abdomen as previously described[94]. Longitudinal sampling was performed according to Fig. 1a. To define the humoral response elicited by 10014.F8.SOSIP immunization, we evaluated longitudinal plasma antibody binding titers over the course of the immunization schedule, and evaluated avidity indices, neutralization, and Fc-mediated effector activity (antibody dependent cellular cytotoxicity and antibody dependent cellular phagocytosis) at week 22, or 2 weeks post final immunization (Fig. 1). Across animals, 10014.F8.SOSIP immunization elicited high titer Env-specific serum responses, indicating antigen engagement.

All animals were responsive to vaccination, and IgG endpoint binding titers to the autologous Env, 10014.F8.SOSIP, increased progressively over the course of immunization and peaked at an endpoint titer of approximately 3.1×10^5 following the third protein boost (fourth total vaccination) at week 20 (Fig. 1b). To assess whether these responses also showed evidence of qualitative maturation, we measured serum antibody avidity two weeks post each immunization using ammonium thiocyanate displacement ELISA (Fig. 1c) to determine an avidity index, which provides a surrogate readout of B cell maturation[127,128]. 10014.F8.SOSIP immunization induced a progressive increase in avidity from week 2 to week 12, indicating that repeated antigen exposure promoted measurable maturation of the Env-specific serum antibody response. In contrast, the increase from week 12 to week 22 was not significant, indicating that the final boost produced little additional improvement in apparent avidity. This plateau suggests that, although 10014.F8.SOSIP vaccination successfully initiated and amplified affinity-matured antibody responses, the serum response reached a maturation ceiling after repeated boosting.

Antiviral functions mediated by interactions of the Fc region of IgG with Fc gamma receptors (FcγRs) are associated with reduced acquisition risk in human clinical trials and may be important components of a protective vaccine response[40,129–131], and thus, we evaluated the ability of vaccine-elicited antibodies to mediate ADCC and ADCP. ADCP activity was evaluated

by measuring phagocytosis of 10014.F8 gp120 coated neutravidin beads into THP-1 macrophage cells by flow cytometry[3]. All animals vaccinated with 10014.F8.SOSIP exhibited potent ADCP compared to pre-immune controls (Fig. 1d). ADCC was evaluated in a luciferase based assay using 10014.F8 infectious virion-infected MT4 cells[12] as the target cells and CD16-expressing KHYG-1 cells as the effector. All animals developed ADCC activity against the autologous virus at week 22, compared to paired pre-immune control samples (Fig. 1e). Thus, vaccination with 10014.F8.SOSIP elicited antibodies capable of mediating Fc-dependent antiviral functions.

We evaluated antibody neutralization against the autologous virus, and a Tier 1 and Tier 2 panel of heterologous HIV-1 isolates in the TZM-bl assay[132–134]. Week 22 plasma showed detectable but weak neutralizing activity against 10014.F8 pseudovirus, which exhibits a Tier 2 neutralization phenotype[10,94,135], with 4 of 6 rhesus macaques exceeding 50% neutralization at a 1:10 plasma dilution (Fig. 1f). We evaluated heterologous neutralization at a 1:50 plasma dilution against a panel of Tier 1 isolates from clades, A, B, and C (Fig. 1g), with significant neutralization evident against only SF162.LS, a highly neutralization-sensitive clade B *env*, whereas responses to the remaining Tier 1 viruses were weak or inconsistent. We also evaluated neutralization at a 1:50 plasma dilution against the Tier 2 Global Reference panel [136], a collection of Tier 2 viruses from clades, A, B, C, and G, as well as the recombinant forms CRF01_AE, CRF07_BC, and AC, assembled to represent global diversity (Fig. 1h). Serum from all RMs neutralized the clade A *env* 398F1, but exhibited weak neutralization against all other viruses in the panel. Thus, although serum antibodies elicited by 10014.F8.SOSIP exhibited Tier 2 autologous and sporadic Tier 1/Tier 2 heterologous neutralizing activity, overall neutralizing antibody responses were low potency and relatively narrow in activity.

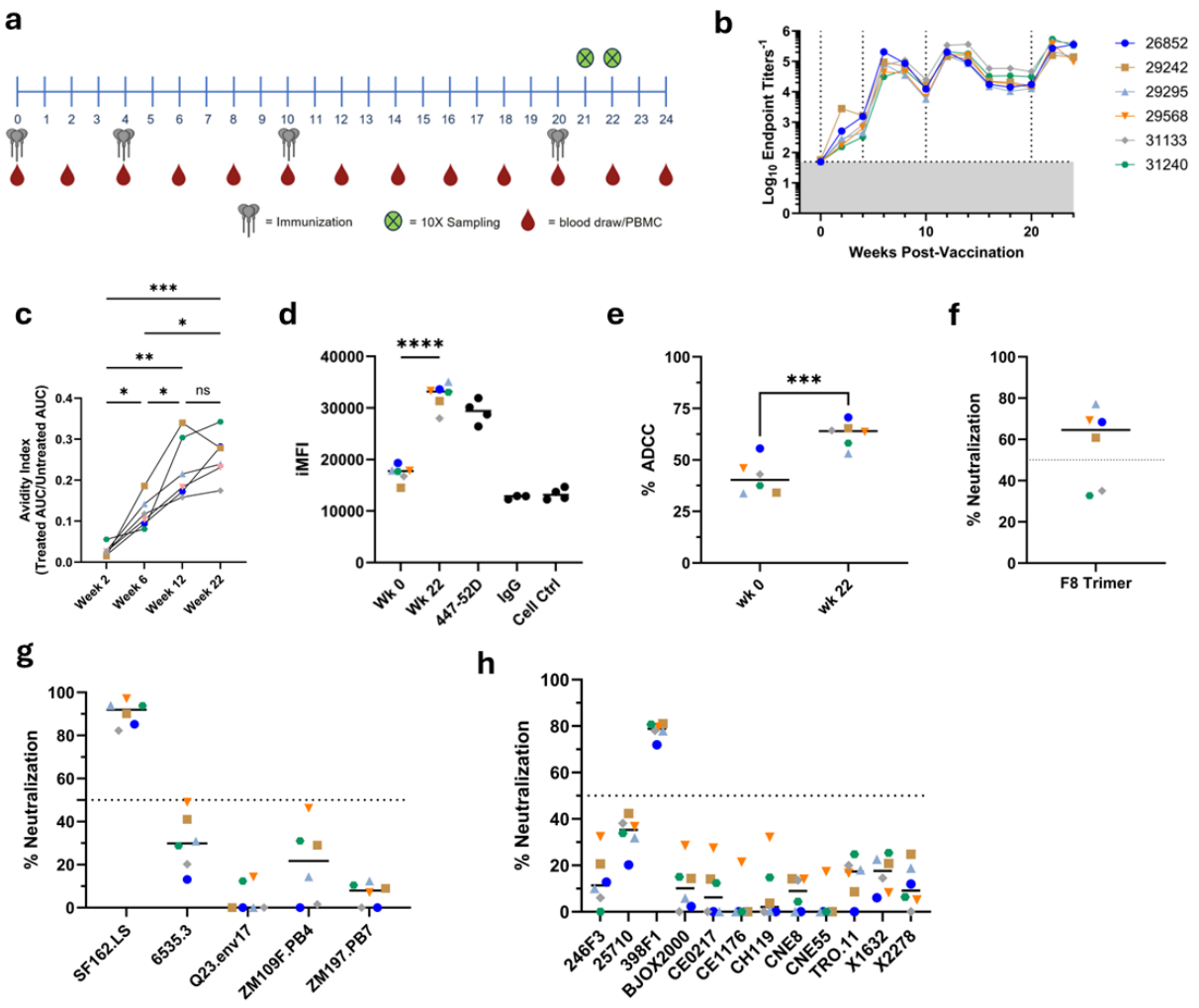

Figure 1. 10014.F8.SOSIP trimer immunization elicited Env-binding plasma antibodies with increasing avidity and measurable Fc-mediated function but limited neutralization breadth.

a, Immunization and sampling schedule for six female rhesus macaques immunized with HIV-1 10014.F8.SOSIP trimer. Animals received immunizations at weeks 0, 4, 10, and 20, with longitudinal blood draws for plasma and PBMC collection. Bulk and/or single-cell sequencing was performed after the final immunization. **b,** Longitudinal autologous Env-binding IgG endpoint titers measured by ELISA against 10014.F8.SOSIP. Endpoint titers are shown as log10 reciprocal plasma dilution values for each animal across the immunization time course. The shaded region indicates values below the assay detection threshold. **c,** Plasma antibody avidity

measured by ammonium thiocyanate displacement ELISA two weeks after each immunization, at weeks 2, 6, 12, and 22. Avidity index was calculated as the ratio of the area under the binding curve after NH_4SCN treatment to the corresponding PBS-treated control. Time points were compared using repeated-measures one-way ANOVA with Geisser-Greenhouse correction followed by Tukey's multiple-comparisons test; overall $p < 0.0001$. Adjusted p values were: week 2 vs week 6, $p = 0.0192$; week 2 vs week 12, $p = 0.0040$; week 2 vs week 22, $p = 0.0004$; week 6 vs week 12, $p = 0.0395$; week 6 vs week 22, $p = 0.0237$; week 12 vs week 22, $p = 0.6055$. **d,** Antibody-dependent cellular phagocytosis measured using fluorescent antigen-coated beads and THP-1 monocytes. Phagocytic activity is reported as integrated mean fluorescence intensity. Week 0 and week 22 values were compared using a two-sided paired t test; $p < 0.0001$. **e,** Antibody-dependent cellular cytotoxicity measured using infected MT4-CCR5-Luc target cells and KHYG-1 effector cells, with plasma tested at a 1:50 dilution. Week 0 and week 22 values were compared using a two-sided paired t test; $p = 0.0003$. **f,** Autologous neutralization activity against 10014.F8 pseudovirus measured using plasma tested at a 1:10 dilution. **g,** Plasma neutralization activity against Tier 1 pseudoviruses measured at a 1:50 dilution. **h,** Plasma neutralization activity against a multi-clade Tier 2/global pseudovirus panel measured at a 1:50 dilution. Dotted horizontal lines indicate the 50% neutralization threshold. Each point represents an individual animal; horizontal bars indicate group medians.

Vaccine	Animal ID	Age (yrs)	Sex
10014.F8.SOSIP Trimer	26852	11.9	Female
	29242	9.0	Female
	29295	9.0	Female
	29568	9.0	Female
	31133	7.0	Female
	31240	7.0	Female

Table 1. Soluble 10014.F8.SOSIP trimer cohort animal identifiers.

Animals are listed by vaccine group, animal ID, age, and sex. The cohort included six female rhesus macaques immunized with soluble 10014.F8.SOSIP trimer. All animals underwent bulk memory B cell immunoglobulin G heavy-chain RNA sequencing by Hinge-Seq. Underlined animal IDs indicate animals that also underwent 10x Genomics single-cell V(D)J sequencing.

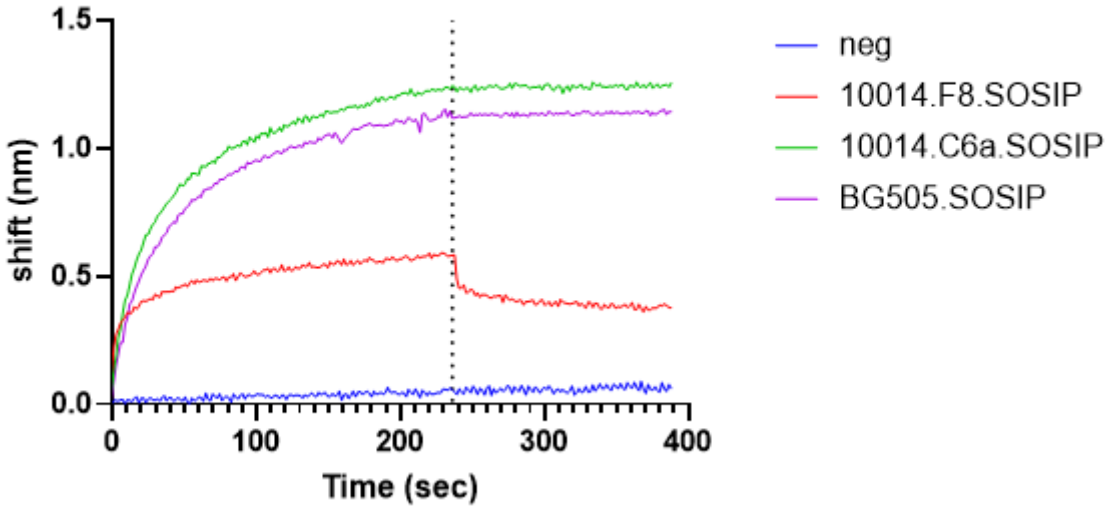

Supplemental Figure 1. Validation of SOSIP Envelopes via Bio-Layer Interferometry analysis of PGT151 binding.

Bio-Layer Interferometry (BLI) was used to assess binding of the trimer-specific monoclonal antibody PGT151 to recombinant 10014.F8.SOSIP, 10014.C6a.SOSIP, and BG505.SOSIP Env proteins. Sensorgrams show the binding response over time for each antigen, with the negative control shown in blue. The dotted vertical line indicates the transition from the association phase to the dissociation phase. PGT151 bound all three SOSIP trimers above background, consistent with preservation of native-like trimer conformation.

2.3.2 Functional Validation Identifies Env-specific and Non-Env-binding Lineages in the Bulk Repertoire

Serological analyses revealed robust generation of vaccine-elicited IgG with Fc-mediated effector function but limited neutralization. However, serological readouts don't directly link serum antibody features to the underlying immunological processes that shape the B cell response during vaccination, limiting our ability to diagnose the mechanisms underlying vaccine hypo-efficacy. We hypothesized that the Env-specific BCR repertoire contains quantifiable sequence imprints of GC processes, and that identifying those features would enable the implication of specific immunological processes underlying vaccine hypo-efficacy. Understanding these mechanisms is key to enabling the development of strategies to overcome these limitations, but it requires deep profiling of Env-specific B cell lineages elicited by vaccination. To do so, we developed a hybrid next generation sequencing approach that employed Env-specific sorting and 10x Genomics single-cell sequencing to identify Env-specific lineages coupled with deep 5'RACE profiling of the IgG MBC BCR IgH cell repertoire to enable compilation of Env-specific clonal lineages.

To deeply profile the IgG+ memory B cell repertoire inclusive of IgG subclass usage, we developed a dual amplicon Illumina-based sequencing approach covering the variable and

constant regions of IgG, which enabled the high fidelity reconstruction variable Fv and IgG subclass constant region Fc repertoires (Fig. 2a). The Fv and Fc amplicons were amplified separately because short-read sequencing could not reliably span both regions in a single contiguous read. 5'RACE unique molecular identifier (UMI)-encoded libraries were generated using a universal forward primer and primers specific to the C1 and C3 regions of the IgG Fc, which ensured that two amplicon sequences from the same cDNA molecule had identical UMIs. The Fv and Fc amplicons were sequenced separately on a MiSeq 600 cycle kit. Long composite sequences were reconstructed by creating contigs from identical UMIs. Reads were quality filtered, collapsed into consensus sequences based on UMI grouping to define unique template molecules, and annotated using IgBLAST[137] against a rhesus macaque immunoglobulin reference database. Productive IgH sequences were retained for downstream clonal analysis. IgG MBC BCR IgH repertoires were clustered into clonal families using SCOPer[14,15], grouping sequences by shared V and J gene family usage and CDRH3 length, followed by hierarchical clustering based on length-normalized nucleotide distances within the CDRH3 region. Clonal thresholds were determined using nearest-neighbor distance distributions implemented in *Alakazam* to distinguish intra-clonal from inter-clonal relationships[14].

This method enabled us to identify the repertoire of IgG subclasses (IgG1, 2, 3 and 4) expressed by a given B cell lineage, directly sampling the degree of class switch the clone had undergone during maturation. This procedure was carried out on all six rhesus macaques, and after processing and annotation we quantified IgHV family usage. The animals expressed repertoires dominated by IgHV4 (Fig. 2b, 2c) family segments, in line with recent studies profiling the rhesus macaque memory B cell repertoire[86,92,138–140]. The animals expressed comparable distributed ranges of CDRH3 lengths, in agreement with previous reports (Fig. 2d). Overall, the animals contained B cell repertoires with expected sequence features, supporting the conclusion that these data represented a reasonable sampling of the memory IgG compartment.

To identify Env-specific B cell lineages, we applied a functional anchoring approach linking mAb specificity to its IgG MBC BCR IgH repertoire (Fig. 2a). B cells from three immunized macaques were cultured in activation media, and CD3-, CD20+, IgG+, Ag+, Decoy- cells were sorted using tetramerized 10014.F8 gp120 as bait (Supplemental Fig. 2). Matched heavy (H) and light (L) chain pairs were recovered from sorted cells by 10x Genomics 5'RACE VDJ enrichment protocols using custom NHP-specific primers. 48 H+L pairs were expressed as recombinant antibodies. 15 antibodies (Table 2) bound Env SOSIP or gp120 by ELISA (Supplemental Fig. 3) and by Bio-Layer Interferometry (Supplemental Fig. 4) . The remainder were classified as non-Env-binding BCRs, and were retained as a comparator set in subsequent analyses to represent the features of the "average" member of the memory B cell compartment (Table 3).

To reconstruct clonal lineages, mAb-derived heavy chain sequences from the single-cell workflow were incorporated directly into the bulk IgG MBC BCR IgH datasets prior to clonal inference. Clonal families were then inferred jointly using SCOPer, grouping all sequences into clusters[14,15]. Following clustering, clonal families containing at least one sequence corresponding to an Env-specific mAb were classified as vaccine-specific lineages, whereas clonal families containing only sequences from non-Env-binding antibodies were classified as non-binding lineages. Clonal families without associated mAb sequences were designated as IgG MBC-only clusters. Two Env-specific antibody pairs, ab22/B4_84 and ab26/B4_40, were inferred to be clonally related by SCOPer clustering, indicating that these independently recovered antibodies likely represent members of the same vaccine-engaged B cell lineage.

After antigen specificity was assigned at the clonal level, we compared repertoire features between Env-specific and non-Env-binding antibody-anchored clusters. IgHV4 remained the dominant V family among both Env-specific and non-Env-binding clusters (Fig. 2c), indicating that vaccine-specific lineages were not distinguished by unusual V-family usage. In contrast, Env-specific clusters were generally shifted toward shorter CDRH3 lengths, with a

few extended CDRH3 outliers, compared with non-Env-binding clusters (Fig. 2e), indicating that 10014.F8.SOSIP-specific lineage recruitment did not preferentially or exclusively enrich for long-CDRH3 antibodies. This framework enabled direct comparison of the features of vaccine-engaged and non-binding lineages within the same B cell repertoires. With antigen specificity assigned at the clonal level, we next analyzed the biophysical and functional characteristics of the 15 vaccine-specific lineages.

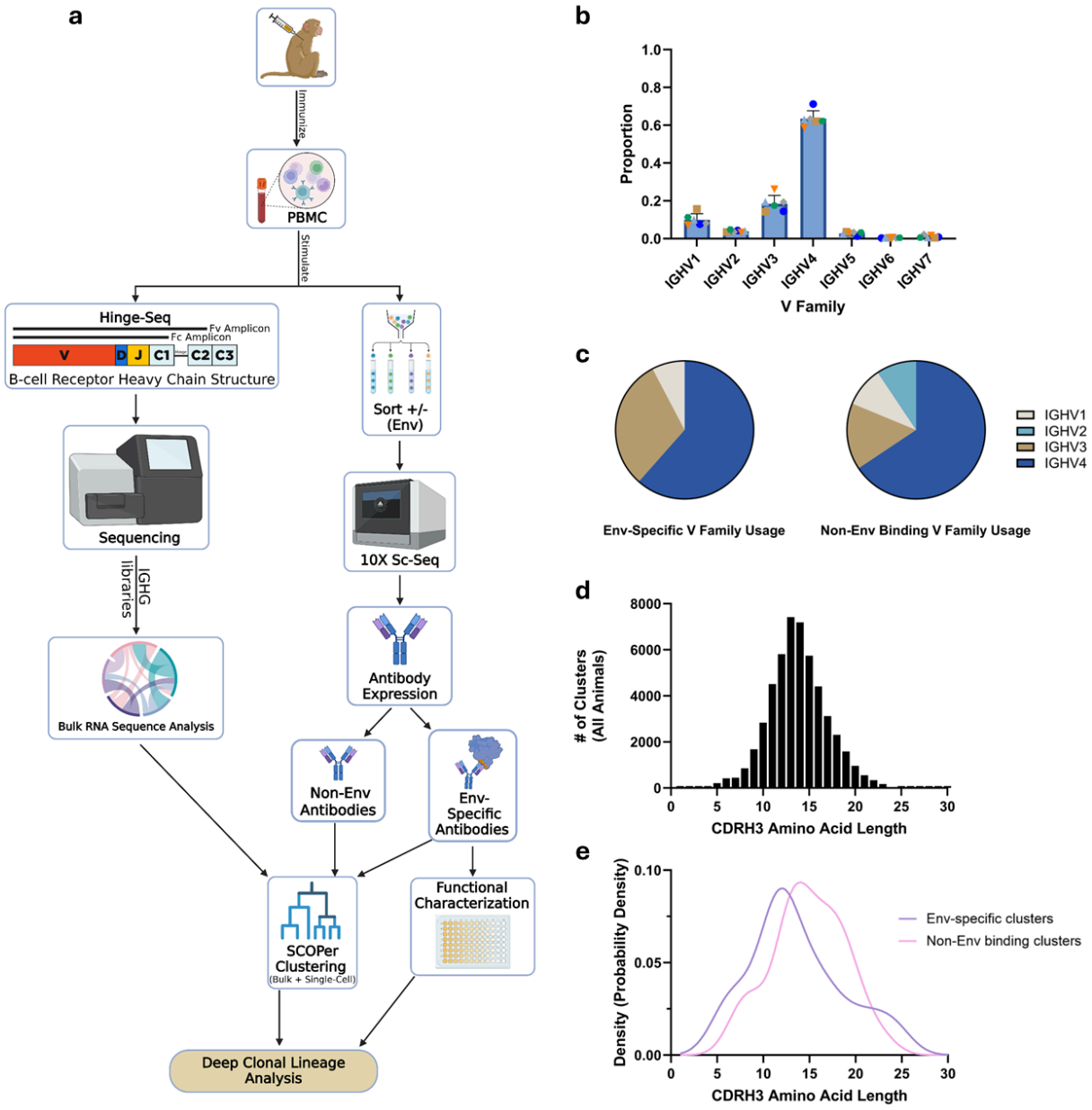

Figure 2. Functional anchoring links single-cell antibody specificity to bulk IGH repertoire lineages.

a, Workflow for integrating Hinge-Seq bulk IGH sequencing with single-cell antibody recovery. PBMCs were processed for bulk IGH repertoire analysis and antigen-specific single-cell sorting. Recovered monoclonal antibody sequences were expressed, functionally characterized, and used to anchor vaccine-specific or non-Env-binding clonal lineages within the bulk repertoire. **b,**

Bulk IGH V family usage across immunized animals. SCOPer clustering was performed on bulk libraries, and each cluster was treated as one unit contributing a V family assignment within each animal. Points show animal-level proportions. **c,** V family usage among vaccine-specific and non-Env-binding anchored clusters. Pie charts show the proportion of antibody-anchored clusters assigned to each IGH V family, allowing comparison of V family composition between Env-binding and non-Env-binding lineages identified through functional anchoring. **d,** CDRH3 amino acid length distribution across bulk IGH clonal clusters from all animals. **e,** Kernel density distributions of CDRH3 amino acid lengths among vaccine-specific and non-Env-binding anchored clusters. Density curves are normalized to equal area, so curve height reflects relative probability density rather than cluster count. Purple indicates vaccine-specific clusters; pink indicates non-Env-binding clusters.

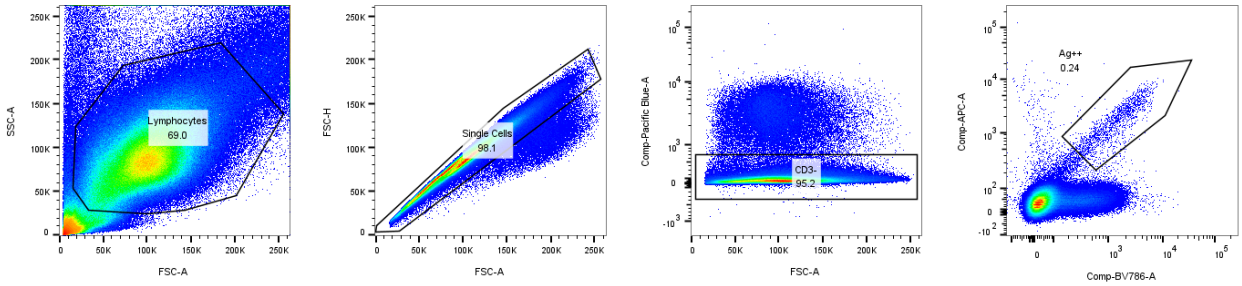

Supplemental Figure 2. Representative gating strategy for sorting 10014.F8.SOSIP Env-specific memory B cells.

Day 7 stimulated rhesus macaque memory B cells were sorted to recover antigen-positive cells for downstream single-cell V(D)J sequencing. Cells were first gated on the lymphocyte population by forward and side scatter, followed by singlet selection using FSC-A and FSC-H. T cells were excluded by gating on CD3-negative cells, and antigen-positive B cells were identified as double-positive for tetramerized 10014.F8 gp120 probes labeled with APC and

BV786. The final sorted population consisted of CD3− antigen double-positive cells, which were collected into FBS and processed for 10x Genomics 5′ V(D)J sequencing.

mAb	V gene	J gene	CDRH3 amino acid	% VH identity	Animal
ab21	IGHV1-Korf4	IGHJ5-I1	TRSTIFGLIDV	94.898	29568
ab22	IGHV4-S57	IGHJ4-I1	AGLANS	83.000	26852
ab24	IGHV4-S22	IGHJ5-I1	GREERLIWSL	88.776	26852
ab25	IGHV3-S33	IGHJ5-I2*02	TRSGAVYNSLDV	93.537	26852
ab26	IGHV4-Korf2	IGHJ4-I1	VRDTLFGLGILI	93.266	29568
B4_1	IGHV3-Korf2	IGHJ5-I1	TRDSTGLADGNWFDV	93.515	26852
B4_16	IGHV3-Korf9	IGHJ4-I1	ARTDCDH	93.836	26852
B4_31	IGHV4-K7	IGHJ5-I1	AGEWGITKMVTVTTTARWSNV	92.857	Undetermined
B4_39	IGHV4-K7	IGHJ6-I1	AATPPVVVSPSMISNIDSFYGFDS	93.878	26852
B4_40	IGHV4-Korf2	IGHJ4-I1	ARDTLFGLGILI	95.623	29568
B4_42	IGHV4-Korf2	IGHJ4-I1	ARDTSDYLAFDY	92.929	31240
B4_50	IGHV3-Korf9	IGHJ4-I1	AKGSSGWYVGIDY	95.862	Undetermined
B4_68	IGHV4-S38	IGHJ5-I1	MSRGVTRTDVMFPFDV	94.502	29568
B4_78	IGHV4-S40	IGHJ5-I2*02	ARDHEYNFWRGFYTSLDV	92.593	Undetermined
B4_84	IGHV4-S57	IGHJ4-I1	AGFANS	83.221	26852

Table 2. Sequence features of recovered 10014.F8.SOSIP-binding monoclonal antibodies.

Recovered Env-binding monoclonal antibodies are listed with inferred IGH V gene assignment, IGH J gene assignment, CDRH3 amino acid sequence, percent VH identity, and assigned animal of origin. Percent VH identity was calculated relative to the inferred germline V gene sequence. Animal assignment was inferred by matching monoclonal antibody heavy-chain sequences to associated bulk IGH clonal lineages. Because single-cell samples were pooled in a three-animal group, antibodies were listed as undetermined when no associated bulk sequences passed post-filtering stringency thresholds within the matched cluster; in these cases, the clone could not be assigned to one specific animal within the pooled set.

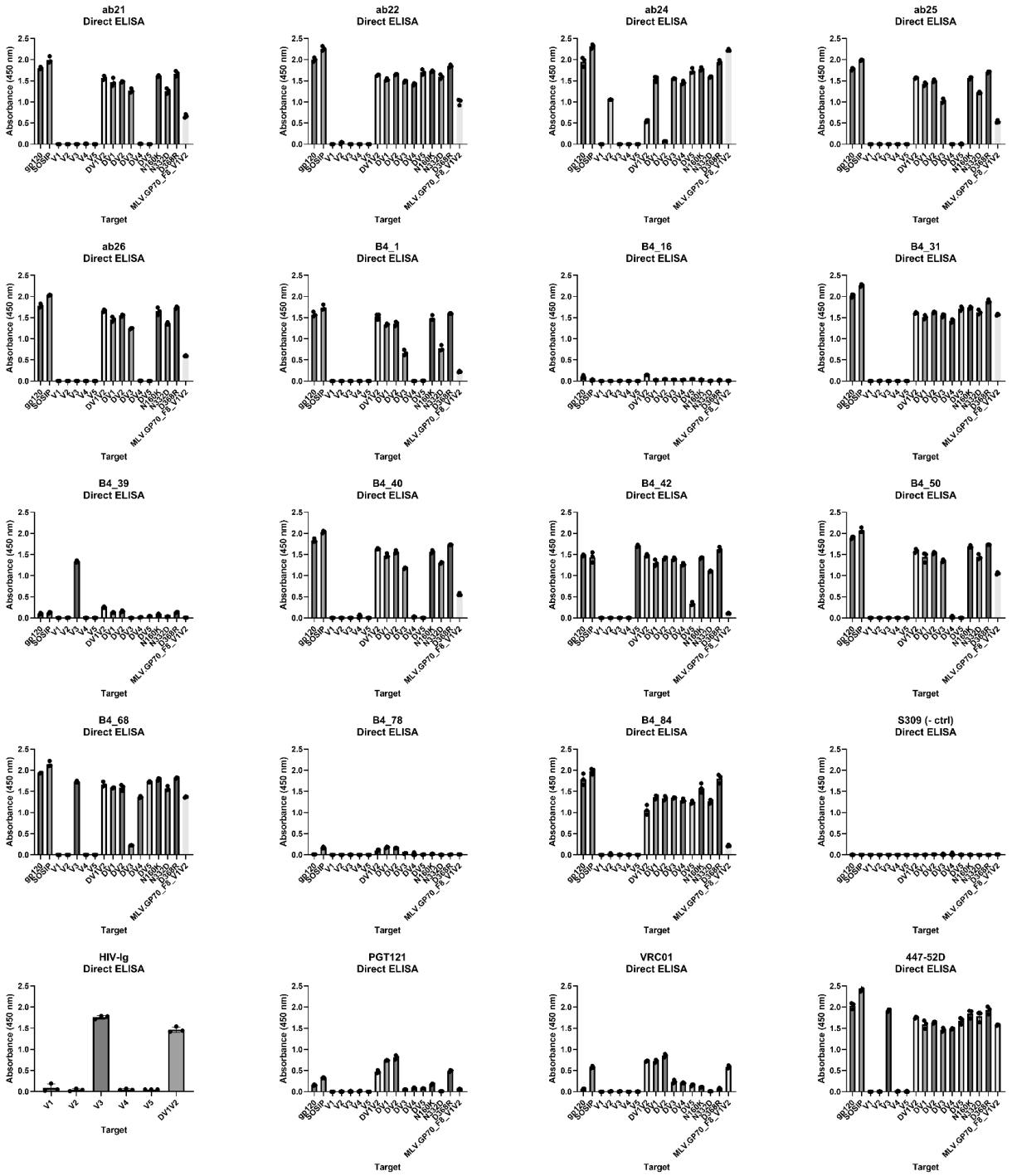

Supplemental Figure 3. Direct ELISA validation and epitope-mapping screen of 10014.F8.SOSIP Env-specific monoclonal antibodies.

Monoclonal antibodies recovered from 10014.F8.SOSIP-immunized rhesus macaques were evaluated by direct ELISA for binding to 10014.F8 Env antigens (Table 4) and epitope-mapping

probes. Plates were coated with 10014.F8 gp120, 10014.F8.SOSIP, variable-loop deletion or mutant gp120 proteins, variable-loop peptides, MLV gp70-F8 V1V2 scaffold protein, and control antigens. Binding was measured as absorbance at 450 nm. The panel was used both to confirm antibody binding to 10014.F8 gp120 and/or 10014.F8.SOSIP and to infer candidate epitope specificities based on differential binding to Env variants and peptide/scaffold targets. HIV-Ig, PGT121, VRC01, and 447-52D were included as positive/control antibodies, and S309 was included as a negative control. Bars show replicate absorbance values for each antigen-antibody combination.

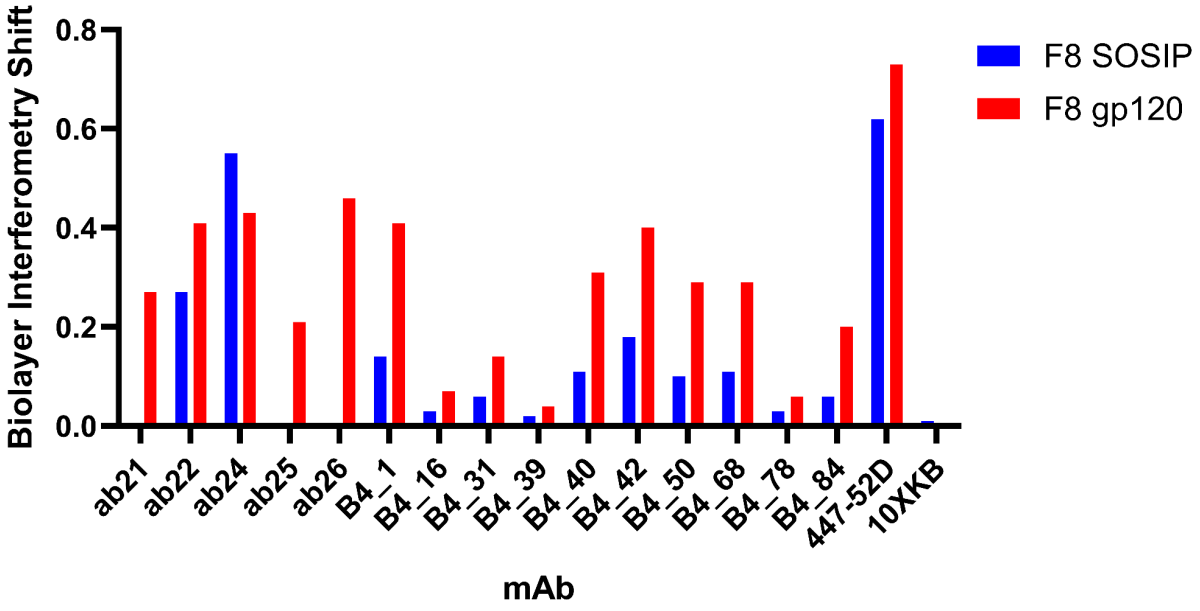

Supplemental Figure 4. Bio-Layer Interferometry validation of 10014.F8 Env binding by monoclonal antibodies.

Bio-Layer Interferometry (BLI) was performed on a GatorBio GatorPlus instrument to confirm monoclonal antibody binding to 10014.F8 Env antigens. Biotinylated 10014.F8.SOSIP trimer or 10014.F8 gp120 was immobilized on streptavidin biosensors, and antigen-loaded sensors were dipped into monoclonal antibody solutions to measure binding responses. BLI response shifts

are shown for each monoclonal antibody against 10014.F8.SOSIP (blue) and 10014.F8 gp120 (red). All monoclonal antibodies shown were considered positive Env-binding hits because binding to 10014.F8.SOSIP, 10014.F8 gp120, or both antigens exceeded background signal observed with KB running buffer alone. Response magnitudes varied across antibodies, consistent with differences in antigen specificity, epitope accessibility, and/or binding strength.

mAb	V gene	J gene	CDRH3 amino acid	% VH identity	Animal
ab11	IGHV2-S62	IGHJ4-I1	ARVGHCSDMECSSRIDY	90.301	29568
ab12	IGHV3-S6	IGHJ4-I1	VREGFDY	88.079	29568
ab13	IGHV3-KSeq21	IGHJ6-I1	ARVGGPYYGMDS	94.218	Undetermined
ab14	IGHV4-S22	IGHJ5-I2*02	AKYPLGLDV	84.483	31240
ab15	IGHV3-S54	IGHJ4-I1	AKGGGSYN	93.289	Undetermined
ab16	IGHV1-Kn,IGHV1-Korf1	IGHJ6-I1	ARSHYGYDWPAGPYALDF	85.567	31240
ab17	IGHV2-Korf1	IGHJ1-I1	ARLYGGDYNTFGYFDF	89.527	31240
ab18	IGHV2-Korf1	IGHJ4-I1	ARLNRVSTALLHY	90.909	26852
ab19	IGHV3-Korf2	IGHJ5-I2*02	PRGFSLDV	91.126	26852
ab20	IGHV4-S35	IGHJ5-I1	AKTGSRVTRFGRLSPQSYNWFDV	84.068	Undetermined
ab23	IGHV4-S11,IGHV4-S26	IGHJ4-I1	ARPDIAGAHHFYY	90.816	29568
ab27	IGHV1-Kn	IGHJ4-I1	ARAGYADEDNQYSRYYYFDY	81.973	29568
ab28	IGHV4-S11	IGHJ2-I1	ARHFPDNGNFNWYFDL	91.837	29568
B4_2	IGHV3-Korf8	IGHJ5-I2*02	TRWSGGGYYTESLDV	90.941	Undetermined
B4_5	IGHV4-K39,IGHV4-S22	IGHJ4-I1	VRVNTYNYLHYFDH	88.435	Undetermined
B4_12	IGHV4-S26	IGHJ4-I1	ARDPGYCTGNTCSTRGDY	85.811	Undetermined
B4_14	IGHV4-K32	IGHJ4-I1	ARHMGSFNEWTGYYPALDD	88.014	Undetermined
B4_18	IGHV4-K32	IGHJ5-I1	ASPHKSPLHV	87.713	26852
B4_21	IGHV4-K39	IGHJ5-I2*02	ARDGLDTARTGRGSSLDL	93.537	Undetermined
B4_25	IGHV4-K4	IGHJ4-I1	ARGGPGYGPWSFY	89.42	Undetermined
B4_26	IGHV4-K4	IGHJ5-I1	ARVYLFYDDDYGYTTGLWFDV	85.034	Undetermined
B4_32	IGHV4-S22	IGHJ5-I1	VRHGEYCGGSHCLLRFDV	88.435	29568
B4_36	IGHV4-Korf2	IGHJ6-I1	ARIDYGNYQGWDS	91.582	26852
B4_43	IGHV4-K9,IGHV4-Korf2	IGHJ4-I1	SRPLRESWTEYYFDY	87.542	Undetermined
B4_46	IGHV4-Korf2,IGHV4-Korf4	IGHJ5-I1	ASLPMAATIRLEV	88.851	Undetermined
B4_59	IGHV4-S37	IGHJ4-I1	ARPRLGIIIRGAFSY	92.833	Undetermined
B4_63	IGHV1-Kg	IGHJ5-I2*02	ARGGLGSCRGGVCFAMDV	85.959	Undetermined
B4_65	IGHV4-S37	IGHJ5-I2*02	ARDGGRSVTTILDV	86.824	31240
B4_66	IGHV4-S37	IGHJ5-I2*02	ARRGWGDRYVFNSLDL	91.753	Undetermined
B4_69	IGHV4-S38	IGHJ5-I2*02	ARDGLDTARTGRGSSLDL	90.97	Undetermined
B4_74	IGHV4-S40	IGHJ2-I1	ARVYSNSWQFDI	95.623	Undetermined
B4_77	IGHV4-S40	IGHJ4-I1	ASRYSTGWFSFDY	84.459	29568
B4_80	IGHV4-S40	IGHJ5-I2*02	ARPPRYCTTTACFTFHSLDV	95.973	29568

Table 3. Sequence features of recovered non-Env-binding monoclonal antibodies.

Recovered non-Env-binding monoclonal antibodies are listed with inferred IGH V gene assignment, IGH J gene assignment, CDRH3 amino acid sequence, percent VH identity, and assigned animal of origin. Percent VH identity was calculated relative to the inferred germline V gene sequence. Animal assignment was inferred by matching monoclonal antibody heavy-chain sequences to associated bulk IGH clonal lineages. Bulk sequences were required to pass post-filtering stringency thresholds, including support from at least three reads. Because single-cell samples were pooled in a three-animal group, antibodies were listed as undetermined when no associated bulk sequences passing these thresholds were present within the matched cluster; in these cases, the clone could not be assigned to one specific animal within the pooled set.

2.3.3 10014.F8.SOSIP-elicited B Cell Lineages Target Diverse Epitopes but Display Limited Antiviral Function

To determine the binding characteristics of the Env-specific mAbs, we evaluated binding by ELISA against a panel of antigens designed to identify the epitope targets they recognize (Supplemental Fig. 3). The antigen panel included the SOSIP native-like trimer, and an 10014.F8 gp120 protein. Additional gp120 variants were produced with epitope deletions, including variable loop deletions (DV1, 2, 3, 4, and 5), D368R (CD4-BS), N332D (V3 glycan supersite), and N160K (V2 glycan), and an MLV.GP70.F8.V1V2 construct. We also generated variable loop peptides spanning each of the variable loops (details on the antigens are provided in Table 4). A schematic summary of the assigned epitope specificities is shown in Fig. 3a, mapped onto a surface rendering of the gp140 BG505 SOSIP.664 structure (pdb_00006v0r[141]). The majority of the mAbs bound to both gp120 and SOSIP by ELISA and BLI (Fig. 3b, Supplemental Fig. 3 and 4, respectively), with one mAb binding weakly to SOSIP but not gp120

(B4_78). We successfully identified candidate epitopes for 10/15 mAbs with this panel, encompassing the V2, V3, V4, and V5 loops (Fig. 3a, Supplemental Fig. 3). The V4 and V4/5 region was the most heavily targeted, with 7 of 10 mAbs targeting here. The V4 focused immune response is interesting, given that the antibody response naturally acquired by donor subject 10014 was similarly focused on the V4 region[10]. We were unable to identify the specific binding epitopes for five of the 10 mAbs, beyond identifying that they bind to gp120. However, these findings confirm that we isolated a diverse panel of anti-Env mAbs, both in their BCR rearrangement and the epitopes they target. To assess whether vaccine-engaged lineages progressed through maturation to develop antiviral functions, we characterized the binding and effector properties of mAbs isolated from 10014.F8.SOSIP-immunized animals (Fig. 3).

Only two of the mAbs exhibited neutralization against the autologous 10014.F8 pseudovirus, but they lacked significant potency. The mAb B4_68, which targets the V3, had an IC50 of around 3 μg/ml, and B4_78 (undetermined epitope) neutralized at 50% at 10 μg/ml (Fig. 3c). All other mAbs failed to reach 50% neutralization at 20 μg/ml. 12 of 15 mAbs mediated phagocytosis of 10014.F8 gp120 in the ADCP assay (Fig. 3d), including the two neutralizing mAbs. No mAbs exhibited ADCC above background levels against replication-competent 10014.F8 virus (Fig. 3e). Thus, except for ADCP, the panel of mAbs exhibited weak or no antiviral activity. This is in contrast to the ADCC activity observed in serum (Fig. 1e), where all six animals mediated robust ADCC against the autologous virus. However, the recovered mAbs were expressed as macaque IgG1, whereas serum ADCC reflects a polyclonal antibody pool that may include multiple IgG subclasses and Fc glycoforms. Although they are not represented in this panel of antibodies, ADCC-mediating antibodies were elicited by vaccination. Overall, the panel of 15 B cell lineages captures a broad diversity of gene usage, epitope specificity, and functional activity, providing a functionally diverse sampling of a polyclonal vaccine-elicited B cell response.

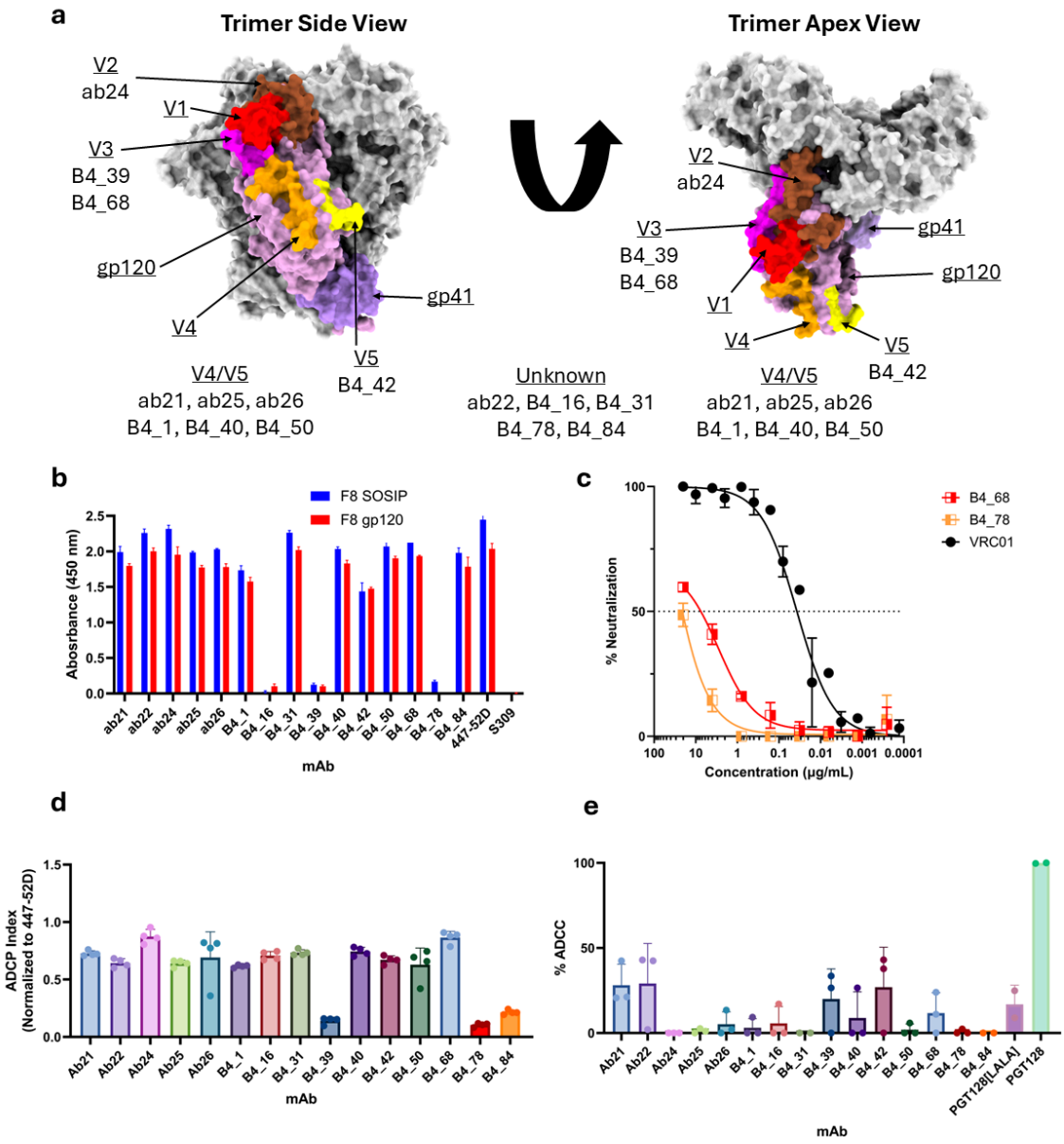

Figure 3. 10014.F8.SOSIP-elicited monoclonal antibodies targeted multiple Env variable-loop regions but showed limited antiviral function.

a, Approximate epitope mapping of vaccine-elicited monoclonal antibodies shown on two surface renderings of the same gp140 BG505 SOSIP.664 trimer structure, pdb_00006v0r, displayed in side and apex orientations. The BG505 Env structure was visualized in ChimeraX, and variable-loop regions were colored according to HXB2 numbering. Antibody epitope bins

were assigned from ELISA binding patterns against 10014.F8.SOSIP, gp120, and variable-loop deletion or modification constructs. Antibodies were classified as targeting V1, V2, V3, V4, V5, V4/V5, or unknown regions. **b,** Binding of recovered monoclonal antibodies to 10014.F8.SOSIP and 10014.F8 gp120 measured by ELISA. 450 nm absorbance is shown for each antibody. **c,** Neutralization activity of selected monoclonal antibodies against autologous 10014.F8 pseudovirus measured by TZM-bl assay. VRC01 is shown as a positive control, and the dotted line indicates 50% neutralization. **d,** Antibody-dependent cellular phagocytosis activity of monoclonal antibodies measured using antigen-coated fluorescent beads and THP-1 monocytes. ADCP index values were normalized to 447-52D. **e,** Antibody-dependent cellular cytotoxicity activity of monoclonal antibodies measured using infected MT4-CCR5-Luc target cells and KHYG-1 effector cells. PGT151 and PGT126 are shown as positive controls. Bars show mean values with replicate points overlaid.

Construct	Purpose	AA boundaries	Deleted AA boundaries
10014.F8.SOSIP	Native-like trimeric Env antigen; used to measure binding to the vaccine-matched folded Env immunogen	31T-664D	
10014.F8.gp120	Monomeric gp120 antigen; used to assess gp120-directed binding independent of gp41/trimer context	31T-502K	
Linear V1 Loop	Linear peptide antigen; used to detect antibodies targeting linear V1-loop epitopes	136N-151K	
Linear V2 Loop	Linear peptide antigen; used to detect antibodies targeting linear V2-loop epitopes	156N-197N	
Linear V3 Loop	Linear peptide antigen; used to detect antibodies targeting linear V3-loop epitopes	295N-332N	
Linear V4 Loop	Linear peptide antigen; used to detect antibodies targeting linear V4-loop epitopes	390L-408T	
Linear V5 Loop	Linear peptide antigen; used to detect antibodies targeting linear V5-loop epitopes	456R-471G	
DV1V2.gp120	V1/V2-deleted gp120; used to test whether binding depends on the V1/V2 region	31T-502K	132T-195S
DV1.gp120	V1-deleted gp120; used to test whether binding depends on the V1 region	31T-502K	132T-156N
DV2.gp120	V2-deleted gp120; used to test whether binding depends on the V2 region	31T-502K	158N-195S
DV3.gp120	V3-deleted gp120; used to test whether binding depends on the V3 loop	31T-502K	296T-330H
DV4.gp120	V4-deleted gp120; used to test whether binding depends on the V4 loop	31T-502K	386N-417P
DV5.gp120	V5-deleted gp120; used to test whether binding depends on the V5 loop	31T-502K	461S-470P
N160K.gp120	Glycan-site mutant; used to assess dependence on the N160 glycan-associated V1/V2 epitope region	31T-502K	N160K
N332D.gp120	Glycan-site mutant; used to assess dependence on the N332 glycan-associated outer-domain/V3-base epitope region	31T-502K	N332D
D368R.gp120	CD4-binding-site mutant; used to assess binding sensitivity to disruption of the CD4-binding site	31T-502K	D368R
MLV.gp70.F8.V1V2	V1/V2 scaffold antigen; used to detect V1/V2-directed binding outside the full gp120 context	115S-209S	

Table 4. Sequence features of recovered non-Env-binding monoclonal antibodies.

Recovered non-Env-binding monoclonal antibodies are listed with inferred IGH V gene assignment, IGH J gene assignment, CDRH3 amino acid sequence, percent VH identity, and assigned animal of origin. Percent VH identity was calculated relative to the inferred germline V gene sequence. Animal assignment was inferred by matching monoclonal antibody heavy-chain sequences to associated bulk IGH clonal lineages. Bulk sequences were required to pass post-filtering stringency thresholds, including support from at least three reads. Because single-cell samples were pooled in a three-animal group, antibodies were listed as undetermined when no associated bulk sequences passing these thresholds were present within the matched cluster; in these cases, the clone could not be assigned to one specific animal within the pooled set.

2.3.4 Vaccine-specific Lineages Undergo Class Switching but Do Not Exhibit Distinct Subclass Bias

Given the minimal antiviral functionality of the mAbs, we analyzed the sequence and evolutionary characteristics of each B cell lineage to evaluate whether there were sequence features encoded in the BCR repertoire that could implicate specific immunological processes associated with hypo-efficacy. After encountering antigen, B cells proliferate and undergo class switch recombination, creating a pool of cells with identical VDJ rearrangements but with diverse IgG subclass usage[70]. Because our Hinge-Seq approach captures the IgG Fc region and subclass, we were able to assign the exact IgG subclass of all members of the clonal family that were identified from the IgG MBC BCR IgH repertoires. We analyzed IgG subclass usage within and across clonal clusters, comparing vaccine-specific and non-Env-binding lineages (Fig. 4).

We first examined subclass usage within bulk IgG MBC BCR IgH NGS libraries for all clonal families for each animal (i.e., total MBC BCR repertoire) to establish the background

subclass structure present across the immunized animals (Fig. 4a). Across all animals, IgG1 and IgG2 subclasses were the most abundant, with an average of 45% of all clonal clusters containing IGHG1 (range 35%-70%) and 47% containing IgG2 (range 30%-55%). IgG3 and IgG4 were far less abundant, with an average of 5% of clusters containing IgG3, and 7% of clusters containing IgG4. The distribution of IgG subclass across BCR repertoires in RMs is understudied, but the relative abundance of IgG subclasses observed in the IgG MBC BCR IgH repertoires here is in agreement with a recent study using single cell analyses[138]. Thus, the IgHV usage and IgG subclass distribution observed in the IgG MBC BCR IgH repertoires is consistent with previous studies, and provides a representative baseline for interpreting subclass usage among functionally anchored lineages, allowing vaccine-specific and non-binding clusters to be evaluated relative to the broader activated IgG repertoire.

To compare IgG subclass distribution within functionally anchored Env-specific B cell lineages compared to non-Env-binding lineages, we analyzed each clonal family and assigned subclass usage to individual members, defining the frequency with which each subclass was found among the lineages (Fig. 4b). 80% of Env-specific lineages contained one or more members that expressed IgG1, whereas all lineages contained members expressing IgG2. IgG3 and IgG4 were less frequently expressed, with 15% of clonal families expressing IgG3 and 22% containing IgG4. By comparison, the non-Env-binding lineages expressed IgG2 less frequently, but otherwise the two lineage groups were similar. Importantly, the abundance of multiple subclasses within lineages is an indication that Env-specific B cell lineages underwent similar levels of class switching to non-Env-binding lineages, and that Env vaccination did not appear to result in detectable subclass bias.

We then analyzed the total relative subclass composition for all Env-specific clusters and all non-Env-binding B cell clusters (Fig. 4c). In both vaccine-specific and non-binding clusters, IGHG1 and IGHG2 accounted for most subclass assignments, while IGHG3 and IGHG4 contributed smaller fractions. However, IgG1 was observed less frequently in Env-specific

lineages compared to the non-Env-binding repertoire. Conversely, IgG2 was more frequent in Env-specific lineages than in non-Env lineages. This global proportional view reinforced the pattern observed at the individual-subclass level, that Env-specific and non-binding lineages differed modestly in relative subclass contribution, but both were composed primarily of the same dominant IgG subclasses observed in the IgG MBC BCR IgH repertoire.

Finally, we asked whether differences in subclass diversity were detectable within individual clonal families by quantifying the number of IgG subclasses observed per clonal family (Fig. 4d). Vaccine-specific and non-binding lineages both included clonal members containing more than one subclass, indicating that subclass diversity was present within clonal families and across unrelated clones. Vaccine-specific lineages commonly contained multiple subclasses, with some expressing three or more subclasses, supporting the interpretation that 10014.F8.SOSIP-engaged lineages underwent extensive class-switch diversification. These data show that 10014.F8-specific lineages entered class-switched IgG compartments and, in most cases, contained multiple subclass identities within the same clonal family. However, their subclass profiles largely reflected the broader IgG MBC BCR IgH repertoire and did not show a dominant subclass signature distinguishing them from non-Env-binding lineages. Thus, it is unlikely that the maturation bottleneck observed in the 10014.F8-specific antibody response is due to limitations in class-switch recombination processes.

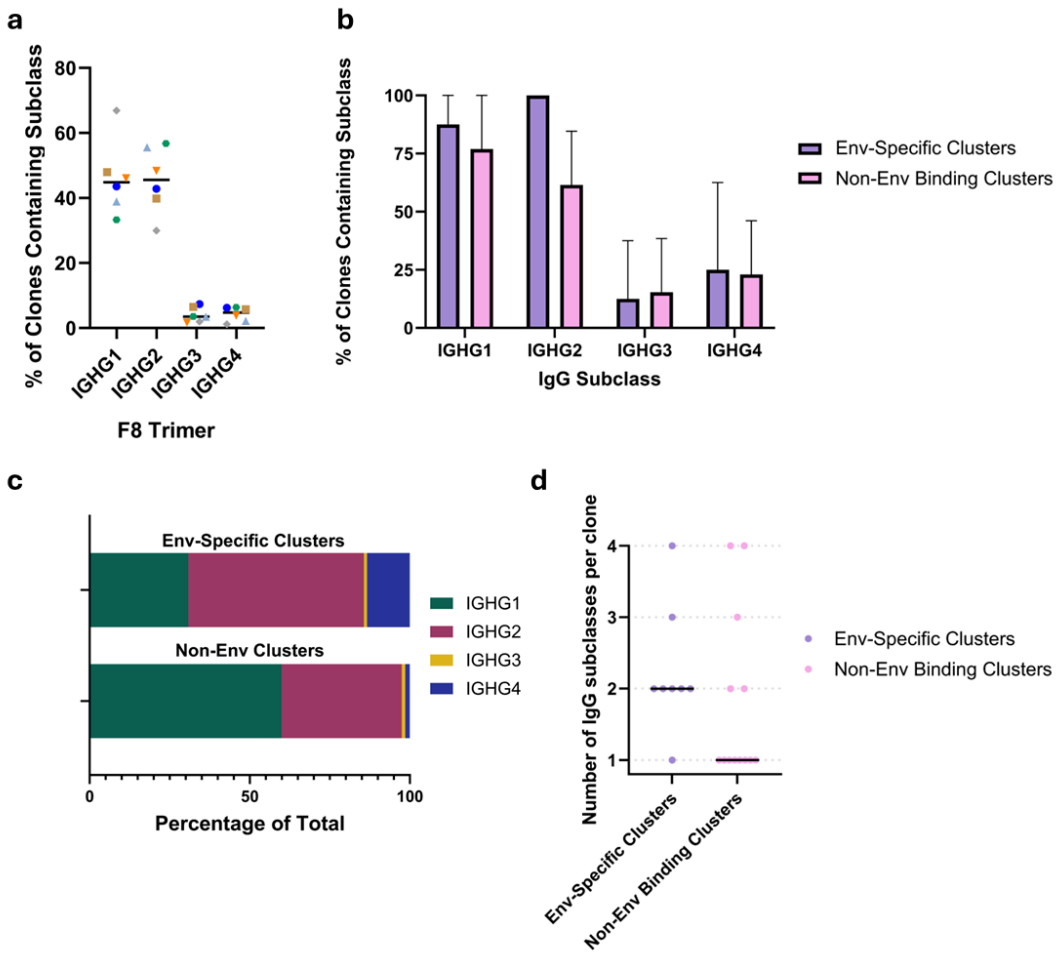

Figure 4. Vaccine-specific and non-Env-binding IGH lineages showed overlapping IgG subclass profiles.

a, IgG subclass distribution across bulk IGH clonal clusters from 10014.F8.SOSIP trimer-immunized animals. Subclass usage was quantified as the percentage of clonal clusters containing each IgG subclass within each animal. Points show individual animals; horizontal bars indicate group medians. **b,** Percentage of vaccine-specific and non-Env-binding anchored clusters containing each IgG subclass. Bars show group means with error bars. **c,** Clone-weighted IgG subclass composition among vaccine-specific and non-Env-binding clusters. Each cluster contributed a total weight of 1.0 distributed across detected subclasses in proportion to the number of retained cluster members assigned to each subclass. Stacked bars show the resulting subclass-fraction contributions normalized within each lineage group. **d,**

Subclass richness per clone among vaccine-specific and non-Env-binding clusters. Each point represents one clone, and the y-axis shows the number of distinct IgG subclasses detected within that clone. Black horizontal bars indicate group medians.

2.3.5 Vaccine-specific Lineages Exhibit Limited Diversification and Remain Restricted to Intermediate SHM States

To determine whether vaccine-engaged lineages progressed through affinity maturation, we quantified SHM across clonal clusters and compared Env-specific, non-Env-binding, and IgG MBC BCR IgH repertoires (Fig. 5). We first examined overall SHM levels at the clonal level in each mAb-derived lineage (Fig. 5a). Overall, Env-specific lineages (dark purple circles) exhibited lower somatic mutation levels compared to non-Env-binding lineages (pink circles). Thus, comparatively, Env-specific clones did not accumulate mutations to the same extent as the broader activated non-Env repertoire. To assess the mutation state of the mAbs relative to the SHM distribution within their own clonal lineages (Fig. 5a), all members of each clonal lineage were plotted as a function of % divergence (as grey circles) within each clonal family. The expressed mAbs were distributed across the range of mutation levels present within each lineage, indicating that they represent a continuum of mutational states within their clonal families and are not biased toward extremes within their own distribution. In aggregate, Env-specific lineages occupied a lower absolute SHM range compared to non-binding clusters (Fig. 5b; $p=0.0015$), consistent with the reduced SHM observed across each lineage. Together, these observations indicate that the vaccine-elicited Env-specific lineages were generally constrained to lower overall mutation states compared to the class-switched MBC compartment.

To assess whether this difference reflected sequence region-specific effects within the VDJ rearrangement, SHM was partitioned across complementarity-determining (CDR) and framework (FWR) regions (Figs. 5c and d, respectively). Env-specific mAbs exhibited lower

mutation within CDRs compared to non-Env lineages (Fig. 5c; p=0.012). Similarly, Env-specific mAbs exhibited lower mutation rates within the FWR compared to non-Env-binding mAbs (Fig. 5d; p=0.012). Thus, reduced mutation levels in Env-specific clones were observed in both antigen contact and framework regions, reflecting a generalized lower mutation rate compared to the IgG MBC compartment. To assess SHM levels across the populations of BCR sequences, we plotted the SHM of Env-specific, non-Env-binding, and IgG MBC BCR IgH populations as a probability density distribution and overlaid the distribution curves for comparison (Fig. 5e). The SHM distribution of the non-Env-binding mAb clones (pink line) neatly overlapped with the deep-profiling IgG MBC BCR IgH repertoire (black line), indicating that the non-Env-binding clones reflected mutation rates representative of the circulating class-switched MBC compartment. In contrast, the Env-binding clone distribution sharply peaked below the average class-switched IgG MBC BCR IgH repertoire and non-Env-binding clones, with a few outliers showing average or above average SHM.

Together, these data indicate that vaccine-elicited Env-specific B cell lineages exhibited significantly lower SHM levels compared to the broader class-switched MBC compartment. Whereas non-Env-binding clones mirrored the typical mutational distribution of circulating MBCs, the Env-specific clones were generally constrained to much lower mutational states. Thus, Env-specific clones experienced a restricted progression through affinity maturation relative to the general memory B cell repertoire.

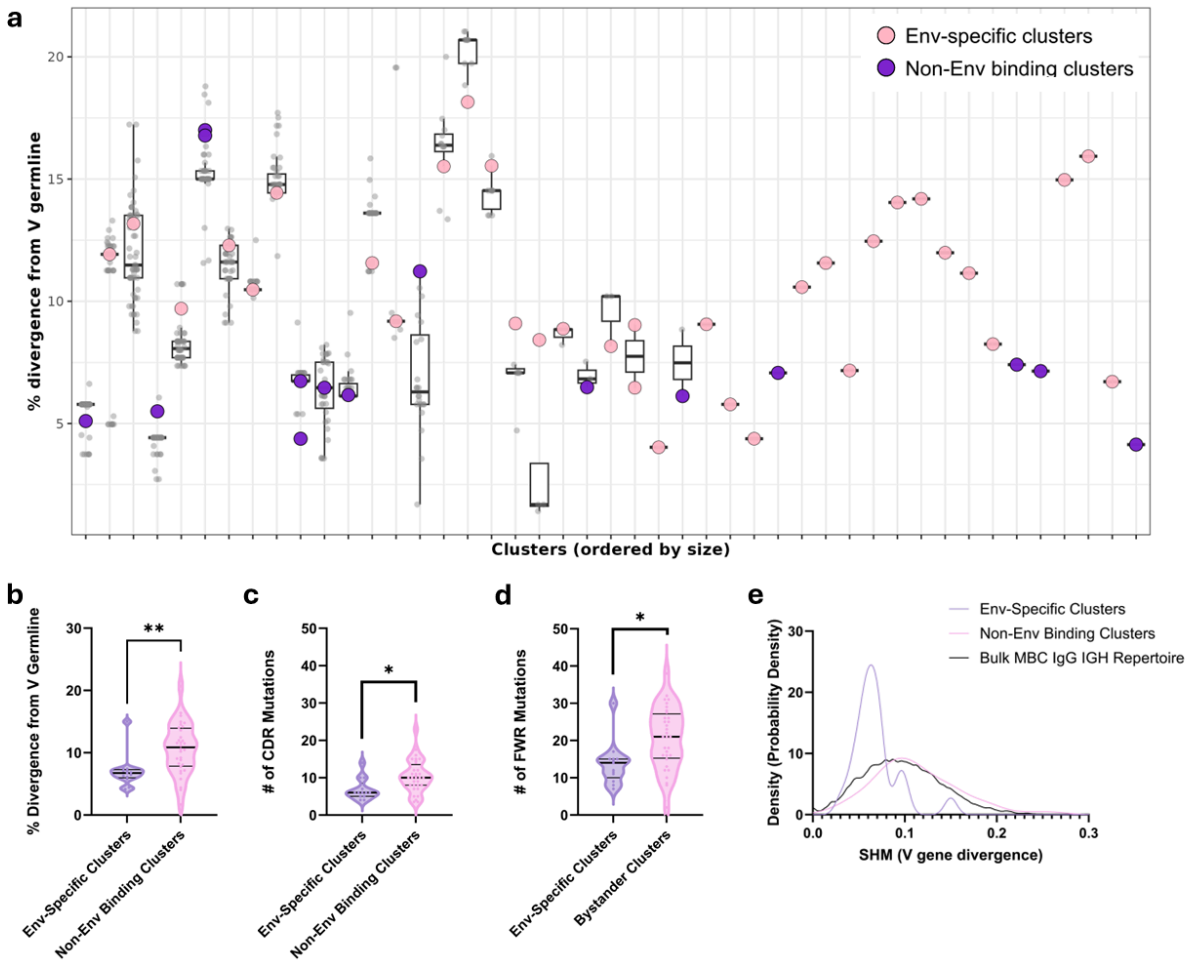

Figure 5. Vaccine-specific IGH lineages showed lower SHM than non-Env-binding lineages.

a, V gene divergence across antibody-anchored clonal clusters ordered by clone size. Grey points show bulk IGH sequences within each cluster, with boxplots summarizing sequence-level divergence from inferred V germline. Colored points indicate monoclonal antibodies mapped into each cluster, with Env-positive mAbs shown in purple and non-Env-binding mAbs shown in pink. **b,** Clone-level V gene divergence among vaccine-specific and non-Env-binding clusters. Each point represents one antibody-anchored clone, with clone-level divergence calculated as the median sequence-level SHM rate, defined as 1 − V gene identity. Groups were compared using a two-sided Mann-Whitney U test; p = 0.0015. **c,** Clone-level CDR mutation counts among

vaccine-specific and non-Env-binding clusters. Each point represents one antibody-anchored clone, with the plotted value calculated as the median number of CDR mutations across sequences in that clone. **d,** Clone-level framework-region mutation counts among vaccine-specific and non-Env-binding clusters. Each point represents one antibody-anchored clone, with the plotted value calculated as the median number of framework-region mutations across sequences in that clone. For **c** and **d**, groups were compared using two-sided Mann-Whitney U tests, and p-values were adjusted using the Benjamini-Hochberg method; adjusted p = 0.012 for both comparisons. **e,** Kernel density distributions of sequence-level SHM, measured as V gene divergence, among vaccine-specific clusters, non-Env-binding clusters, and the bulk IGH repertoire. Density curves are normalized to equal area, so curve height reflects relative probability density rather than absolute sequence count.

2.4 Discussion

A persistent challenge in evaluating pre-clinical HIV-1 vaccine studies is interpreting outcomes where regimens induce robust antibody responses but yield little to no antiviral function. Relying mainly on traditional serological readouts makes it difficult to diagnose specific immunological bottlenecks or generate testable hypotheses regarding which precise developmental stage of the immune response is implicated in the lack of efficacy. We approached this analytical barrier by utilizing novel next-generation sequencing (NGS) analytical tools to deeply interrogate the memory B cell repertoire in the context of characterized serum responses, directly linking serological phenotypes to features encoded within the B cell repertoire.

By employing our functionally-anchored deep IgG MBC BCR IgH profiling Hinge-Seq approach alongside 10x Genomics single B cell analysis, we demonstrated that the 10014.F8.SOSIP immunogen successfully drove B cell activation, GC entry, and class-switch

recombination, resulting in a diverse pool of B cells recognizing distinct epitopes. However, these expanding lineages exhibited a shared truncated maturation phenotype. Vaccine-elicited clones did not undergo the continuous, iterative SHM typically required to develop broadly neutralizing activity. Instead, they appeared to plateau at an intermediate mutational ceiling despite evidence of lineage diversification, regardless of genetic origin or epitope specificity. These findings imply that the primary bottleneck in this Env vaccine study was an inability to sustain iterative, targeted, GC-driven somatic evolution. More broadly, this provides a mechanistic explanation for the persistent disconnect between robust antibody responses and weak antiviral function observed in many HIV-1 vaccine studies, and suggests that high-frequency clonal expansion can be deceptive if the underlying GC reactions fail to drive significant affinity maturation.

Crucially, our data indicate that the NHP immune system fundamentally responded to the 10014.F8.SOSIP immunogen as expected. The successful expansion, diversification, and class-switch recombination observed within the functionally anchored lineages demonstrated that the basic machinery of B cell activation was intact. However, the arrest of these lineages at an intermediate mutation ceiling exposes a limitation in how vaccine efficacy is currently evaluated. In recent studies, the presence of robust GC reactions, measured via GC longevity, elevated CD4+ T follicular helper (Tfh) cell frequencies, or markers of GC-experienced B cells, is frequently interpreted as direct evidence of ongoing affinity maturation[72,142–145]. Our findings urge caution in this assumption, showing that features consistent with GC-derived maturation, including clonal expansion, class switching, increased avidity, and measurable SHM, can occur alongside plateaued SHM levels. This implies that a B cell clone can actively participate in a GC reaction yet still hit a strict mutational ceiling, underscoring that prolonged GC duration does not inherently guarantee continuous, productive somatic evolution within desired lineages.

A prevailing strategy in the field to overcome this maturation barrier focuses on artificially prolonging GC activity[146]. For example, studies employing slow-delivery mechanisms or

near-continual antigen exposure during the priming phase have successfully correlated extended GC residency with improved neutralizing outcomes[144,147]. While these studies provide proof-of-concept that prolonged antigen availability can enhance neutralizing responses, it remains unclear whether these extended GC responses achieve somatic mutation rates higher than those of traditional approaches. Furthermore, even if continuous antigen exposure can drive deeper SHM, such complex dosing regimens may be highly impractical for mass global deployment. Standard, clinically translatable prime-boost regimens must be capable of intrinsically initiating and sustaining productive GC responses. Our data highlight the profound difficulty of achieving this with current approaches and suggest that overcoming the SHM bottleneck may rely on the discovery of novel adjuvants or immunomodulatory factors capable of enhancing GC efficacy without requiring continuous antigen infusion.

Our functionally anchored profiling of the non-Env-specific comparator group strongly supports truncated maturation as a specific feature of the immunization approach. This is evidenced by significantly higher SHM frequencies in the class-switched MBC and non-Env-binding B cell lineages compared to the Env-specific clones. This stark contrast demonstrates that the rhesus macaque immune system is fully capable of executing and sustaining high levels of SHM. Therefore, the observed maturation bottleneck is not a reflection of an inherent host limitation, but rather a barrier specific to the vaccine regimen or the structural nature of the Env immunogen itself. While the heavily mutated non-Env lineages likely represent the accumulation of SHM through chronic, lifelong exposure to endemic environmental pathogens or the microbiome, their existence highlights a fundamental disparity: the episodic, acute antigen exposures provided by standard prime-boost immunizations are insufficient to replicate the sustained evolutionary pressure required to push Env-specific lineages past their intermediate mutational ceiling.

While our study implicates restricted SHM as a primary developmental roadblock, the precise mechanisms enforcing this bottleneck require further investigation. The mutational

ceiling we observed could be a consequence of rapid antigen clearance limiting GC residency time, inefficient follicular antigen presentation, or intense cross-competition for antigen among highly diverse, immunodominant B cell clones. Furthermore, the bottleneck may be exacerbated by the cellular dynamics of the boost itself. Emerging immunological evidence suggests that upon re-immunization, the majority of B cells that form secondary GCs are newly recruited from the naïve pool, rather than pre-existing MBCs re-entering to undergo further affinity maturation[89]. If Env-specific MBCs preferentially adopt a plasmablast differentiation fate upon boosting rather than re-entering the GC cycle, iterative SHM across multiple immunizations is effectively halted. Overcoming this specific limitation will likely require novel vaccine strategies explicitly engineered to encourage or enable existing MBCs to re-enter germinal centers, thereby unlocking the deep, sequential somatic hypermutation required for broad neutralization.

In conclusion, our findings highlight that while eliciting bNAbs likely requires initial recruitment of specific B cell precursors, the subsequent failure of HIV-1 trimer regimens to achieve broad neutralization is likely driven by restricted vaccine-driven maturation. This premature arrest in somatic evolution leaves Env-specific lineages plateaued in intermediate SHM states and demonstrates that robust clonal expansion and successful B cell activation are insufficient without sustained germinal center selective pressure. As such, these findings support the development of future vaccine strategies that couple the recruitment of appropriate precursors with methods designed to sustain continuous affinity maturation across iterative immunizations, potentially by utilizing approaches that encourage re-entry of MBCs back into secondary GCs or enhance follicular antigen presentation.

Chapter 3. Comparative Effects of 10014.F8.SOSIP Env Antigen Multimerization on Humoral Function and B Cell Repertoire Maturation

3.1 Introduction and Rationale

3.1.1 Building on Soluble Trimer-induced B Cell Responses

In Chapter 2 we showed that soluble 10014.F8.SOSIP trimer immunization was sufficient to recruit Env-binding B cells and generate vaccine-engaged clonal lineages, but the response remained functionally limited. Serum binding responses were detectable, and 10014.F8-specific mAbs could be recovered. However, antiviral function was limited, and Env-specific clusters did not show the degree of SHM expected (or required) for highly matured HIV-1 antibody responses. These findings implicated an incomplete or inadequate degree of B cell maturation as a central barrier: soluble 10014.F8.SOSIP trimer could recruit Env-reactive B cells, but did not drive sufficient SHM, lineage maturation, or functional antibody development to generate broad and potent antiviral activity. One possible explanation for this bottleneck is that soluble trimeric Env does not provide sufficient BCR crosslinking and signaling to strongly stimulate naïve B cells for activation and GC selection. B cells respond not only to antigen sequence or epitope identity, but also to antigen density, spacing, and valency[66,75,85,148]. Repetitive antigen display can overcome weak 1:1 interactions between soluble antigen and low-affinity naïve BCRs by allowing a single antigenic particle to engage multiple BCRs simultaneously. This multivalent binding increases the avidity of the antigen-B cell interaction, stabilizes antigen

capture at the B cell surface, and strengthens early antigen-dependent signalling. This logic is especially relevant for HIV-1 Env vaccination because many antibody lineages with potential relevance for protection may be difficult to initiate due to the weak interaction of the antigen with naïve BCRs[25,57]. A soluble trimer may engage some Env-reactive clones, as shown in Chapter 2, but still fail to recruit/mature a sufficiently broad or developmentally productive pool of B cells. Presenting the same Env sequence in a multivalent format may be able to increase recruitment of lower-affinity Env-reactive B cells and alter the founder population available for GC maturation.

Multimerization may also influence later stages of B cell maturation and evolution. After activation, B cells entering GCs undergo SHM and compete for antigen and T follicular helper cell help. By altering which B cells enter GCs, how efficiently they capture antigen, or how effectively they receive Tfh-derived selection signals, antigen format may shape clonal expansion, SHM accumulation, class switching, memory formation, and antibody function.

For this reason, the broader Env vaccination study in which the Chapter 2 vaccine group was conducted also compared three formats of the same 10014.F8.SOSIP Env immunogen: soluble 10014.F8.SOSIP trimer, ferritin-displayed 10014.F8.SOSIP Env nanoparticles, and liposome-displayed 10014.F8.SOSIP Env trimers. This design allowed this dissertation to separate two related questions. Chapter 2 asked what kind of B cell response was induced by soluble 10014.F8.SOSIP trimer and why that response remained functionally limited. Chapter 3 asks whether increasing antigen valency improved the vaccine response compared to trimeric delivery, including serum binding, antiviral function, clonal expansion, SHM, IgG subclass usage, and repertoire-level maturation.

3.1.2 Chapter Hypothesis

Based on the rationale that antigen valency can influence BCR engagement and downstream B cell fate, we hypothesized that increasing the valency of the 10014.F8.SOSIP

Env immunogen would improve both the magnitude and quality of the vaccine-induced antibody response. Specifically, we predicted that multivalent 10014.F8.SOSIP Env display would enhance early B cell activation and broaden clonal recruitment by increasing antigen avidity at the B cell surface. This would cause stronger serum binding responses, improved antibody functional activity, greater clonal expansion, increased SHM, and altered IgG subclass distributions consistent with changes in GC output and Fc-mediated effector potential.

This hypothesis was tested by comparing humoral and repertoire features across animals immunized with soluble 10014.F8.SOSIP trimers, ferritin-displayed 10014.F8.SOSIP nanoparticles, or liposome-displayed 10014.F8.SOSIP trimers. If increasing antigen valency improved vaccine-induced maturation, then the ferritin or liposome groups would be expected to show coordinated improvements across multiple layers of the response[66,75,85]. These would include increased Env-specific binding titers, higher avidity, broader or stronger neutralization, enhanced Fc-mediated effector function, increased clonal expansion, higher SHM, and shifts in subclass usage or subclass diversity.

However, an alternative possibility was that multimerization would primarily increase antigen engagement without improving the downstream quality of the response. In that case, higher-valency antigen formats might increase serum binding magnitude or recruit more Env-reactive B cells, but still fail to drive the deeper maturation required for effective antiviral function. This would produce a disconnect between quantitative immunogenicity and qualitative antibody development, where antibody titers increase without corresponding improvements in neutralization, Fc-effector function, SHM accumulation, or lineage maturation.

This chapter tests these possibilities by comparing serological function, bulk IgG MBC BCR IgH repertoire features, and functionally anchored Env-specific versus non-Env-binding clusters across the three 10014.F8.SOSIP Env presentation formats. In doing so, it extends the central question raised by Chapter 2: whether the incomplete maturation observed after soluble 10014.F8.SOSIP trimer vaccination reflects a broader limitation of the 10014.F8.SOSIP Env

response, or whether changing antigen valency can redirect the response toward more functionally mature antibody lineages. By applying the same functional anchoring framework across the full cohort, this chapter evaluates whether multimerization altered not only serum-level antibody activity, but also the clonal and sequence-level features of Env-specific B cell clusters.

3.2 Experimental Design

The analyses in this chapter extend the same experimental and analytical framework described in Chapter 2 to the full multimerization cohort. Serum assays, bulk IgG MBC BCR IgH repertoire sequencing, single-cell V(D)J sequencing, and mAb expression were performed using the same approaches described for the soluble trimer group. The purpose of this chapter is therefore not to introduce a separate analytical strategy, but to apply the Chapter 2 framework across all three vaccine groups.

3.2.1 Animal Cohorts and Vaccine Groups

To test whether antigen presentation format altered the humoral and repertoire response to 10014.F8.SOSIP Env vaccination, the study compared three vaccine groups that used the same HIV-1 10014.F8.SOSIP Env sequence but differed in antigen valency (Table 5). Eighteen rhesus macaques were enrolled and divided into three experimental groups of six animals each. This design allowed vaccine responses to be compared across presentation formats while holding Env sequence constant.

The first group received soluble 10014.F8.SOSIP trimers, representing the lowest-valency antigen format evaluated in this study. This group served as the reference condition for interpreting the effects of multimerized antigen display and is examined in greater depth in Chapter 2. The second group received ferritin-displayed 10014.F8.SOSIP Env nanoparticles, in which 10014.F8.SOSIP Env was presented in an 8-copy nanoparticle format.

This group tested whether moderate multivalent display would enhance B cell activation, antibody magnitude, or repertoire maturation compared with soluble trimer. The third group received liposome-displayed 10014.F8.SOSIP Env trimers, a high-valency format designed to present many copies of Env on a lipid particle surface. This group tested whether dense membrane-associated antigen display could further enhance humoral responses and B cell maturation.

Together, these three groups created a valency gradient, ranging from soluble trimer to intermediate-valency ferritin nanoparticles to high-density liposomal Env display. Because all groups used the same 10014.F8.SOSIP Env sequence, differences in serum binding, antibody function, clonal expansion, SHM, IgG subclass usage, or repertoire composition could be interpreted in relation to antigen presentation format rather than Env sequence identity.

Vaccine Group	Animal ID	Age (yrs)	Sex
Soluble Trimer	26852	11.9	Female
	29242	9.0	Female
	29295	9.0	Female
	29568	9.0	Female
	31133	7.0	Female
	31240	7.0	Female
Ferritin-display	25312	17.0	Female
	25849	16.0	Female
	27318	13.8	Female
	28550	13.2	Female
	30945	10.2	Female
	33823	7.7	Female
Liposome-Display	25746	15.9	Female
	25891	15.9	Female
	26565	15.1	Female
	28127	12.8	Female
	28398	12.9	Female
	31472	9.9	Female

Table 5. Immunization groups and animal identifiers for the multimerization cohort.

Animals are listed by vaccine group, animal ID, age, and sex. Vaccine groups included soluble 10014.F8.SOSIP trimer, ferritin-displayed 10014.F8.SOSIP Env, and liposome-displayed 10014.F8.SOSIP Env. All animals underwent bulk IgG MBC BCR IgH RNA sequencing by Hinge-Seq. Underlined animal IDs indicate animals that also underwent 10x Genomics single-cell sequencing.

3.2.2 Immunization and Sampling Schedule

The three vaccine groups followed the same immunization and sampling schedule described in Chapter 2. Briefly, animals received a DNA prime at week 0 followed by protein boosts at weeks 4, 10, and 20 with their assigned 10014.F8.SOSIP Env antigen format. Blood and peripheral blood mononuclear cell (PBMC) samples were collected longitudinally to measure serum antibody binding, antiviral function, Fc-mediated effector activity, and bulk IgG MBC BCR IgH repertoire features across the vaccine course. Because the timing of immunization and sample collection was held constant across groups, differences observed among the soluble trimer, ferritin, and liposome groups could be interpreted in relation to antigen presentation format rather than differences in vaccine schedule. The full immunization and sampling timeline is shown in Fig. 1a.

3.2.3 Analytical Overview

Animals immunized with soluble 10014.F8.SOSIP trimer, ferritin-displayed 10014.F8.SOSIP Env, or liposome-displayed 10014.F8.SOSIP Env were compared using the same major data layers described in Chapter 2: serum binding titers, avidity, neutralization, antibody-dependent cellular phagocytosis (ADCP), ADCC, bulk IgG MBC BCR IgH repertoire metrics, single-cell V(D)J recovery, and expressed mAb binding or function. This allowed antibody binding, antibody function, clonal expansion, SHM, IgG subclass usage, V/J family usage, and mAb recovery to be compared across antigen presentation formats. Specifically, the analysis asked whether multimerization improved antibody magnitude, antiviral function, clonal recruitment, SHM accumulation, IgG subclass distribution, or repertoire composition.

3.3 Serum Binding Responses Across Antigen Formats

3.3.1 Longitudinal 10014.F8.SOSIP Binding Titers

To determine whether antigen format altered the magnitude of the Env-specific antibody response, longitudinal 10014.F8.SOSIP endpoint titers were compared across the three vaccine groups. All groups generated detectable 10014.F8-specific binding responses that increased after repeated immunization, indicating that each antigen format was immunogenic (Fig. 6a).

Although binding responses were induced across all groups, endpoint titers differed by antigen format. Ferritin-displayed 10014.F8.SOSIP produced the highest serum binding titers, with mean endpoint titers reaching approximately 10^6 after boosting, exceeding the responses observed in the soluble trimer and liposome groups. Moderate multivalent display therefore increased the magnitude of the 10014.F8-specific serum antibody response relative to the other antigen formats (Fig. 6b). These results show that antigen multimerization can enhance quantitative serum binding, but they do not determine whether increased binding magnitude reflects improved antibody quality or antiviral function.

3.3.2 Serum Avidity

To determine whether differences in endpoint titers were accompanied by differences in apparent binding strength, serum avidity was compared across the three vaccine groups. Avidity was assessed by measuring retention of 10014.F8.SOSIP binding after ammonium thiocyanate treatment, allowing comparison of binding stability rather than binding magnitude alone, measured two weeks post final boost. Ferritin-immunized animals showed the highest avidity indices, significantly exceeding the liposome group, while the soluble trimer group showed an intermediate profile. This suggests that ferritin display increased not only the magnitude of the 10014.F8-specific serum response, but also the apparent stability of serum antibody binding. Together with the endpoint titer data, these results indicate that the ferritin display produced the

strongest quantitative and apparent binding-quality response among the three antigen formats (Fig. 6c).

3.4 Fc-mediated Antibody Function Across Antigen Formats

3.4.1 ADCC Activity

The ADCC activity observed in the trimer group in Chapter 2 was not observed in the multimerized antigen formats. Although ferritin-immunized animals generated the highest 10014.F8-specific binding titers and avidity indices, this group showed no detectable ADCC activity. Liposome-immunized animals similarly showed minimal ADCC activity. Ferritin and liposome display therefore did not improve Fc-mediated cytotoxic function relative to the soluble trimer response (Fig. 6d).

3.4.2 ADCP Activity

A similar pattern was observed for ADCP. In the trimer group, serum ADCP against 10014.F8 gp120 increased substantially from week 0 to week 22, indicating induction of phagocytic Fc-effector activity after vaccination. In contrast, ferritin- and liposome-immunized animals showed no increase in ADCP activity between timepoints, with no clear post-immunization increase. The ADCP activity induced by soluble trimer immunization was therefore not reproduced by the multimerized antigen formats (Fig. 6e).

3.4.3 Integrated Fc-function Interpretation

The Fc-function data revealed a clear disconnect between binding magnitude and Fc-mediated antibody activity. Multimerized 10014.F8.SOSIP display did not improve ADCC or ADCP relative to soluble trimer immunization. Instead, ferritin and liposome display failed to reproduce the Fc-effector activity observed in the trimer group. This was particularly notable for ferritin immunization, which produced the highest 10014.F8-specific binding titers and avidity

indices but showed little to no detectable ADCC or ADCP. These results indicate that increased Env-specific binding magnitude was not sufficient to predict Fc-effector function. Rather, serum binding, avidity, and Fc-mediated activity appeared to behave as partly separable outputs of the antibody response. This distinction is important because the ferritin group could appear improved if evaluated only by binding-based serology, yet it lacked the Fc-functional activity detected after soluble trimer immunization.

3.5 Neutralization Breadth and Potency Across Antigen Formats

3.5.1 Autologous Neutralization of 10014.F8

Autologous 10014.F8 neutralization was compared across vaccine groups to determine whether 10014.F8-specific binding responses translated into antiviral activity against the matched virus. Neutralization was detectable in subsets of animals across the study, with several animals in the trimer and ferritin groups exceeding 50% neutralization at the 1:50 dilution. Responses in the liposome group were more variable, although several animals reached similar levels of activity (Fig. 6f).

Despite detectable autologous neutralization in individual animals, activity was not uniform within any vaccine group. Ferritin immunization produced the highest binding titers and avidity indices, but this did not translate into a clearly superior autologous neutralization profile across the group. Autologous neutralization was therefore induced in some animals, but did not scale directly with serum binding magnitude.

3.5.2 Tier 1 Neutralization Panel

The tier 1 neutralization profile observed in Chapter 2 was not substantially improved by ferritin or liposome display. Across the entire multimerization cohort, activity remained concentrated against SF162, while neutralization of the remaining tier 1 viruses was weak or inconsistent (Fig. 6g).

3.5.3 Tier 2 Neutralization Panel

A similar pattern was observed against the tier 2 panel. Neutralizing activity remained sparse across vaccine groups, with measurable activity for all groups largely restricted to the 398F1 isolate identified as susceptible to neutralization in the trimer analysis (Fig. 6h).

Together, the tier 1 and tier 2 data show that multimerized antigen display did not convert the 10014.F8 response into a broader neutralizing antibody response. Ferritin display increased serum binding magnitude and avidity, but those improvements were not accompanied by a corresponding expansion of neutralization breadth.

3.6 Summary of Serological Effects of Multimerization

Together, the serological data show that all three antigen formats induced detectable 10014.F8 Env-specific antibody responses, but increasing antigen valency did not produce a coordinated improvement in antibody function. Ferritin display generated the highest binding titers and avidity indices, indicating that moderate multivalent display enhanced the magnitude and apparent binding stability of the serum response. However, this stronger binding profile did not translate into broader neutralization or improved Fc-mediated activity. Neutralization remained narrow across groups, and the ADCC and ADCP activity observed after soluble trimer immunization was not reproduced by the ferritin or liposome groups.

These findings indicate that antigen multimerization altered some quantitative features of the antibody response without clearly improving qualitative antiviral function. Serum binding magnitude, avidity, neutralization, ADCC, and ADCP were not coordinated across vaccine groups, suggesting that antigen format can shape different features of the humoral response independently. Therefore, serological measurements alone were insufficient to explain how antigen presentation format affected the underlying B cell response. To address this, the next

analyses compared bulk IgG MBC BCR IgH repertoire features across vaccine groups, including clonal expansion, SHM, IgG subclass usage, and V/J family composition.

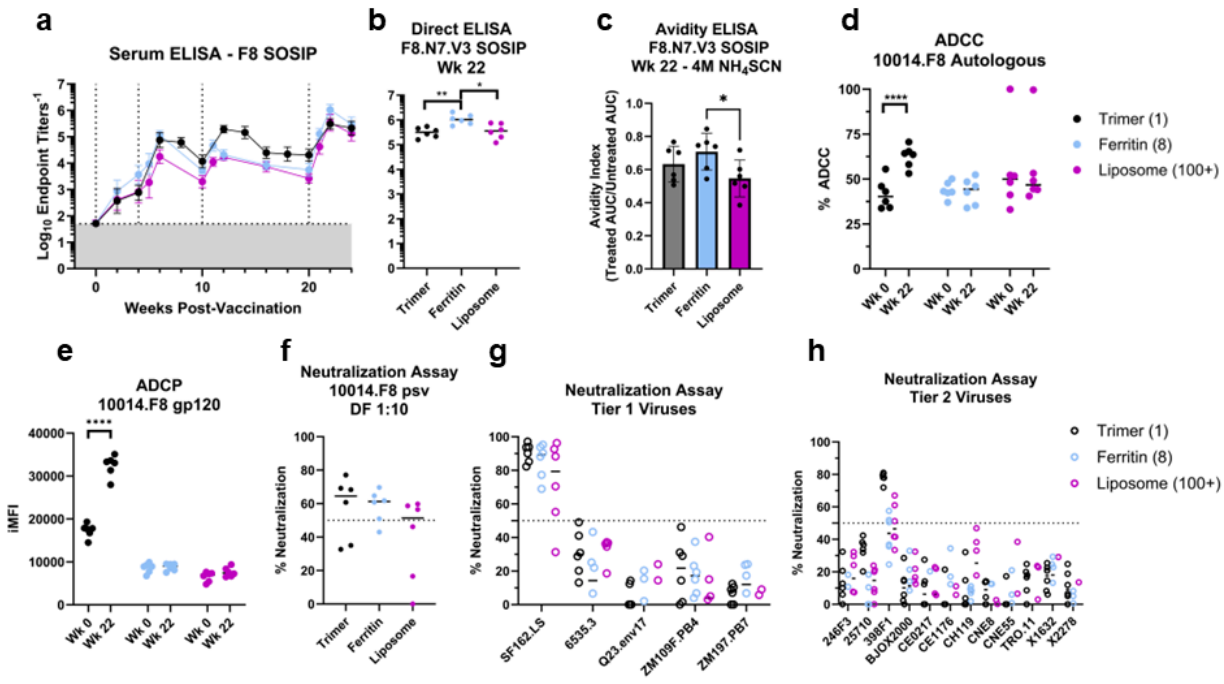

Figure 6. 10014.F8.SOSIP Env multimerization increased binding titers but did not improve neutralization breadth.

a, Longitudinal serum IgG endpoint titers measured by ELISA against 10014.F8.SOSIP in macaques immunized with soluble trimer, ferritin-displayed Env, or liposome-displayed Env. Dotted vertical lines indicate immunizations; the grey shaded region indicates values below the assay limit of detection. **b,** Week 22 serum IgG binding titers to 10014.F8.SOSIP. Planned pairwise comparisons used two-sided Welch's t tests with Holm correction; Trimer vs Ferritin, adjusted p = 0.0022; Ferritin vs Liposome, adjusted p = 0.0122. **c,** Week 22 plasma antibody avidity to 10014.F8.SOSIP measured by 4 M NH_4SCN displacement ELISA. Avidity index was calculated as treated AUC divided by untreated AUC. Ferritin and Liposome were compared by two-sided Welch's t test; p = 0.0306. **d,** ADCC against autologous 10014.F8-infected target cells at week 0 and week 22. Trimer week 0 and week 22 values were compared by two-sided paired

t test; p = 0.0003. **e,** ADCP against 10014.F8 gp120-coated beads at week 0 and week 22, reported as integrated mean fluorescence intensity. Trimer week 0 and week 22 values were compared by two-sided paired t test; p < 0.0001. **f,** Autologous neutralization against 10014.F8 pseudovirus measured at 1:10 plasma dilution. **g,** Tier 1 pseudovirus neutralization measured at 1:50 plasma dilution. **h,** Tier 2 pseudovirus neutralization measured at 1:50 plasma dilution. Dotted horizontal lines indicate 50% neutralization. Each point represents one animal; horizontal bars indicate group medians.

3.7 Repertoire Sequencing Across Vaccine Formats

3.7.1 Incorporation of Multimerization Groups into the Env-specific Versus Non-Env-binding Cluster Analysis

Antigen valency improved some serological measures, including ferritin-associated increases in endpoint titers and avidity, but did not produce a coordinated improvement in neutralization or Fc-mediated function. Bulk IgG MBC BCR IgH repertoire sequencing was used to compare the underlying B cell response across vaccine formats. The same Hinge-Seq and functional anchoring framework described in Chapter 2 in Fig. 2a was applied to animals from the soluble trimer, ferritin, and liposome groups. This allowed repertoire-level features to be compared across antigen presentation formats and enabled the Env-specific versus non-Env-binding cluster analysis to be expanded beyond the soluble trimer group.

As in Chapter 2, expressed mAbs were used as functional anchors for bulk IgG MBC BCR IgH clonal families. Clusters containing Env-binding mAbs were classified as Env-specific, while clusters containing non-Env-binding mAbs were classified as non-Env-binding or background clusters. Bulk IgG MBC BCR IgH sequences clonally related to these mAbs were then used to compare cluster size, SHM, root-to-tip divergence, CDR mutation burden, and the relationship between clonal expansion and mutation.

Because the number of functionally anchored Env-specific lineages differed substantially across vaccine groups, these analyses were not powered for separate vaccine-group comparisons of Env-specific clusters. The soluble trimer group contributed the largest number of Env-specific mAbs, while fewer Env-specific mAbs were recovered from the ferritin and liposome groups. Specifically, the functional anchoring dataset included 15 Env-specific mAbs from trimer-immunized animals, 8 from ferritin-immunized animals, and 2 from liposome-immunized animals. Given this uneven sampling, especially the limited number of liposome-derived Env-specific anchors, the primary repertoire analysis pooled anchored clusters across vaccine formats and compared Env-specific clusters with non-Env-binding clusters. This approach increased the number of anchored Env-specific lineages available for analysis and tested whether the maturation pattern observed in the soluble trimer group persisted after inclusion of mAbs recovered from the multimerized vaccine groups.

Incorporating the ferritin and liposome groups increased the number of functionally anchored clonal families available for Env-specific versus non-Env-binding comparison, totaling 25 Env-binding and 80 non-Env-binding mAbs. This expanded analysis asked whether the major cluster-level pattern observed in the soluble trimer group, recruitment of Env-binding lineages with limited progression toward highly mutated states, persisted across the broader multimerization cohort. Rather than serving as a powered between-format comparison of anchored Env-specific lineages, this analysis tested whether adding ferritin- and liposome-derived anchors changed the overall conclusion that Env-specific clusters remained less mature than the non-Env-binding background compartment.

3.7.2 Clonal Expansion of Env-specific and Non-Env-binding Clusters

Clonal expansion was compared between Env-specific and non-Env-binding clusters (Fig. 7a). The expanded dataset increased the number of anchored clusters available for

comparison and allowed the relationship between antigen binding and sampled clonal representation to be evaluated across the broader multimerization cohort.

Env-specific clusters showed a trend toward larger cluster size than non-Env-binding clusters when summarized at the animal level. Although this comparison did not reach conventional statistical significance (p=0.0625), the direction of the effect was consistent with ongoing antigen-engaged B cell recruitment and expansion after vaccination. Within that limitation, the expanded Env-specific versus non-Env-binding comparison supports the conclusion that Env-binding lineages were recruited and expanded across the vaccine study.

3.7.3 Somatic Hypermutation by Vaccine Group

SHM was next evaluated within the expanded functional anchoring framework (Fig. 7b). As in Chapter 2, the goal was to determine whether Env-specific clusters showed evidence of sequence-level maturation relative to non-Env-binding clusters. Incorporating the ferritin and liposome groups allowed for the SHM patterns observed in the soluble trimer group to be tested across the broader multimerization cohort.

Env-specific clusters showed lower median SHM than non-Env-binding clusters. This indicates that Env-binding clusters were generally closer to germline than the non-Env-binding compartment, even after expanding the analysis beyond the soluble trimer group. A similar pattern was observed when mutation was evaluated using additional cluster-level metrics, including root-to-tip distance and CDR mutation counts (Fig. 7c, 7d). Non-Env-binding clusters tended to occupy more highly mutated sequence states, while Env-specific clusters were concentrated at lower-to-intermediate mutation levels.

These results extend the Chapter 2 finding that Env-specific clusters were detectable but incompletely matured. The expanded analysis suggests that this pattern was not unique to the soluble trimer group. Instead, Env-specific clusters across the multimerization cohort showed

evidence of antigen engagement and clonal representation, but did not accumulate the same mutation burden observed in non-Env-binding clusters.

3.7.4 Relationship Between Clonal Expansion and SHM

The relationship between cluster size and SHM was examined to determine whether clonal expansion and mutation accumulation were positively correlated within Env-specific and non-Env-binding clusters (Fig. 7e). This analysis tested whether larger Env-specific clusters also showed higher mutation, which would be consistent with expansion-linked maturation after antigen engagement.

Among Env-specific clusters, median SHM showed a positive relationship with median clone size. This suggests that, within Env-specific clusters, greater sampled clonal representation was associated with greater mutation accumulation. In contrast, non-Env-binding clusters showed effectively no relationship between SHM and clone size, indicating that highly mutated background lineages were not necessarily the most expanded. This distinction suggests that Env-specific clusters were not simply low-SHM background clones, but instead showed evidence of coordinated expansion and mutation.

However, the absolute mutation burden of Env-specific clusters remained lower than that of non-Env-binding clusters. Therefore, the expanded analysis supports two related conclusions: Env-specific clusters were recruited into maturation pathways, but their maturation remained limited relative to the broader non-Env-binding repertoire. This pattern is consistent with incomplete vaccine-driven B cell maturation rather than absence of antigen engagement.

3.7.5 Repertoire-wide SHM Distribution of Env-specific Clusters

To visualize the mutational landscape of the vaccine response relative to the broader immune system, the density distribution of SHM was plotted and compared across Env-specific clusters, non-Env-binding clusters, and the general bulk IgG MBC BCR IgH repertoire (Fig. 7f). When overlaid, the SHM distribution of the non-Env-binding clusters closely matched the overall

bulk IgG MBC BCR IgH repertoire. This overlap indicates that the non-Env-binding clusters were representative of the broader IgG MBC BCR IgH repertoire, supporting their use as a background comparison for assessing the maturation state of Env-specific lineages.

In contrast, while the Env-specific clusters fell within this dominant SHM landscape rather than forming a distinct outlier population, their distribution exhibited a modest but consistent shift toward lower mutation levels. Most notably, the Env-specific distribution was enriched at intermediate mutation levels but distinctly lacked the highly mutated "right shoulder" observed in both the non-Env-binding and bulk IgG MBC BCR IgH repertoires.

This reduced representation in the highly mutated tail visually reinforces the conclusions of the previous clonal analyses. It clearly demonstrates that while the 10014.F8.SOSIP immunogen successfully recruits and expands antigen-specific B cells, their mutational trajectory is prematurely truncated. Consequently, Env-specific clusters fail to accumulate the extensive somatic hypermutation that the broader background repertoire routinely achieves.

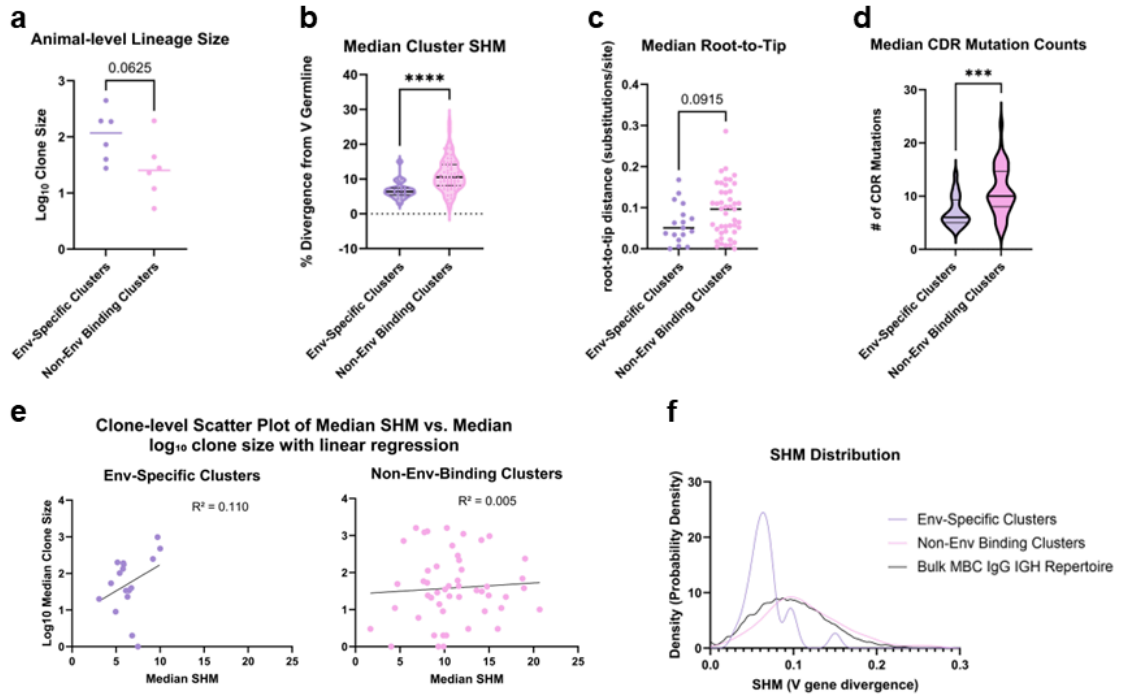

Figure 7. Env-specific IGH clusters showed lower mutation accumulation than non-Env-binding clusters.

a, Animal-level clone size comparison between Env-specific and non-Env-binding clusters after sampling control. Each point represents an animal-level log10 clone-size summary. Groups were compared by two-sided Wilcoxon matched-pairs signed-rank test; p = 0.0625. **b,** Median cluster SHM, measured as percent divergence from inferred V germline. Groups were compared by two-sided Mann-Whitney U test; p < 0.0001. **c,** Median root-to-tip distance from clone-level phylogenies, reported as substitutions per site; p = 0.0915. **d,** Median CDR mutation counts per clone. Groups were compared by two-sided Mann-Whitney U test; p = 0.0001. **e,** Clone-level relationship between median SHM and median log10 clone size. Lines show simple linear regression fits; Env-specific clusters, $R^2 = 0.110$, p = 0.1946; non-Env-binding clusters, $R^2 = 0.005$, p = 0.6421. **f,** Kernel density distributions of sequence-level SHM, measured as V gene divergence, among Env-specific clusters, non-Env-binding clusters, and the bulk IgG MBC BCR IgH repertoire. Density curves are normalized to equal area.

3.8 IgG Subclass Usage and Class-switching Across Vaccine Formats

3.8.1 Bulk IgG MBC BCR IgH Subclass Distributions

IgG subclass use was compared across vaccine groups to determine whether antigen presentation format altered class-switching patterns in the bulk IgG MBC BCR IgH repertoire (Fig. 8a). Because IgG subclass influences Fc-mediated antibody function, differences in subclass distribution could provide a potential explanation for the discordance between serum binding magnitude and Fc-effector activity observed across vaccine groups.

Across the bulk IgG MBC BCR IgH repertoire, subclass distributions were broadly similar among animals immunized with soluble trimer, ferritin-displayed Env, or liposome-displayed Env. Sequence-weighted subclass frequencies were dominated by IGHG1 and IGHG2, while IGHG3 and IGHG4 were present at lower frequencies. Individual subclass frequencies did not differ significantly across vaccine groups by Kruskal-Wallis testing, indicating that antigen format did not strongly reshape the overall subclass composition of the circulating IgG repertoire.

These results suggest that the differences in Fc-effector activity observed across vaccine groups were not explained by broad shifts in sequence-weighted bulk IgG MBC BCR IgH subclass frequencies. Although ferritin immunization produced the highest serum binding titers and avidity indices and soluble trimer immunization demonstrated appreciable Fc-effector activity, they were not accompanied by a distinct shift in the relative abundance of individual IgG subclasses.

3.8.2 Clone-level Subclass Usage in Env-specific and Non-Env-binding Clusters

Clone-level subclass usage was next evaluated within the expanded Env-specific versus non-Env-binding cluster framework (Fig. 8b). Rather than comparing subclass frequencies

across vaccine formats, this analysis asked whether Env-binding clusters differed from non-Env-binding clusters in their class-switching patterns.

Env-specific and non-Env-binding clusters showed broadly similar clone-level subclass usage. IGHG1 and IGHG2 were the most frequently represented subclasses in both groups, while IGHG3 and IGHG4 were detected less frequently. None of the individual subclasses differed significantly between Env-specific and non-Env-binding clusters. This indicates that Env-binding clusters were not distinguished from non-Env-binding clusters by a major shift in clone-level subclass composition.

These results support the interpretation that Env-specific clusters underwent class switching, but their limited functional maturation was not explained by failure to access a particular IgG subclass. Instead, differences between Env-specific and non-Env-binding clusters were more apparent in clonal expansion and mutation-related metrics than in individual subclass usage.

3.8.3 Subclass Entropy

Subclass diversity was assessed to determine whether antigen format altered the breadth or balance of class-switching within the bulk IgG MBC BCR IgH repertoire (Fig. 8c). While individual subclass frequencies describe the overall relative abundance of IGHG1, IGHG2, IGHG3, and IGHG4 sequences within each animal, clone-level subclass entropy captures how evenly those subclasses are represented within individual clonal families. For each clone, Shannon entropy was calculated from the proportions of subclass-assigned sequences belonging to IGHG1, IGHG2, IGHG3, and IGHG4, and clone-level entropy values were then averaged per animal. Higher entropy reflects greater within-clone subclass diversification, whereas lower entropy indicates dominance by fewer subclasses within clones.

Although individual IgG subclass frequencies were broadly similar across vaccine groups, subclass entropy differed by antigen format. The soluble trimer group showed higher

subclass entropy than the multimerized groups, with a significant difference observed between trimer and liposome animals. This indicates that trimer immunization generated a more balanced and diverse IgG subclass repertoire, while ferritin and liposome clones were more restricted to containing fewer subclasses.

Taken together, the subclass analyses indicate that antigen format did not strongly alter the relative abundance of individual IgG subclasses, but did affect the balance of subclass usage across animals. This distinction is important for interpreting Fc-effector function. The lack of improved ADCC or ADCP in the ferritin and liposome groups was unlikely to reflect a broad failure to generate class-switched IgG responses. Instead, Fc-functional differences may reflect more specific features of the antibody response, including antibody specificity, epitope targeting, affinity, subclass balance, Fc glycosylation, or other functional properties not captured by individual subclass frequency alone.

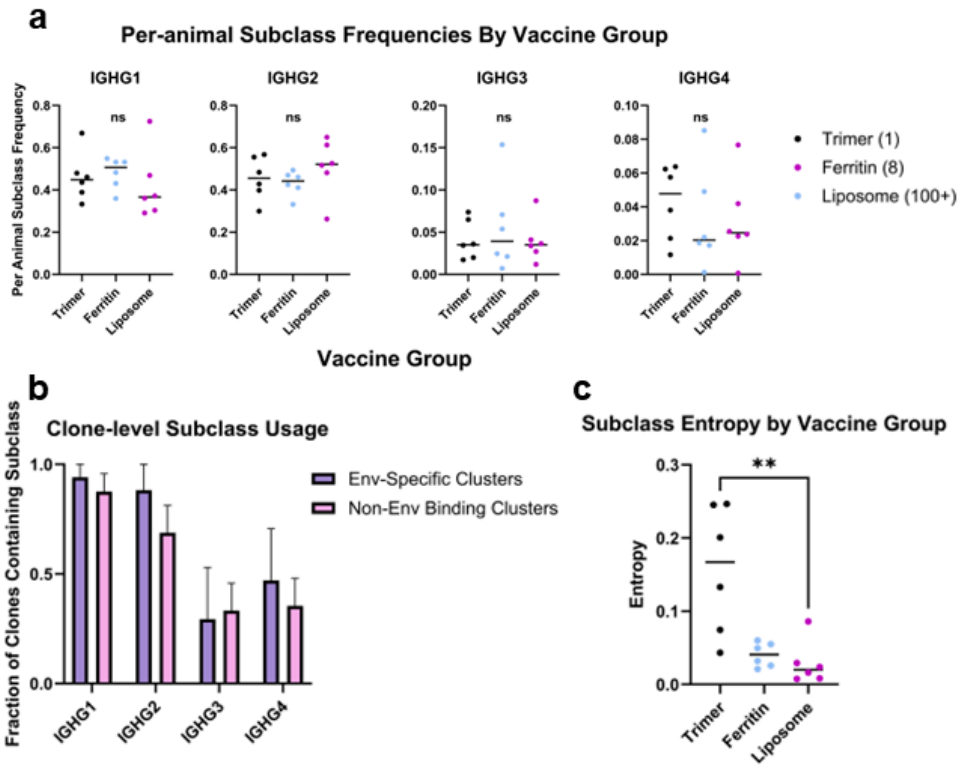

Figure 8. IgG subclass frequencies in bulk IgG MBC BCR IgH repertoires and functionally anchored clusters.

a, Per-animal IgG subclass frequencies calculated from bulk IgG MBC BCR IgH sequencing across trimer-, ferritin-, and liposome-immunized macaques. Each point represents one animal, and horizontal lines indicate group medians. Groups were compared by Kruskal-Wallis test for each subclass; all comparisons were not significant. **b,** Clone-level subclass usage among functionally anchored Env-specific and non-Env-binding clusters pooled across vaccine groups. Bars show the fraction of clusters containing at least one sequence assigned to each IgG subclass. Error bars indicate bootstrap 95% confidence intervals from cluster-level resampling. **c,** Bulk IgG MBC BCR IgH repertoire subclass entropy calculated at the clonal level and averaged per animal across all vaccine groups. Each point represents the mean clone-level subclass entropy for one animal, and horizontal lines indicate group medians. Groups were compared by Kruskal-Wallis test followed by Dunn's multiple comparisons test; trimer versus

ferritin, adjusted p = 0.1363; trimer versus liposome, adjusted p = 0.0074; ferritin versus liposome, adjusted p = 0.9127.

3.9 Discussion

3.9.1 Antigen Multimerization Improved Binding but Not Coordinated Antibody Function

The central hypothesis of this chapter was that increasing the valency of 10014.F8.SOSIP Env would improve both the magnitude and quality of the vaccine-induced antibody response. Based on prior work showing that repetitive antigen display can strengthen BCR engagement, lower activation thresholds, and enhance germinal center recruitment, ferritin- and liposome-displayed Env were expected to produce coordinated improvements across multiple layers of the humoral response[66,75,85]. These expected improvements included higher Env-specific binding titers, increased avidity, broader neutralization, stronger Fc-mediated effector activity, greater expansion of Env-specific lineages, increased SHM, and altered subclass patterns consistent with improved antibody function.

This expectation was only partially met. Ferritin display produced the clearest increase in binding-based serological readouts, with higher endpoint titers and higher avidity than the other antigen formats. This indicates that intermediate-valency ferritin display enhanced quantitative antigen engagement and apparent binding stability. However, this improved binding profile did not translate into a broader or more functional antibody response. Neutralization breadth remained limited, and the ADCC and ADCP activity observed after soluble trimer immunization was not reproduced by either multimerized format.

The loss of detectable Fc-effector activity in the ferritin and liposome groups was one of the chapter's most significant findings. Ferritin immunization produced the strongest binding and avidity profile, yet showed little to no detectable ADCC or ADCP. The loss of ADCC and ADCP

in the ferritin and liposome groups was especially informative because it showed that multivalent antigen display did not merely fail to improve Fc-mediated function, but appeared to redirect the response away from the Fc-functional profile observed after soluble trimer immunization. This indicates that Env-specific binding magnitude and Fc-mediated activity are not interchangeable measures of antibody quality. Rather, they appear to represent at least partially separable features of the antibody response. Antigen format may increase the quantity or apparent binding strength of Env-specific antibodies while failing to induce the antibody epitope specificities, subclass features, immune-complex properties, Fc receptor engagement, or other qualitative characteristics required for Fc-effector function.

This distinction is especially important in HIV-1 vaccine development because Fc-mediated functions have been implicated in protective responses when protective broadly neutralizing antibody activity is absent or incomplete. If the ferritin group had been evaluated only by binding titers or avidity, it would appear to be the most successful vaccine format. However, the lack of detectable ADCC and ADCP shows that stronger binding did not correspond to improved antiviral antibody function. These data therefore argue against using binding magnitude alone as a proxy for response quality.

3.9.2 Multimerization Did Not Overcome the Env-specific Maturation Bottleneck

The repertoire analyses showed that the serological effects of multimerization were not matched by coordinated improvements in B cell maturation. Expanding the functional anchoring framework across the trimer, ferritin, and liposome groups increased the number of Env-specific and non-Env-binding clusters available for comparison, allowing the patterns observed in Chapter 2 to be tested across the broader multimerization cohort.

Across this expanded dataset, Env-specific clusters were detectable and showed evidence of sampled clonal expansion. This supports the conclusion that 10014.F8.SOSIP Env vaccination recruited Env-specific B cells across vaccine formats. However, these clusters remained less mutated than non-Env-binding clusters across multiple measures, including median SHM, root-to-tip distance, and CDR mutation burden. Therefore, increasing antigen valency did not shift Env-specific clusters toward the highly mutated states expected for deeply matured HIV-1 antibody responses.

The relationship between clone size and SHM further suggested that Env-specific clusters were not simply random background lineages. Among Env-specific clusters, larger clone size was associated with higher SHM (Fig. 7e), consistent with some degree of expansion-linked mutation after antigen engagement[69,101,149]. However, the absolute mutation burden of these clusters remained lower than that of non-Env-binding clusters. This pattern supports a model in which Env-specific B cells were recruited and expanded, but did not progress into the highly mutated states associated with more advanced antibody maturation. This restricted maturation profile may suggest that the sequential vaccine response is encountering biological bottlenecks in B cell fate decisions, preventing previously engaged lineages from re-entering active GC reactions to accumulate deeper mutations.

Together, these findings extend the conclusion from Chapter 2. Soluble trimer immunization recruited Env-specific B cells but did not drive them to high levels of mutation or broad antiviral function. Incorporating ferritin and liposome groups showed that this limitation was not eliminated by increasing antigen valency. Multimerization altered some measurable features of the humoral response, particularly ferritin-associated binding titers and avidity, but did not overcome the underlying maturation constraint observed in Env-specific clusters.

3.9.3 Subclass Patterns Suggest Fc-function Differences Are Not Explained by Subclass Frequency Alone

The subclass analyses provided a potential link between antigen format and Fc-mediated function, but did not yield a simple one-to-one explanation for the loss of ADCC and ADCP in the multimerized groups. Across the bulk IgG MBC BCR IgH repertoire, IGHG1 and IGHG2 dominated the class-switched response, whereas IGHG3 and IGHG4 were less frequent. This general pattern was observed across vaccine groups, indicating that all antigen formats induced class-switched antibody responses.

At the clone level, Env-specific and non-Env-binding clusters also showed broadly overlapping subclass profiles. This suggests that the absence of Fc-effector activity in the ferritin and liposome groups was not explained by a complete failure of class switching or by the absence of major IgG subclasses. In other words, the multimerized groups generated Env-specific binding antibodies and class-switched repertoires, but these features were not sufficient to produce detectable ADCC or ADCP.

This interpretation is also consistent with known features of rhesus macaque IgG biology. Unlike human IgG subclasses, which differ substantially in FcγR binding, rhesus IgG subclasses are structurally less divergent and have been reported to bind rhesus FcγRs with similar strength[138]. Therefore, changes in subclass frequency alone may be less likely to fully explain large differences in Fc-effector activity in this model. Subclass balance may still contribute to functional differences, but the absence of ADCC and ADCP in the multimerized groups likely reflects additional qualitative features of the antibody response, such as epitope specificity, Fc glycosylation, or other antibody features not captured by repertoire sequencing.

Subclass entropy was higher in the trimer group, indicating a more balanced subclass distribution than in the multimerized groups. This may be relevant because Fc-mediated activity depends not only on whether antibodies are class-switched, but also on the composition of the

antibody pool and how those antibodies engage antigen and Fc receptors in a functional assay context. However, given the relatively similar FcγR-binding properties of rhesus IgG subclasses, the entropy result should be interpreted as one possible contributor rather than a complete mechanism.

One possible explanation is that multimerized antigen display altered the specificity or composition of the antibody pool rather than simply changing the amount of Env-specific antibody. Ferritin and liposome display may have preferentially recruited or expanded B cells recognizing epitopes that were accessible on the multimerized immunogen but poorly positioned for downstream Fc-effector activity. In this example, multimerization could increase serum binding and apparent avidity while producing antibodies that fail to coat target cells effectively, orient Fc domains appropriately, or form immune complexes capable of productive FcγR engagement. A related possibility is that high-valency antigen lowered the activation threshold for Env-reactive B cells and altered the founder pool of GC selection environment, allowing less functionally useful specificities to expand without being refined into Fc-active lineages. These possibilities are not mutually exclusive and would require additional experiments, such as infected-cell binding, FcγR engagement, and Env-specific glycosylation analyses, to distinguish.

Together, these results suggest that subclass composition may have contributed to the functional differences among vaccine formats, but subclass frequency alone cannot explain the full pattern. Fc-effector activity likely depends on multiple features acting together, including antigen specificity, antibody concentration within functional specificities, immune-complex geometry, Fc receptor engagement, glycosylation, and target-cell antigen presentation. This supports the broader conclusion that antibody binding, class switching, and Fc-mediated function are related but separable outputs of the vaccine response.

3.10 Limitations

Several limitations should be considered when interpreting the multimerization comparisons in this chapter. First, serological assays reflect the activity of the total circulating antibody pool. These measurements are useful for comparing overall binding magnitude, neutralization, ADCP, and ADCC, but they do not identify which B cell lineages or antibody specificities are responsible for the observed activity. This limitation motivated the functional anchoring strategy used in Chapter 2 and expanded here, in which expressed mAbs were used to connect antibody specificity with bulk IgG MBC BCR IgH clusters.

Second, mAb recovery and functional anchoring was not equally comprehensive across vaccine groups. Expressed mAbs represent only a sampled subset of the total Env-specific and non-Env-binding B cell response, and the number of recovered mAbs can be affected by sorting efficiency, cell recovery, expression success, and antigen-binding thresholds. Therefore, Env-specific versus non-Env-binding cluster comparisons should be interpreted as analyses of functionally anchored clusters rather than complete inventories of every Env-reactive clone induced by each vaccine format.

Third, the repertoire analyses were performed on circulating PBMC-derived B cells rather than directly on lymph node GC B cells. Circulating memory B cells and plasmablasts provide important downstream readouts of vaccine-induced B cell maturation, but they may not fully capture the magnitude, timing, or selection dynamics occurring within active GCs. As a result, limited SHM or incomplete functional maturation in the circulating repertoire does not necessarily exclude transient or anatomically restricted GC activity that was not sampled.

Fourth, antigen valency was not the only difference among the vaccine formulations. The soluble trimer and ferritin groups were formulated with Adjuplex, whereas the liposome group used a distinct liposomal formulation containing MPLA and QS-21[150–153]. Because adjuvant composition can influence innate activation, T cell help, GC formation, class switching, and

Fc-functional antibody profiles, differences between the liposome group and the other groups cannot be attributed solely to antigen valency.

Fifth, cluster inference in rhesus macaques is affected by incomplete germline reference information and uncertainty in V gene assignment[92,154]. To reduce the effect of this limitation, clonal clustering used V/J family-level grouping, identical CDRH3 length, and CDRH3 sequence similarity rather than relying exclusively on allele-level germline calls. However, uncertainty in germline assignment can still influence estimates of SHM, cluster structure, and root-to-tip distance.

Finally, the functional assays measured distinct antibody properties and should not be expected to correlate perfectly. Neutralization depends primarily on antibody specificity, epitope accessibility, affinity, and the ability to block viral entry. ADCP and ADCC depend on additional features, including subclass, Fc receptor engagement, antibody orientation, antigen density on the target, and potentially Fc glycosylation. Therefore, the lack of coordination among binding titers, neutralization, ADCP, and ADCC does not indicate assay inconsistency; rather, it reflects the fact that these assays capture different dimensions of antibody quality.

Together, these limitations suggest that the results should be interpreted as evidence that antigen multimerization altered selected features of the 10014.F8.SOSIP Env response, but did not produce a coordinated improvement across serum function and lineage-level maturation. The data support the conclusion that antigen valency alone was insufficient to overcome the maturation bottleneck identified in Chapter 2, while also leaving open the possibility that additional variables, including adjuvant context, immunization timing, GC sampling, and antigen-specific lineage recovery, may influence the outcome of future Env vaccine strategies.

Chapter 4. General Discussion and Future Directions

4.1 Summary of Key Findings Across Chapters

This dissertation examined how HIV-1 10014.F8.SOSIP Env vaccination shaped antibody function and B cell repertoire maturation in rhesus macaques. The central goal was to determine whether serum-level vaccine responses could be connected to the sequence-level features of the B cell lineages that produced them, and whether changing antigen presentation format improved the quality of the response. Across chapters, the major finding was that 10014.F8.SOSIP Env vaccination induced detectable antibody responses and recruited Env-specific B cells, but these responses remained insufficiently mutated and did not produce broad or coordinated antiviral function.

Chapter 2 focused on the soluble 10014.F8.SOSIP trimer group and established the functional anchoring framework used throughout the dissertation. Serum binding responses and 10014.F8-specific mAbs demonstrated that the immunogen was recognized by the humoral immune system. However, neutralization and Fc-mediated activity were limited, indicating that antigen recognition alone was insufficient to generate a broadly functional antibody response. By mapping expressed mAbs back into bulk IgG MBC BCR IgH clonal families, Chapter 2 distinguished Env-specific clusters from non-Env-binding clusters and showed that Env-specific clusters were detectable but remained limited in their progression toward highly mutated antibody states.

Chapter 3 expanded this framework to the full multimerization cohort. The rationale was that increasing antigen valency might improve BCR engagement, lower activation thresholds, broaden clonal recruitment, and enhance GC-driven maturation. This expectation was only

partially supported. Ferritin-displayed 10014.F8.SOSIP produced the highest endpoint titers and avidity indices, showing that moderate multivalent display improved some quantitative serological measures. However, these improvements did not translate into broader neutralization or stronger Fc-mediated activity. The ADCC and ADCP activity observed after soluble trimer immunization was not reproduced by the ferritin or liposome groups.

The expanded repertoire analyses similarly showed that antigen engagement and functional maturation were separable outcomes. Incorporating ferritin and liposome animals increased the number of functionally anchored clusters available for Env-specific versus non-Env-binding comparisons. Env-specific clusters showed evidence of sampled clonal expansion and a relationship between clone size and SHM, consistent with antigen-driven recruitment into maturation pathways. However, even with the addition of multimer-derived clusters, Env-specific clusters remained less mutated than non-Env-binding clusters across multiple mutation-related metrics. These data indicate that Env-specific lineages were recruited but did not progress to the highly mutated states associated with mature HIV-1 antibody responses.

IgG subclass analyses added another layer to this interpretation. Bulk IgG MBC BCR IgH and clone-level subclass usage showed that all vaccine groups generated class-switched IgG repertoires dominated by IGHG1 and IGHG2, with lower representation of IGHG3 and IGHG4. Individual subclass frequencies did not strongly explain differences in Fc-effector activity. However, subclass entropy was higher in the trimer group, suggesting a more balanced subclass repertoire than in the multimerized groups. This may help explain why the trimer group showed the clearest Fc-effector activity despite lower overall binding magnitude than ferritin.

Together, these findings support a model in which 10014.F8.SOSIP Env vaccination successfully initiated humoral responses but failed to drive coordinated functional maturation. Antigen multimerization changed selected features of the response, especially ferritin-associated binding magnitude and avidity, but did not produce a unified improvement in

neutralization, Fc-effector function, SHM, or Env-specific B cell maturation. The key limitation was therefore not complete failure of antigen recognition, but incomplete progression from antigen engagement to functionally mature antibody states.

4.2 **Implications for HIV-1 Vaccine Development**

The results of this dissertation reinforce a central challenge in HIV-1 vaccine development: the type of B cell maturation required for protective HIV-1 antibody responses appears to exceed what conventional vaccination usually achieves. Many HIV-1 bNAbs are highly diverged from germline, often requiring mutation levels on the order of ~20% or more[110]. In contrast, it is difficult to identify approved human vaccines where antigen-specific B cell populations routinely reach comparable levels of SHM. Even vaccine-induced subsets exceeding ~10% SHM appear uncommon. Population-level averages or medians above ~6% are not typical for most conventional vaccine responses[107,108]. This creates a fundamental mismatch between the biology of HIV-1 antibody protection and the maturation trajectories usually produced by vaccination.

This mismatch raises a difficult question for HIV vaccinology: whether current vaccine technologies can realistically generate the degree of antibody evolution needed for broad protection. This does not mean that vaccine-elicited bNAbs are biologically impossible. However, it does suggest that HIV-1 vaccines are being asked to reproduce, through a controlled immunization series, a level of antibody evolution that natural infection often rarely achieves only after years of antigenic exposure, viral escape, and repeated immune selection/tolerance. In this context, the limited SHM observed in Env-specific clusters in this study may not simply reflect a shortcoming of one immunogen or one antigen format. It may reflect a broader limitation of current vaccine approaches: they can recruit Env-reactive B cells,

but they may not sustain or direct those cells through enough iterations of mutation and selection to generate highly matured antibody function.

Several emerging vaccine strategies attempt to address this problem by extending antigen exposure or altering the kinetics of immune stimulation. Escalating-dose regimens, slow-delivery approaches, osmotic pumps, and related technologies are designed to prolong antigen availability, sustain GC activity, and more closely mimic the extended antigenic stimulation that occurs during chronic infection. Conceptually, these approaches are attractive because the desired HIV-1 antibody responses likely require more than a brief pulse of antigen and a standard boost schedule. They may require prolonged or repeated GC selection events that allow rare lineages to accumulate useful mutations over time.

However, these approaches must be weighed against the practical realities of vaccine deployment. A proof-of-concept HIV vaccine regimen can be technically complex, expensive, and labor-intensive if the goal is to show that a particular immune trajectory can be induced under optimized experimental conditions. A deployable vaccine must meet a much higher bar. It would need to be affordable, scalable, stable, acceptable to recipients, and feasible to administer in the populations most affected by HIV-1. Cost-effectiveness modeling highlights this constraint. In one analysis of low-income countries, a three-dose HIV-1 vaccine regimen needed to cost below approximately US $20-25 per full regimen under full scale-up assumptions, or US $35-40 under 50% scale-up assumptions, to be considered highly cost-effective[155]. This emphasizes that vaccine complexity, dose number, and manufacturing cost are not secondary implementation details, but central features of whether an HIV-1 vaccine could have population-level impact. A strategy that depends on implanted pumps, repeated clinic visits, or highly individualized dosing may be scientifically informative while still being difficult to translate into an effective public health intervention. The field may be able to demonstrate that certain bNAb-like pathways can be initiated or pushed forward experimentally, while still falling short of a regimen that can be deployed at the scale needed for HIV prevention.

This problem is especially important given the limited success of other major HIV vaccine strategies. T cell-based vaccine approaches have repeatedly failed to provide reliable protection despite strong theoretical rationale and substantial investment. At the same time, the most notable efficacy signal in the HIV vaccine field, RV144, was not associated with broad neutralization. Instead, protection was linked more closely to non-neutralizing antibody functions, including Fc-mediated activity such as ADCC and related effector mechanisms. This suggests that a successful HIV vaccine may not be built around a single immune mechanism. My interpretation is that the most plausible future HIV vaccine strategy may need to be combinatorial, much like antiretroviral therapy. Rather than relying entirely on one immune pathway, an effective vaccine may need to combine approaches that promote bNAb development, Fc-effector function, mucosal protection, and possibly T cell immunity within the same regimen.

If bNAbs are to remain the gold standard for HIV vaccine development, then SHM should be treated as one of the most important early metrics of vaccine success. Binding titers, antigen-specific B cell frequencies, and even clonal expansion are not sufficient if vaccine-induced lineages do not accumulate the mutations needed for bNAb activity. In that framework, SHM is not just a descriptive repertoire feature; it is a necessary intermediate phenotype. Without sufficient mutation, the field should not expect vaccine-induced lineages to reach bNAb-like function. This does not mean that SHM alone proves success, because many highly mutated antibodies are irrelevant or non-neutralizing. However, in the context of bNAb-directed vaccination, insufficient SHM is a clear warning sign that the desired outcome is unlikely.

The results from this dissertation also emphasize that stronger serological immunogenicity does not necessarily indicate better vaccine quality. Ferritin-displayed 10014.F8.SOSIP Env produced the highest binding titers and avidity indices, yet these improvements did not translate into broader neutralization or stronger Fc-mediated function.

ADCC and ADCP were most apparent in the soluble trimer group, not the multimerized groups. This distinction is important because binding magnitude is often used as a primary endpoint for immunogenicity and, by extension, as an early indicator of vaccine success. However, these results support an increasingly apparent disconnect between antibody quantity and antibody function. For HIV-1 Env, more antibody is not necessarily better antibody. A vaccine format can improve endpoint titers while failing to improve the specificities, mutation states, subclass balance, or Fc properties needed for antiviral function.

These findings also argue against blindly treating antigen multimerization as an inherently beneficial design feature. Multimerization can increase BCR engagement, antigen avidity, and serum binding magnitude, but those effects do not guarantee productive maturation. In this study, multimerized antigen formats did not improve neutralization breadth, potency, or Fc-effector activity relative to soluble trimer. In fact, adding multimerization appeared unfavorable for Fc-effector activity in this system, as the trimer group showed the clearest ADCC and ADCP responses. Subclass entropy was also higher in the trimer group and lower in the multimerized groups, suggesting that multimerization may have narrowed the balance of subclass usage. This raises the possibility that antigen display format can shape the immune response in multiple directions at once: increasing some quantitative features, such as binding titers, while reducing or failing to improve qualitative features, such as Fc-effector activity or subclass balance.

A major implication is that antigen engagement and productive maturation should be treated as separable stages of the vaccine response. The vaccine did not fail at the first step. Env-binding B cells were recruited, Env-specific clusters were recovered, and those clusters showed evidence of sampled clonal expansion. The related clone size and SHM dynamic observed in Env-specific clusters further suggests that these lineages were not random background clones, but were engaged in a process consistent with expansion-linked mutation. The limitation was that this process did not progress far enough. Env-specific clusters remained

less mutated than non-Env-binding clusters and did not acquire broad or coordinated antiviral function.

This interpretation raises broader questions about whether traditional vaccine logic is sufficient for HIV-1. Many vaccines work by inducing memory B cells that can rapidly respond upon re-exposure. Recent fate-mapping studies indicate that the immune system populates the MBC compartment with diverse, lower-affinity B cells with limited SHM to maintain a broad repertoire capable of recognizing mutated viral variants upon future exposures[71]. While this evolutionary strategy is highly effective for anticipating standard viral drift, it may be fundamentally counterproductive for HIV-1 vaccine design.

For HIV-1, the desired outcome requires these specific memory lineages to undergo repeated GC participation over extended periods of time to accumulate the extraordinarily high levels of mutation required for broadly neutralizing activity. However, this repeated participation is not guaranteed. Secondary GC responses are often substantially populated by newly recruited naïve B cells, and memory B cell reentry into new GCs can be highly limited or selective[89]. If each boost recruits new naïve clones rather than forcing the desired memory lineages back into productive mutation and selection, then sequential vaccination may not move the same lineages forward in the intended way. This is a central problem for germline-targeting and lineage-guided vaccine strategies.

Addressing this problem may require vaccine approaches that actively regulate GC membership rather than simply providing antigen and adjuvant. Future strategies may need adjuvants or immunization conditions that favor memory B cell reentry, preserve lineage continuity across boosts, and reduce repeated recruitment of naïve competitors. Temporary blockade of naïve B cell recruitment could also be considered as a speculative strategy, if it could be done safely and transiently. The goal would not be broad immunosuppression, but rather selective control over which B cell populations are allowed to compete for antigen and T cell help during later stages of a vaccine regimen. If the desired lineages must accumulate

mutations over multiple rounds of selection, then the field needs ways to ensure that the same lineages actually reenter and persist in GCs.

In my view, B cells are the key unresolved problem in HIV vaccine development. T cell immunity may contribute, Fc-effector function may matter, and antigen design is clearly important, but none of these can substitute for understanding how to control B cell fate. The major challenge is not simply making better Env proteins. It is learning how to manipulate B cell recruitment, GC entry, memory reentry, mutation accumulation, class switching, and functional selection in a predictable way. Current vaccine technologies may be able to demonstrate pieces of this process, but the field may not yet understand enough foundational B cell biology to reliably engineer the complete trajectory needed for a practical HIV vaccine.

Tolerance may represent another major barrier. Some bNAb precursors or intermediates may be autoreactive, polyreactive, or cross-reactive. These features may limit their availability or survival under normal immune conditions. Chronically infected individuals who eventually develop bNAbs may experience altered inflammatory, antigenic, and tolerance environments that permit rare or normally disfavored B cell lineages to survive and evolve. If this is true, then vaccination may fail not only because it provides insufficient antigenic stimulation, but because the immune system actively suppresses or excludes some of the lineages with the greatest antiviral potential. Temporary or localized tolerance modulation is therefore an outlandish but logically relevant possibility. Such an approach would carry obvious safety concerns, but it highlights a central issue: the lineages most useful for HIV protection may not be the lineages that a healthy immune system most readily permits to expand.

A greater focus on mucosal vaccination may also be necessary. HIV acquisition typically occurs at mucosal surfaces, yet many vaccine studies prioritize (due to ease) serum binding and serum neutralization. A vaccine that fails to induce perfect systemic bNAb responses might still provide meaningful protection if it creates a strong local barrier at the portal of entry. Mucosal antibodies, tissue-resident immune cells, Fc-effector activity, and local innate responses may all

contribute to preventing founder virus expansion. This would represent a different model of success: not necessarily sterilizing neutralization in serum, but rapid containment/elimination or prevention of establishment at the mucosal site of exposure. Given the difficulty of eliciting mature bNAbs through conventional vaccination, mucosal and Fc-focused strategies may deserve more attention as practical components of a combined HIV vaccine approach.

A related interpretive issue concerns how repertoire sequencing is used to infer vaccine-driven maturation. High SHM in a bulk IgG MBC BCR IgH repertoire is not evidence of successful vaccine-driven maturation unless antigen specificity is established. We demonstrated in this work that mature primate immune repertoires already contain highly mutated memory B cells, most likely generated by prior environmental exposures. These background lineages can dominate the high-SHM compartment and obscure the features of Env-specific clones. Without functional anchoring or binding validation, a study could mistake highly mutated background sequences for evidence that vaccination drove extensive maturation. This is especially problematic in HIV-1 vaccine studies, where the desired antigen-specific lineages may be rare and the relevant functional phenotypes are difficult to infer from sequence alone.

For this reason, high-throughput sequencing should be coupled with functional validation whenever possible. Bulk repertoire sequencing provides depth, but it is traditionally antigen-agnostic. Antigen-specific single-cell sorting improves specificity, but sorting alone should be treated as enrichment rather than proof of binding. Probe binding can be affected by avidity, non-specific staining, cell handling, gating strategy, and sorting thresholds[156]. Sorting strategies may also miss low-affinity B cells that would still be biologically relevant *in vivo*. A B cell with weak measurable binding to a soluble probe may fail to sort cleanly, yet still participate in a GC response where antigen is presented in a native, membrane-associated, or immune-complexed form[66,101,157,158]. Therefore, sorted antigen-positive cells are not necessarily a complete representation of the vaccine-relevant precursor or responding pool, and

antigen-negative sorted cells cannot be assumed to represent an entirely vaccine-irrelevant population.

This problem may be even more complicated for HIV-1 bNAb precursors. Some precursor B cells may be autoreactive, polyreactive, or cross-reactive in ways that make them difficult to identify with standard antigen probes. Others may not bind the vaccine antigen strongly until after specific intermediate mutations have accumulated. In chronically infected individuals, years of viral evolution may create unusual selection environments that eventually permit these lineages to emerge. Standard sorting strategies may never capture the full set of cells capable of giving rise to bNAbs because the relevant starting cells may be weak binders, off-target binders, autoreactive cells subject to tolerance, or cells whose future potential is not obvious from their current binding phenotype. This means that even antigen-specific sequencing may systematically miss some of the cells that matter most.

Sequencing without functional validation can describe a repertoire, but it cannot prove that a sequence encodes the antibody function being inferred from it. Binding validation requires antibody expression. A subset of antibodies should be expressed and tested directly for antigen binding and function. As antibody expression becomes cheaper and faster, this should become a standard part of vaccine repertoire studies rather than an optional follow-up. This is particularly important when conclusions depend on whether lineages are truly Env-specific, whether they bind native-like Env, whether they target relevant epitopes, or whether they mediate neutralization or Fc-effector function.

A major technological limitation is that antibody sequence alone still cannot reliably determine epitope specificity or functional potential. High-throughput sequencing has made it possible to characterize B cell repertoires at enormous depth, but the interpretive value of those data remains limited by the inability to confidently map sequence to specificity. In principle, if epitope specificity could be accurately predicted from antibody sequence, repertoire sequencing would become far more powerful. It would allow near-complete characterization of the

antigen-specific response to vaccination, including which epitopes were targeted, which lineages were expanding, which lineages were maturing, and whether the response was moving toward or away from desired antibody classes.

This would be especially valuable for HIV-1 vaccine development because the relevant lineages are rare, the background repertoire is complex, and the difference between useful and distracting Env-binding responses can be subtle. Many Env-reactive antibodies bind immunodominant but non-protective surfaces, while the lineages with the greatest protective potential may be rare, weakly binding, or developmentally constrained. If sequence alone could consistently and accurately identify whether an antibody targeted the CD4 binding site, V3 glycan supersite, V1/V2 apex, fusion peptide, gp120-gp41 interface, base epitopes, or non-neutralizing exposed surfaces, vaccine studies could be evaluated with much greater resolution. Instead of relying on limited mAb panels and partial sorting strategies, investigators could ask whether the entire responding repertoire was being directed toward protective or non-protective epitope classes.

Current technologies are not yet able to do this reliably. Antibody sequence contains important information about clonality, SHM, CDRH3 length, germline gene usage, and in some cases recognizable public antibody classes. However, for most antibodies, sequence features alone are insufficient to consistently determine exact antigen specificity, epitope targeting, binding orientation, neutralization potential, or Fc-functional relevance. This is why antibody expression and functional validation remain necessary. Sequencing can prioritize candidates, define clusters, and suggest maturation patterns, but it cannot yet replace direct measurement of binding and function.

That said, this is an area where aggressive technological development could substantially change the field. Advances in structural modeling, including tools conceptually related to AlphaFold and related antibody-antigen modeling frameworks, should be pursued as far as technically possible[159–161]. If antibody structure, antigen docking, and epitope recognition

could be predicted accurately from sequence at scale, high-throughput repertoire sequencing could move from descriptive immunology toward functional repertoire reconstruction. Even imperfect models could be useful if they reliably classified broad epitope families or excluded irrelevant binders. Such tools would not eliminate the need for experimental validation, but they could make validation more efficient by prioritizing the most informative antibodies and lineages for expression.

In my view, this kind of sequence-to-specificity prediction would be one of the most important technological advances for HIV vaccinology. It would address a core limitation of current studies: we can generate far more sequence data than we can functionally interpret. Without reliable specificity prediction, most repertoire sequencing remains partially blind. With it, vaccine studies could begin to evaluate not only whether B cells expanded and mutated, but whether the right B cells expanded and mutated. For a vaccine problem as lineage-dependent as HIV-1, that distinction is central.

Another possibility raised by these data is that HIV vaccine failure may not only reflect insufficient promotion of desired lineages, but also insufficient suppression of undesired lineages. Vaccination induces a competitive B cell response. The problem may not be simply that rare protective precursors fail to mature, but that immunodominant, non-neutralizing, or otherwise unhelpful lineages are preferentially recruited and occupy the available GC or T cell help space. In this model, better vaccines would need to do two things simultaneously: promote the lineages with protective potential and limit the expansion or maturation of distracting responses. Multimerization could potentially worsen this problem if it amplifies BCR engagement broadly, increasing the magnitude of binding responses without improving the quality of lineage selection.

This has implications for how HIV-1 vaccine studies should define success. The central question should not simply be whether a vaccine induces Env-specific antibodies. The more important question is whether the vaccine recruits appropriate lineages and moves them

through a trajectory that plausibly leads to protection. Useful readouts should include whether Env-specific lineages expand, whether they accumulate SHM, whether they maintain or improve binding to relevant Env conformations, whether they avoid immunodominant non-protective epitopes, whether they class switch into productive Fc states, whether they persist or recall upon boosting, and whether they are present at relevant mucosal sites. No single assay captures this entire trajectory.

Overall, these findings suggest that future HIV-1 vaccine design should focus less on maximizing any single readout and more on coordinating multiple features of the response. Antigen valency, epitope specificity, antigen persistence, adjuvant choice, boost timing, Tfh support, tolerance constraints, GC reentry dynamics, mucosal immunity, and suppression of distracting lineages are likely to interact. Improving one feature, such as binding titer, may not be sufficient if the response does not also acquire the necessary mutation burden, subclass balance, epitope targeting, anatomical localization, and antiviral function. The challenge is not simply to make Env immunogens more immunogenic, but to design vaccine regimens that guide Env-specific B cells through a maturation pathway that existing vaccine approaches have not yet reliably achieved.

Taken together, this work suggests a sober interpretation of current HIV-1 vaccine technology. It may be possible to generate proof-of-concept responses that resemble early stages of bNAb development, especially with carefully engineered immunogens and complex delivery strategies. However, producing a practical vaccine capable of reliably inducing mature, protective bNAb-like responses in humans may require advances beyond the conventional vaccine framework. A successful HIV vaccine may ultimately need to combine strategies that separately promote bNAb development, Fc-effector function, mucosal immunity, and perhaps T cell immunity, while also suppressing distracting B cell responses that consume immune resources without contributing to protection. The field may need to fully move from simple “prime and boost” models toward more precise control of B cell lineage selection, GC persistence,

tolerance modulation, memory B cell reentry, sequence-guided epitope tracking, mucosal protection, and functional antibody maturation.

4.3 **Future Research Directions**

Future work should directly sample the anatomical sites where vaccine-driven B cell selection and antibody production occur. Lymph node biopsies would allow direct analysis of GC B cells, Tfh cells, and antigen-specific clonal evolution during the vaccine response, while bone marrow and tissue-resident plasma cell analyses would help define the antibody-secreting lineages that contribute directly to serum activity. This would help determine whether the limited maturation observed in PBMC-derived repertoires reflects weak GC induction, premature GC collapse, altered GC selection, or failure of matured GC clones to enter the circulating memory, plasmablast, or plasma cell compartments, or discordance between peripheral repertoires and the cells responsible for serum antibody production.

A second priority is to expand antigen-specific mAb recovery across all vaccine groups and timepoints. Deeper mAb sampling would improve the resolution of functional anchoring and reduce uncertainty caused by uneven lineage recovery. Larger panels of expressed antibodies would also allow more detailed analysis of epitope targeting, neutralization potential, ADCP, ADCC, subclass effects, and sequence-function relationships. This would be especially useful for determining whether ferritin and liposome groups generated Env-binding clones with distinct specificities or whether they primarily expanded non-neutralizing or poorly functional antibody populations. Future studies should determine whether the loss of Fc-mediated activity after multimerized Env vaccinations reflects altered infected-cell Env recognition, shifted epitope specificity, reduced FcγR engagement, altered Env-specific Fc-glycosylation, changes in Tfh/cytokine-driven class-switch programming, or differences in antigen trafficking and follicular retention.

Future studies should also test immunization regimens designed to extend or redirect maturation. Delayed fractional dosing, prolonged antigen exposure, sequential Env immunization, or modified boost timing could be used to determine whether Env-specific lineages can be pushed beyond the intermediate SHM states observed in this study. Because HIV-1 bNAbs often require extensive maturation, altering the kinetics of antigen exposure and GC selection may be as important as altering antigen valency.

Additional work should examine how adjuvant context interacts with antigen format. In this study, antigen valency and formulation were not completely separable, especially for the liposome group. Future experiments could compare antigen formats using matched adjuvants or compare adjuvants using the same antigen format. This would help determine whether differences in Fc-effector activity, subclass entropy, or SHM are driven by antigen display, innate immune programming, T cell help, or combinations of these variables.

Another direction is to integrate Fc profiling more deeply into repertoire analysis. Subclass frequency alone did not explain functional differences across groups, and Fc-effector function likely depends on additional features such as Fc glycosylation, antibody orientation, epitope specificity, and target-cell antigen density. Pairing Hinge-Seq or single-cell BCR sequencing with Fc glycan profiling and mAb functional assays would provide a more complete view of how B cell sequence features translate into Fc-mediated activity.

Bibliography

1. Sather, D. N. *et al.* Factors associated with the development of cross-reactive neutralizing antibodies during human immunodeficiency virus type 1 infection. *J. Virol.* **83**, 757–769 (2009).
2. Sather, D. N. *et al.* Broadly neutralizing antibodies developed by an HIV-positive elite neutralizer exact a replication fitness cost on the contemporaneous virus. *J. Virol.* **86**, 12676–12685 (2012).
3. Fisher, B. S. *et al.* Oral Immunization with HIV-1 Envelope SOSIP trimers elicits systemic immune responses and cross-reactive anti-V1V2 antibodies in non-human primates. *PLoS One* **15**, e0233577 (2020).
4. Sanders, R. W. *et al.* Stabilization of the soluble, cleaved, trimeric form of the envelope glycoprotein complex of human immunodeficiency virus type 1. *J. Virol.* **76**, 8875–8889 (2002).
5. Binley, J. M. *et al.* A recombinant human immunodeficiency virus type 1 envelope glycoprotein complex stabilized by an intermolecular disulfide bond between the gp120 and gp41 subunits is an antigenic mimic of the trimeric virion-associated structure. *J. Virol.* **74**, 627–643 (2000).
6. Sanders, R. W. *et al.* A next-generation cleaved, soluble HIV-1 Env trimer, BG505 SOSIP.664 gp140, expresses multiple epitopes for broadly neutralizing but not non-neutralizing antibodies. *PLoS Pathog.* **9**, e1003618 (2013).
7. Pugach, P. *et al.* A native-like SOSIP.664 trimer based on an HIV-1 subtype B env gene. *J. Virol.* **89**, 3380–3395 (2015).
8. Guenaga, J. *et al.* Structure-guided redesign increases the propensity of HIV Env to generate highly stable soluble trimers. *J. Virol.* **90**, 2806–2817 (2015).
9. Klasse, P. J. *et al.* Influences on trimerization and aggregation of soluble, cleaved HIV-1

SOSIP envelope glycoprotein. *J. Virol.* **87**, 9873–9885 (2013).

10. Sather, D. N. *et al.* Emergence of broadly neutralizing antibodies and viral coevolution in two subjects during the early stages of infection with human immunodeficiency virus type 1. *J. Virol.* **88**, 12968–12981 (2014).
11. Ackerman, M. E. *et al.* A robust, high-throughput assay to determine the phagocytic activity of clinical antibody samples. *J. Immunol. Methods* **366**, 8–19 (2011).
12. Thomas, A. S. *et al.* A new cell line for assessing HIV-1 antibody dependent cellular cytotoxicity against a broad range of variants. *J. Immunol. Methods* **480**, 112766 (2020).
13. Zhang, F. *et al.* Phenotypic characterization of Chinese rhesus macaque plasmablasts for cloning antigen-specific monoclonal antibodies. *Front. Immunol.* **10**, 2426 (2019).
14. Gupta, N. T. *et al.* Change-O: a toolkit for analyzing large-scale B cell immunoglobulin repertoire sequencing data. *Bioinformatics* **31**, 3356–3358 (2015).
15. Gupta, N. T. *et al.* Hierarchical clustering can identify B cell clones with high confidence in Ig repertoire sequencing data. *J. Immunol.* **198**, 2489–2499 (2017).
16. Katoh, K., Misawa, K., Kuma, K.-I. & Miyata, T. MAFFT: a novel method for rapid multiple sequence alignment based on fast Fourier transform. *Nucleic Acids Res.* **30**, 3059–3066 (2002).
17. Minh, B. Q. *et al.* IQ-TREE 2: New models and efficient methods for phylogenetic inference in the genomic era. *Mol. Biol. Evol.* **37**, 1530–1534 (2020).
18. Knight, L. *UNAIDS: The First 10 Years, 1996-2006*. (UNAIDS Office, Geneva, 2008).
19. 2025 UN AIDS Global HIV Factsheet.
20. Ghosn, J., Taiwo, B., Seedat, S., Autran, B. & Katlama, C. HIV. *Lancet* **392**, 685–697 (2018).
21. Ng'uni, T., Chasara, C. & Ndhlovu, Z. M. Major scientific hurdles in HIV vaccine development: Historical perspective and future directions. *Front. Immunol.* **11**, 590780 (2020).

22. Pejchal, R. *et al.* A potent and broad neutralizing antibody recognizes and penetrates the HIV glycan shield. *Science* **334**, 1097–1103 (2011).
23. Piantadosi, A. *et al.* Breadth of neutralizing antibody response to human immunodeficiency virus type 1 is affected by factors early in infection but does not influence disease progression. *J. Virol.* **83**, 10269–10274 (2009).
24. Simonich, C. A. *et al.* Kappa chain maturation helps drive rapid development of an infant HIV-1 broadly neutralizing antibody lineage. *Nat. Commun.* **10**, 2190 (2019).
25. Hoot, S. *et al.* Recombinant HIV envelope proteins fail to engage germline versions of anti-CD4bs bNAbs. *PLoS Pathog.* **9**, e1003106 (2013).
26. Wu, X. *et al.* Focused evolution of HIV-1 neutralizing antibodies revealed by structures and deep sequencing. *Science* **333**, 1593–1602 (2011).
27. West, A. P., Jr, Diskin, R., Nussenzweig, M. C. & Bjorkman, P. J. Structural basis for germ-line gene usage of a potent class of antibodies targeting the CD4-binding site of HIV-1 gp120. *Proc. Natl. Acad. Sci. U. S. A.* **109**, E2083–90 (2012).
28. Zhou, T. *et al.* Multidonor analysis reveals structural elements, genetic determinants, and maturation pathway for HIV-1 neutralization by VRC01-class antibodies. *Immunity* **39**, 245–258 (2013).
29. Coulson, M. Why Don't We Have an HIV Vaccine? *John Hopkins University* https://publichealth.jhu.edu/2022/why-dont-we-have-an-hiv-vaccine (2022).
30. Barré-Sinoussi, F. *et al.* Isolation of a T-lymphotropic retrovirus from a patient at risk for acquired immune deficiency syndrome (AIDS). *Science* **220**, 868–871 (1983).
31. Gallo, R. C. *et al.* Frequent detection and isolation of cytopathic retroviruses (HTLV-III) from patients with AIDS and at risk for AIDS. *Science* **224**, 500–503 (1984).
32. Finzi, D. *et al.* Identification of a reservoir for HIV-1 in patients on highly active antiretroviral therapy. *Science* **278**, 1295–1300 (1997).
33. Korber, B. *et al.* Evolutionary and immunological implications of contemporary HIV-1

variation. *Br. Med. Bull.* **58**, 19–42 (2001).

34. Zagury, D. *et al.* Immunization against AIDS in humans. *Nature* **326**, 249–250 (1987).
35. Zagury, D. *et al.* A group specific anamnestic immune reaction against HIV-1 induced by a candidate vaccine against AIDS. *Nature* **332**, 728–731 (1988).
36. Dolin, R. *et al.* The safety and immunogenicity of a human immunodeficiency virus type 1 (HIV-1) recombinant gp160 candidate vaccine in humans. NIAID AIDS Vaccine Clinical Trials Network. *Ann. Intern. Med.* **114**, 119–127 (1991).
37. Cooney, E. L. *et al.* Safety of and immunological response to a recombinant vaccinia virus vaccine expressing HIV envelope glycoprotein. *Lancet* **337**, 567–572 (1991).
38. Pitisuttithum, P. *et al.* Randomized, double-blind, placebo-controlled efficacy trial of a bivalent recombinant glycoprotein 120 HIV-1 vaccine among injection drug users in Bangkok, Thailand. *J. Infect. Dis.* **194**, 1661–1671 (2006).
39. Flynn, N. M. *et al.* Placebo-controlled phase 3 trial of a recombinant glycoprotein 120 vaccine to prevent HIV-1 infection. *J. Infect. Dis.* **191**, 654–665 (2005).
40. Rerks-Ngarm, S. *et al.* Vaccination with ALVAC and AIDSVAX to prevent HIV-1 infection in Thailand. *N. Engl. J. Med.* **361**, 2209–2220 (2009).
41. Tomaras, G. D. *et al.* Vaccine-induced plasma IgA specific for the C1 region of the HIV-1 envelope blocks binding and effector function of IgG. *Proc. Natl. Acad. Sci. U. S. A.* **110**, 9019–9024 (2013).
42. Chung, A. W. *et al.* Polyfunctional Fc-effector profiles mediated by IgG subclass selection distinguish RV144 and VAX003 vaccines. *Sci. Transl. Med.* **6**, 228ra38 (2014).
43. Robb, M. L. *et al.* Risk behaviour and time as covariates for efficacy of the HIV vaccine regimen ALVAC-HIV (vCP1521) and AIDSVAX B/E: a post-hoc analysis of the Thai phase 3 efficacy trial RV 144. *Lancet Infect. Dis.* **12**, 531–537 (2012).
44. Chung, A. W. & Alter, G. Systems serology: profiling vaccine induced humoral immunity against HIV. *Retrovirology* **14**, 57 (2017).

45. Rerks-Ngarm, S. *et al.* Randomized, Double-Blind Evaluation of Late Boost Strategies for HIV-Uninfected Vaccine Recipients in the RV144 HIV Vaccine Efficacy Trial. *J. Infect. Dis.* **215**, 1255–1263 (2017).
46. Easterhoff, D. *et al.* Boosting of HIV envelope CD4 binding site antibodies with long variable heavy third complementarity determining region in the randomized double blind RV305 HIV-1 vaccine trial. *PLoS Pathog.* **13**, e1006182 (2017).
47. Pitisuttithum, P. *et al.* Late boosting of the RV144 regimen with AIDSVAX B/E and ALVAC-HIV in HIV-uninfected Thai volunteers: a double-blind, randomised controlled trial. *Lancet HIV* **7**, e238–e248 (2020).
48. Costanzo, M. C. *et al.* ALVAC-HIV and AIDSVAX B/E vaccination induce improved immune responses compared with AIDSVAX B/E vaccination alone. *JCI Insight* **8**, (2023).
49. Bekker, L.-G. *et al.* Subtype C ALVAC-HIV and bivalent subtype C gp120/MF59 HIV-1 vaccine in low-risk, HIV-uninfected, South African adults: a phase 1/2 trial. *Lancet HIV* **5**, e366–e378 (2018).
50. Gray, G. E. *et al.* Vaccine Efficacy of ALVAC-HIV and Bivalent Subtype C gp120-MF59 in Adults. *N. Engl. J. Med.* **384**, 1089–1100 (2021).
51. Gray, G. E. *et al.* HVTN 097: Evaluation of the RV144 vaccine regimen in HIV uninfected south African adults. *AIDS Res. Hum. Retroviruses* **30**, A33–A34 (2014).
52. Hammer, S. M. *et al.* Efficacy trial of a DNA/rAd5 HIV-1 preventive vaccine. *N. Engl. J. Med.* **369**, 2083–2092 (2013).
53. Kenny, A. *et al.* Immune correlates analysis of the Imbokodo (HVTN 705/HPX2008) efficacy trial of a mosaic HIV-1 vaccine regimen evaluated in Southern African people assigned female sex at birth: a two-phase case-control study. *EBioMedicine* **108**, 105320 (2024).
54. Mayr, L. M., Su, B. & Moog, C. Non-Neutralizing Antibodies Directed against HIV and Their Functions. *Front. Immunol.* **8**, 1590 (2017).
55. Corey, L. *et al.* Two Randomized Trials of Neutralizing Antibodies to Prevent HIV-1

Acquisition. *N. Engl. J. Med.* **384**, 1003–1014 (2021).

56. Caniels, T. G. *et al.* Precise targeting of HIV broadly neutralizing antibody precursors in humans. *Science* **389**, eadv5572 (2025).
57. McGuire, A. T. *et al.* Engineering HIV envelope protein to activate germline B cell receptors of broadly neutralizing anti-CD4 binding site antibodies. *J. Exp. Med.* **210**, 655–663 (2013).
58. Jardine, J. *et al.* Rational HIV immunogen design to target specific germline B cell receptors. *Science* **340**, 711–716 (2013).
59. Jardine, J. G. *et al.* HIV-1 VACCINES. Priming a broadly neutralizing antibody response to HIV-1 using a germline-targeting immunogen. *Science* **349**, 156–161 (2015).
60. Jardine, J. G. *et al.* HIV-1 broadly neutralizing antibody precursor B cells revealed by germline-targeting immunogen. *Science* **351**, 1458–1463 (2016).
61. Cohen, K. W. *et al.* A first-in-human germline-targeting HIV nanoparticle vaccine induced broad and publicly targeted helper T cell responses. *Sci. Transl. Med.* **15**, eadf3309 (2023).
62. Bonsignori, M. *et al.* Staged induction of HIV-1 glycan-dependent broadly neutralizing antibodies. *Sci. Transl. Med.* **9**, (2017).
63. Haynes, B. F., Kelsoe, G., Harrison, S. C. & Kepler, T. B. B-cell-lineage immunogen design in vaccine development with HIV-1 as a case study. *Nat. Biotechnol.* **30**, 423–433 (2012).
64. Leggat, D. J. *et al.* Vaccination induces HIV broadly neutralizing antibody precursors in humans. *Science* **378**, eadd6502 (2022).
65. Williams, W. B. *et al.* Vaccine induction of heterologous HIV-1-neutralizing antibody B cell lineages in humans. *Cell* **187**, 2919–2934.e20 (2024).
66. Kato, Y. *et al.* Multifaceted effects of antigen valency on B cell response composition and differentiation in vivo. *Immunity* **53**, 548–563.e8 (2020).
67. Victora, G. D. & Nussenzweig, M. C. Germinal Centers. *Annu. Rev. Immunol.* **40**, 413–442 (2022).
68. Heesters, B. A., van der Poel, C. E., Das, A. & Carroll, M. C. Antigen presentation to B

cells. *Trends Immunol.* **37**, 844–854 (2016).

69. Gitlin, A. D., Shulman, Z. & Nussenzweig, M. C. Clonal selection in the germinal centre by regulated proliferation and hypermutation. *Nature* **509**, 637–640 (2014).
70. Roco, J. A. *et al.* Class-Switch Recombination Occurs Infrequently in Germinal Centers. *Immunity* **51**, 337–350.e7 (2019).
71. Viant, C. *et al.* Antibody Affinity Shapes the Choice between Memory and Germinal Center B Cell Fates. *Cell* **183**, 1298–1311.e11 (2020).
72. Turner, J. S. *et al.* SARS-CoV-2 mRNA vaccines induce persistent human germinal centre responses. *Nature* **596**, 109–113 (2021).
73. Tam, H. H. *et al.* Sustained antigen availability during germinal center initiation enhances antibody responses to vaccination. *Proc. Natl. Acad. Sci. U. S. A.* **113**, E6639–E6648 (2016).
74. Caradonna, T. M. & Schmidt, A. G. Protein engineering strategies for rational immunogen design. *NPJ Vaccines* **6**, 154 (2021).
75. Ols, S. *et al.* Multivalent antigen display on nanoparticle immunogens increases B cell clonotype diversity and neutralization breadth to pneumoviruses. *Immunity* **56**, 2425–2441.e14 (2023).
76. Rodrigues, M. Q., Alves, P. M. & Roldão, A. Functionalizing Ferritin Nanoparticles for Vaccine Development. *Pharmaceutics* **13**, (2021).
77. He, L. *et al.* Presenting native-like trimeric HIV-1 antigens with self-assembling nanoparticles. *Nat. Commun.* **7**, 12041 (2016).
78. Mascola, J. R. *et al.* Immunization with envelope subunit vaccine products elicits neutralizing antibodies against laboratory-adapted but not primary isolates of human immunodeficiency virus type 1. The National Institute of Allergy and Infectious Diseases AIDS Vaccine Evaluation Group. *J. Infect. Dis.* **173**, 340–348 (1996).
79. Wyatt, R. & Sodroski, J. The HIV-1 envelope glycoproteins: fusogens, antigens, and

immunogens. *Science* **280**, 1884–1888 (1998).

80. Dey, B. *et al.* Characterization of human immunodeficiency virus type 1 monomeric and trimeric gp120 glycoproteins stabilized in the CD4-bound state: antigenicity, biophysics, and immunogenicity. *J. Virol.* **81**, 5579–5593 (2007).
81. Sanders, R. W. *et al.* HIV-1 VACCINES. HIV-1 neutralizing antibodies induced by native-like envelope trimers. *Science* **349**, aac4223 (2015).
82. Hofmeyer, T. *et al.* Arranged sevenfold: structural insights into the C-terminal oligomerization domain of human C4b-binding protein. *J. Mol. Biol.* **425**, 1302–1317 (2013).
83. Lin, Y.-R. *et al.* HIV-1 VRC01 germline-targeting immunogens select distinct Epitope-specific B cell receptors. *Immunity* **53**, 840–851.e6 (2020).
84. McGuire, A. T. *et al.* Specifically modified Env immunogens activate B-cell precursors of broadly neutralizing HIV-1 antibodies in transgenic mice. *Nat. Commun.* **7**, 10618 (2016).
85. Ingale, J. *et al.* High-density array of well-ordered HIV-1 spikes on synthetic liposomal nanoparticles efficiently activate B cells. *Cell Rep.* **15**, 1986–1999 (2016).
86. Cottrell, C. A. *et al.* Mapping the immunogenic landscape of near-native HIV-1 envelope trimers in non-human primates. *PLoS Pathog.* **16**, e1008753 (2020).
87. Dai, K. *et al.* Rhesus macaque B-cell responses to an HIV-1 trimer vaccine revealed by unbiased longitudinal repertoire analysis. *MBio* **6**, e01375–15 (2015).
88. Agrawal, P. *et al.* Increased immunogen valency improves the maturation of vaccine-elicited HIV-1 VRC01-like antibodies. *PLoS Pathog.* **21**, e1013039 (2025).
89. Mesin, L. *et al.* Restricted Clonality and Limited Germinal Center Reentry Characterize Memory B Cell Reactivation by Boosting. *Cell* **180**, 92–106.e11 (2020).
90. Wang, Y., Liu, J., Burrows, P. D. & Wang, J.-Y. B Cell Development and Maturation. *Adv. Exp. Med. Biol.* **1254**, 1–22 (2020).
91. Sundling, C. *et al.* High-resolution definition of vaccine-elicited B cell responses against the HIV primary receptor binding site. *Sci. Transl. Med.* **4**, 142ra96 (2012).

92. Vigdorovich, V. *et al.* Repertoire comparison of the B-cell receptor-encoding loci in humans and rhesus macaques by next-generation sequencing. *Clin Transl Immunology* **5**, e93 (2016).
93. Chu, T. H., Patz, E. F., Jr & Ackerman, M. E. Coming together at the hinges: Therapeutic prospects of IgG3. *MAbs* **13**, 1882028 (2021).
94. Hessell, A. J. *et al.* Achieving potent autologous neutralizing antibody responses against Tier 2 HIV-1 viruses by strategic selection of envelope immunogens. *J. Immunol.* **196**, 3064–3078 (2016).
95. Malherbe, D. C. *et al.* Envelope variants circulating as initial neutralization breadth developed in two HIV-infected subjects stimulate multiclade neutralizing antibodies in rabbits. *J. Virol.* **88**, 12949–12967 (2014).
96. Hessell, A. J. *et al.* Virus control in vaccinated rhesus macaques is associated with neutralizing and capturing antibodies against the SHIV challenge virus but not with V1V2 vaccine-induced anti-V2 antibodies alone. *J. Immunol.* **206**, 1266–1283 (2021).
97. Sarkar, S. *et al.* IL-33 enhances the kinetics and quality of the antibody response to a DNA and protein-based HIV-1 Env vaccine. *Vaccine* **37**, 2322–2330 (2019).
98. Sarkar, S. *et al.* CD4+ T cells are dispensable for induction of broad heterologous HIV neutralizing antibodies in rhesus macaques. *Front. Immunol.* **12**, 757811 (2021).
99. Spencer, D. A. *et al.* Polyfunctional tier 2-neutralizing antibodies cloned following HIV-1 env macaque immunization mirror native antibodies in a human donor. *J. Immunol.* **206**, 999–1012 (2021).
100. Matchett, W. E. *et al.* Divergent HIV-1-Directed Immune Responses Generated by Systemic and Mucosal Immunization with Replicating Single-Cycle Adenoviruses in Rhesus Macaques. *J. Virol.* **93**, (2019).
101. Abbott, R. K. *et al.* Precursor frequency and affinity determine B cell competitive fitness in germinal centers, tested with germline-targeting HIV vaccine immunogens. *Immunity* **48**,

133–146.e6 (2018).

102. Burton, D. R., Poignard, P., Stanfield, R. L. & Wilson, I. A. Broadly neutralizing antibodies present new prospects to counter highly antigenically diverse viruses. *Science* **337**, 183–186 (2012).

103. Kwong, P. D. & Mascola, J. R. HIV-1 vaccines based on antibody identification, B cell ontogeny, and Epitope structure. *Immunity* **48**, 855–871 (2018).

104. Haynes, B. F. *et al.* Strategies for HIV-1 vaccines that induce broadly neutralizing antibodies. *Nat. Rev. Immunol.* 1–17 (2022).

105. Teixeira, A. R. & Caskey, M. What's Hot in HIV in 2025-A basic and translational science review from IDWeek 2025. *J. Infect. Dis.* jiag135 (2026).

106. Griffith, S. A. & McCoy, L. E. To bnAb or not to bnAb: Defining broadly neutralising antibodies against HIV-1. *Front. Immunol.* **12**, 708227 (2021).

107. Galson, J. D., Trück, J., Kelly, D. F. & van der Most, R. Investigating the effect of AS03 adjuvant on the plasma cell repertoire following pH1N1 influenza vaccination. *Sci. Rep.* **6**, 37229 (2016).

108. Paschold, L. *et al.* Rapid hypermutation B cell trajectory recruits previously primed B cells upon third SARS-CoV-2 mRNA vaccination. *Front. Immunol.* **13**, 876306 (2022).

109. Wu, X. *et al.* Rational design of envelope identifies broadly neutralizing human monoclonal antibodies to HIV-1. *Science* **329**, 856–861 (2010).

110. Kumar, S., Singh, S. & Luthra, K. An overview of human anti-HIV-1 neutralizing antibodies against diverse epitopes of HIV-1. *ACS Omega* **8**, 7252–7261 (2023).

111. Doores, K. J. The HIV glycan shield as a target for broadly neutralizing antibodies. *FEBS J.* **282**, 4679–4691 (2015).

112. Wagh, K., Hahn, B. H. & Korber, B. Hitting the sweet spot: exploiting HIV-1 glycan shield for induction of broadly neutralizing antibodies: exploiting HIV-1 glycan shield for induction of broadly neutralizing antibodies. *Curr. Opin. HIV AIDS* **15**, 267–274 (2020).

113. Walimbwa, S. I., Maly, P., Kafkova, L. R. & Raska, M. Beyond glycan barriers: non-cognate ligands and protein mimicry approaches to elicit broadly neutralizing antibodies for HIV-1. *J. Biomed. Sci.* **31**, 83 (2024).

114. Walker, L. M. *et al.* Broad and potent neutralizing antibodies from an African donor reveal a new HIV-1 vaccine target. *Science* **326**, 285–289 (2009).

115. Kepler, T. B. *et al.* Immunoglobulin gene insertions and deletions in the affinity maturation of HIV-1 broadly reactive neutralizing antibodies. *Cell Host Microbe* **16**, 304–313 (2014).

116. Klein, F. *et al.* Somatic mutations of the immunoglobulin framework are generally required for broad and potent HIV-1 neutralization. *Cell* **153**, 126–138 (2013).

117. Havenar-Daughton, C. *et al.* Direct probing of germinal center responses reveals immunological features and bottlenecks for neutralizing antibody responses to HIV Env trimer. *Cell Rep.* **17**, 2195–2209 (2016).

118. Pauthner, M. *et al.* Elicitation of robust tier 2 neutralizing antibody responses in nonhuman primates by HIV envelope trimer immunization using optimized approaches. *Immunity* **46**, 1073–1088.e6 (2017).

119. Saunders, K. O. *et al.* Stabilized HIV-1 envelope immunization induces neutralizing antibodies to the CD4bs and protects macaques against mucosal infection. *Sci. Transl. Med.* **14**, eabo5598 (2022).

120. Antanasijevic, A. *et al.* Polyclonal antibody responses to HIV Env immunogens resolved using cryoEM. *Nat. Commun.* **12**, 4817 (2021).

121. Wagh, K. *et al.* Completeness of HIV-1 envelope glycan shield at transmission determines neutralization breadth. *Cell Rep.* **25**, 893–908.e7 (2018).

122. Yang, Y. R. *et al.* Autologous antibody responses to an HIV envelope glycan hole are not easily broadened in rabbits. *J. Virol.* **94**, e01861–19 (2020).

123. Horvath, A. *et al.* Systematic comparison of HIV-1 Envelope-specific IgG responses induced by different vaccination regimens: Can we steer IgG recognition towards regions of

viral vulnerability? *Front. Immunol.* **13**, 1075606 (2022).

124. Cottrell, C. A. *et al.* Heterologous prime-boost vaccination drives early maturation of HIV broadly neutralizing antibody precursors in humanized mice. *Sci. Transl. Med.* **16**, eadn0223 (2024).

125. Wang, X. *et al.* mRNA-LNP prime boost evolves precursors toward VRC01-like broadly neutralizing antibodies in preclinical humanized mouse models. *Sci. Immunol.* **9**, eadn0622 (2024).

126. Ringe, R. P. *et al.* Improving the Expression and Purification of Soluble, Recombinant Native-Like HIV-1 Envelope Glycoprotein Trimers by Targeted Sequence Changes. *J. Virol.* **91**, (2017).

127. Pullen, G. R., Fitzgerald, M. G. & Hosking, C. S. Antibody avidity determination by ELISA using thiocyanate elution. *J. Immunol. Methods* **86**, 83–87 (1986).

128. Siegrist, C.-A. *et al.* Co-administration of CpG oligonucleotides enhances the late affinity maturation process of human anti-hepatitis B vaccine response. *Vaccine* **23**, 615–622 (2004).

129. Haynes, B. F. *et al.* Immune-correlates analysis of an HIV-1 vaccine efficacy trial. *N. Engl. J. Med.* **366**, 1275–1286 (2012).

130. Neidich, S. D. *et al.* Antibody Fc effector functions and IgG3 associate with decreased HIV-1 risk. *J. Clin. Invest.* **129**, 4838–4849 (2019).

131. Forthal, D. N., Gabriel, E. E., Wang, A., Landucci, G. & Phan, T. B. Association of Fcγ receptor IIIa genotype with the rate of HIV infection after gp120 vaccination. *Blood* **120**, 2836–2842 (2012).

132. Platt, E. J., Wehrly, K., Kuhmann, S. E., Chesebro, B. & Kabat, D. Effects of CCR5 and CD4 cell surface concentrations on infections by macrophagetropic isolates of human immunodeficiency virus type 1. *J. Virol.* **72**, 2855–2864 (1998).

133. Wei, X. *et al.* Emergence of resistant human immunodeficiency virus type 1 in patients

receiving fusion inhibitor (T-20) monotherapy. *Antimicrob. Agents Chemother.* **46**, 1896–1905 (2002).

134. Montefiori, D. C. Evaluating neutralizing antibodies against HIV, SIV, and SHIV in luciferase reporter gene assays. *Curr. Protoc. Immunol.* **Chapter 12**, 12.11.1–12.11.17 (2005).

135. Seaman, M. S. *et al.* Tiered categorization of a diverse panel of HIV-1 Env pseudoviruses for assessment of neutralizing antibodies. *J. Virol.* **84**, 1439–1452 (2010).

136. deCamp, A. *et al.* Global panel of HIV-1 Env reference strains for standardized assessments of vaccine-elicited neutralizing antibodies. *J. Virol.* **88**, 2489–2507 (2014).

137. Ye, J., Ma, N., Madden, T. L. & Ostell, J. M. IgBLAST: an immunoglobulin variable domain sequence analysis tool. *Nucleic Acids Res.* **41**, W34–40 (2013).

138. Chan, A. K. P. & Griffin, D. E. The B cell subtypes and VDJ repertoire of young adult rhesus macaques. *J. Immunol.* **214**, 3143–3161 (2025).

139. Sundling, C. *et al.* Single-cell and deep sequencing of IgG-switched macaque B cells reveal a diverse Ig repertoire following immunization. *J. Immunol.* **192**, 3637–3644 (2014).

140. Kaduk, M., Corcoran, M. & Karlsson Hedestam, G. B. Addressing IGHV Gene Structural Diversity Enhances Immunoglobulin Repertoire Analysis: Lessons From Rhesus Macaque. *Front. Immunol.* **13**, 818440 (2022).

141. Nogal, B. *et al.* Mapping polyclonal antibody responses in non-human primates vaccinated with HIV env trimer subunit vaccines. *Cell Rep.* **30**, 3755–3765.e7 (2020).

142. Lee, J. H. *et al.* Long-primed germinal centres with enduring affinity maturation and clonal migration. *Nature* **609**, 998–1004 (2022).

143. Kim, W. *et al.* Germinal centre-driven maturation of B cell response to mRNA vaccination. *Nature* **604**, 141–145 (2022).

144. Marina-Zárate, E. *et al.* Highly functional and prolonged germinal center T follicular helper cell responses are associated with enhanced neutralizing antibody development. *Immunity* **58**, 3094–3112.e7 (2025).

145. Havenar-Daughton, C. *et al.* CXCL13 is a plasma biomarker of germinal center activity. *Proc. Natl. Acad. Sci. U. S. A.* **113**, 2702–2707 (2016).

146. Matz, H. C., McIntire, K. M. & Ellebedy, A. H. Persistent germinal center responses: slow-growing trees bear the best fruits. *Curr. Opin. Immunol.* **83**, 102332 (2023).

147. Cirelli, K. M. *et al.* Slow delivery immunization enhances HIV neutralizing antibody and germinal center responses via modulation of immunodominance. *Cell* **177**, 1153–1171.e28 (2019).

148. El Shikh, M. E. M., El Sayed, R. M., Sukumar, S., Szakal, A. K. & Tew, J. G. Activation of B cells by antigens on follicular dendritic cells. *Trends Immunol.* **31**, 205–211 (2010).

149. MacLean, A. J. *et al.* Affinity maturation of antibody responses is mediated by differential plasma cell proliferation. *Science* **387**, 413–420 (2025).

150. Del Giudice, G., Rappuoli, R. & Didierlaurent, A. M. Correlates of adjuvanticity: A review on adjuvants in licensed vaccines. *Semin. Immunol.* **39**, 14–21 (2018).

151. Martin, M., Michalek, S. M. & Katz, J. Role of innate immune factors in the adjuvant activity of monophosphoryl lipid A. *Infect. Immun.* **71**, 2498–2507 (2003).

152. Ismaili, J. *et al.* Monophosphoryl lipid A activates both human dendritic cells and T cells. *J. Immunol.* **168**, 926–932 (2002).

153. Wegmann, F. *et al.* The Carbomer-Lecithin Adjuvant Adjuplex Has Potent Immunoactivating Properties and Elicits Protective Adaptive Immunity against Influenza Virus Challenge in Mice. *Clin. Vaccine Immunol.* **22**, 1004–1012 (2015).

154. Sundling, C., Phad, G., Douagi, I., Navis, M. & Karlsson Hedestam, G. B. Isolation of antibody V(D)J sequences from single cell sorted rhesus macaque B cells. *J. Immunol. Methods* **386**, 85–93 (2012).

155. Harmon, T. M. *et al.* Exploring the potential health impact and cost-effectiveness of AIDS vaccine within a comprehensive HIV/AIDS response in low- and middle-income countries. *PLoS One* **11**, e0146387 (2016).

156. Boonyaratanakornkit, J. & Taylor, J. J. Techniques to study antigen-specific B cell responses. *Front. Immunol.* **10**, 1694 (2019).

157. Dal Porto, J. M., Haberman, A. M., Shlomchik, M. J. & Kelsoe, G. Antigen drives very low affinity B cells to become plasmacytes and enter germinal centers. *J. Immunol.* **161**, 5373–5381 (1998).

158. Batista, F. D. & Neuberger, M. S. Affinity dependence of the B cell response to antigen: a threshold, a ceiling, and the importance of off-rate. *Immunity* **8**, 751–759 (1998).

159. Jumper, J. *et al.* Highly accurate protein structure prediction with AlphaFold. *Nature* **596**, 583–589 (2021).

160. Yin, R. & Pierce, B. G. Evaluation of AlphaFold antibody-antigen modeling with implications for improving predictive accuracy. *Protein Sci.* **33**, e4865 (2024).

161. Zeng, X., Bai, G., Sun, C. & Ma, B. Recent progress in antibody Epitope prediction. *Antibodies (Basel)* **12**, 52 (2023).